A New Test of Excess Movement in Asset Prices*

Ned Augenblick and Eben Lazarus

JULY 2023

Abstract

We derive new bounds on the rational variation in asset prices over time. We focus specifically on risk-neutral beliefs implied by option prices. While risk preferences distort prices away from physical beliefs, one can nonetheless bound risk-neutral belief movement under a general assumption on the stochastic discount factor. The resulting test requires no knowledge of the objective distribution, and it allows significantly more flexibility in preferences and discount rates than in standard volatility tests. Implementing our test empirically using index options, we find that there is so much movement in risk-neutral beliefs that the bounds are routinely violated.

KEYWORDS: Asset prices, volatility bounds, beliefs, rational expectations, risk aversion

JEL CODES: D84, G13, G14, G41

*This paper subsumes and extends a paper previously circulated as "Restrictions on Asset-Price Movements Under Rational Expectations: Theory and Evidence." We are grateful to Francesca Bastianello, Laura Blattner, Jaroslav Borovička, John Campbell, Gabriel Chodorow-Reich, Emmanuel Farhi, Xavier Gabaix, Niels Gormsen, Sam Hanson, Bryan Kelly, Leonid Kogan, David Laibson, Chen Lian, Ian Martin, Jonathan Parker, Matthew Rabin, Andrei Shleifer, Juan Sotes-Paladino, David Sraer, Jim Stock, Adrien Verdelhan, Jessica Wachter, and seminar and conference participants at Harvard, MIT, UC Berkeley, Chicago Booth, Yale SOM, Stanford GSB, Northwestern Kellogg, Duke Fuqua, LSE, University of Sydney, Bocconi University, City University of Hong Kong, the AEA Annual Meeting, SITE, FIRN, the Chicago Fed Rookie Conference, the NBER Behavioral Finance Meeting, and the NBER Summer Institute Asset Pricing Meeting for advice, comments, and helpful discussions. Augenblick is at the Haas School of Business, University of California, Berkeley (ned@haas.berkeley.edu), and Lazarus is at the MIT Sloan School of Management (eblazarus@gmail.com).

1. Introduction

Are market-implied beliefs about future stock returns excessively volatile? This important question is challenging to answer for at least two reasons. First, asset prices reflect both unobservable physical beliefs and unobservable risk and time preferences. Second, even if one could observe beliefs perfectly, the objectively correct beliefs are unknown period by period.

In this paper, we show that it is nonetheless possible to place bounds on the rational variation in option prices, even without knowledge of the correct beliefs and with significant flexibility in preferences and discount rates. Implementing our bounds empirically, we find that there is so much price variation that the bounds are routinely violated. This implies that there must either be excess volatility in beliefs relative to rationality, or very large, high-frequency variation in the price of risk over small changes in the market index. In additional analysis, we find little evidence that rational variation in the price of risk is a key driver of our results, indicating that excess volatility in beliefs likely plays a role.

We focus our analysis on index option prices, as they provide detailed information about market-implied beliefs over future returns. Specifically, we use standard techniques to transform option prices into so-called *risk-neutral (RN) beliefs*, which are a function of (i) the relative likelihood of different return states and (ii) the relative value of a marginal dollar in each state (which depends on risk preferences). Importantly, as RN beliefs are constructed using the *relative* prices of options with different strike prices but the same maturity, they strip out variation arising from time discounting and common unobservable shocks (e.g., to marginal utility or the quantity of risk) that have the same effect on options with different strikes. We can accordingly make informative statements about rational price variation with significantly weaker assumptions than in past volatility tests for the price of the underlying index.[1]

To introduce the logic of our test, we begin in a stripped-down setting and build up to an empirically realistic environment piece by piece. In order to isolate the first component of RN beliefs, assume for now that we can directly observe a person's physical beliefs $\pi_t(\theta = 1)$ over some binary outcome $\theta \in \{0, 1\}$. Suppose we observe π_t repeatedly oscillating from 0.90 to 0.10 and back as t progresses. While it is of course possible to rationalize this movement ex post by constructing a particular set of signal realizations from some data-generating process (DGP), this amount of movement appears intuitively "rare" for someone with rational expectations (RE). Formalizing this idea, Augenblick and Rabin (2021) note that, when uncertainty is resolved by some period T, the expectation of the sum of squared changes in beliefs across all periods (*belief movement*, $\mathbb{E}\sum_{t=0}^{T-1}(\pi_{t+1} - \pi_t)^2$) must equal *initial uncertainty* ($\pi_0(1 - \pi_0)$) under RE, *regardless* of the DGP. Equivalently, expected *excess movement* — belief movement minus initial uncertainty, which we denote by $\mathbb{E}[X]$ — must always be zero. Intuitively, belief movements imply learning, and rational learning implies a concomitant reduction of uncertainty (from the initial level $\pi_0(1 - \pi_0)$ to 0) on

[1] For example, Shiller (1981) famously documented excess volatility in stock prices relative to a measure of fundamental value, but his measure requires that discount rates over future cash flows remain constant over time. As discount rates appear to vary significantly, what to make of his results remains contested (Fama, 1991).

average. Therefore, if one observes a set of empirical belief streams for which excess movement is far from zero on average, the null of rationality can be statistically rejected at some confidence level. In other words, one can make statements about excess volatility in belief streams even without knowledge of the correct beliefs period by period.

The main theoretical contribution of this paper is to show how this logic — that movement in beliefs must correspond on average to reduction in uncertainty — can be used to restrict excess movement in risk-neutral beliefs, $\mathbb{E}[X^*]$, in the general case in which only risk-neutral rather than physical beliefs are observable. Our task becomes considerably more difficult in this case because risk-preference distortions allow $\mathbb{E}[X^*]$ to be non-zero, and its sign and magnitude depend on the degree of risk aversion and the precise form of the DGP. Put differently, non-zero excess movement in risk-neutral beliefs may in fact be consistent with rational updating. But even while allowing meaningful degrees of freedom in risk preferences and the form of the DGP, we show that the admissible $\mathbb{E}[X^*]$ can be bounded as a simple function of risk aversion over the terminal states (or, more generally, the slope of the stochastic discount factor across states).

The broad intuition carries over from the previous case. Suppose, for illustration, that a person's valuation for a binary option that pays \$1 in state $\theta = 1$ at time T oscillates between \$0.90 and \$0.10, while her valuation for an option that pays \$1 in state $\theta = 0$ oscillates between \$0.10 and \$0.90. Risk-neutral beliefs here are also moving back and forth between 0.90 and 0.10. But physical beliefs are not pinned down, as the relative marginal utility of a dollar in the two states is unknown. For example, the person might initially see the states as equally likely ($\pi_0 = 0.50$), but value the first option nine times higher because she values \$1 in state $\theta = 1$ nine times more. But if this marginal-utility ratio — which we call ϕ — is not changing over time, then a movement in the RN belief from 0.90 to 0.10 means that the physical belief must have shifted to very unlikely ($\pi_1 \approx 0.01$). Physical beliefs are therefore oscillating between 0.50 and 0.01, which is still rare for a Bayesian. The same logic applies for any given value of ϕ as long as this parameter is relatively stable within a belief stream, an assumption we make to begin with and return to below.[2] Intuitively, extreme fluctuations in RN beliefs imply physical belief movements that must be rare regardless of the exact degree of risk aversion.

Our bounds for risk-neutral excess movement $\mathbb{E}[X^*]$ formalize this idea. The first bound we derive is highly conservative: it holds under a particular "worst case" DGP that produces the highest possible movement for a given ϕ. This bound therefore requires no knowledge of the true DGP for option prices, as it applies uniformly over the space of all possible DGPs. We then provide a set of tighter bounds that hold given additional information about the DGP. In both cases, the bounds are simple formulas that depend on the observable RN prior and are increasing in ϕ. Consequently, any observed average excess movement in the data is informative as to the minimal risk-aversion value ϕ required in order for the bound to be satisfied.

How does this seemingly abstract setting apply concretely to real-world financial markets?

[2]Note that if ϕ can move arbitrarily, it becomes difficult to make statements about rational price variation. In the above example, physical beliefs could be stable at $\pi_t = 0.50$, with all variation in option prices caused by swings in ϕ from 9 to $\frac{1}{9}$. But as will be discussed further, such variation in ϕ is also difficult to make sense of under RE.

In our empirical setting, the states indexed by θ correspond to the value of the market index as of fixed option expiration date T (or equivalently, the return on the market over the life of the option). Specializing the above example further, assume that state $\theta = 1$ is realized if the index return from $t = 0$ to T is equal to (or within a neighborhood of) 0%, and the other state is realized if the index return is 5%. In this context, the marginal-utility ratio ϕ is equal to $\frac{\mathbb{E}[M_T \mid R_T=0\%]}{\mathbb{E}[M_T \mid R_T=5\%]}$, where M_T is the stochastic discount factor (SDF) and R_T is the market return. This ratio of expected SDF realizations can be thought of as the market's local relative risk aversion, or price of risk, in a neighborhood around a 0% return realized at T. The assumption that ϕ is stable within a belief stream is therefore equivalent to assuming that the local price of risk in this neighborhood is constant. This is significantly weaker than the assumption of constant discount rates used, for example, by Shiller (1981): it allows for time-varying discount rates arising from multiple sources, including general changes in interest rates or the quantity of risk.[3] It is also met either exactly or approximately under many standard modeling frameworks.

That said, the assumption that the local price of risk ϕ is constant within a belief stream is a knife-edge restriction that is unlikely to hold exactly in reality. We therefore also consider how our bounds change given variation in ϕ. We find, both theoretically and in a set of simulations, that rational variation in ϕ has very limited impact on RN belief movement. This may seem counterintuitive: one might imagine that if ϕ oscillates between 3.1 and 2.9, for example, then RN belief movement can be unbounded even with no movement in physical beliefs. While this is true, it overlooks that these oscillations in ϕ are *also* inconsistent with rational updating: they imply predictable mean reversion in the expected marginal value of \$1 in a fixed terminal state. So while it is possible for variation in the local price of risk to generate significant excess movement in RN beliefs, our results indicate that this variation must likely be non-rational in order for the effect to be large. A bounds violation thus suggests that either physical beliefs or risk prices are excessively volatile. We return to the question of their relative importance in our empirical analysis.

After providing our theoretical results and discussing their interpretation and robustness, we then take our bounds to the data. We obtain S&P 500 index option prices from OptionMetrics, and we use standard methods to infer the risk-neutral distribution over index returns for each option expiration date in the sample. To map to our two-state theoretical setting, we then translate each full distribution into a set of binary RN beliefs $\pi_t^*(R_T = \theta_j \mid R_T \in \{\theta_j, \theta_{j+1}\})$; these correspond to the RN probability that the index return will be equal to (or in a range close to) θ_j, conditional on being either θ_j or θ_{j+1}. (We set our return states to correspond to five-percentage-point ranges for the S&P return, matching the example above in which the return states were 0% and 5%.) We then implement our theoretical bounds, which allow us to infer the minimal local risk-aversion value ϕ (at each point in the return distribution) needed to rationalize the observed variation in RN beliefs over the index return.

[3] For example, suppose that the second-period option prices in the example above were \$0.05 and \$0.45 (for states 1 and 0) rather than \$0.10 and \$0.90, due to a shift in the time-t value of money. This shift induces no change in risk-neutral beliefs relative to the example, because the relative prices are unchanged. Meanwhile, such a change would be problematic for any single-asset volatility test assuming constant discount rates.

Our main empirical finding is that there is so much excess movement in RN beliefs that extremely high risk aversion is needed in order to rationalize the data under our maintained assumptions. In many cases, there is in fact no value of ϕ under which the tight version of the bound is met, and the conservative version of the bound generally implies implausibly large values for ϕ. This suggests that many leading rational frameworks capable of explaining medium-to-low-frequency variation in asset prices have difficulty rationalizing the large degree of observed medium-to-high-frequency variation in RN beliefs.

We are of course not the first to provide evidence that well-known models are inconsistent with various empirical moments. But our results offer progress in understanding specifically what can be deduced from the observed volatility in asset prices, a longstanding question of fundamental interest. In particular, because our bounds are derived under the joint null of RE and a constant local price of risk ϕ, our results suggest that at least one of these two must be violated in order to match the data. Further, because we find excessively *positive* movement, these violations must take the form of significant, predictable mean reversion in either physical beliefs or the price of risk.

We conduct additional tests to try to disentangle these possible explanations for our results. We regress observed excess movement on a set of proxies for both (i) overreaction in expectations and (ii) volatility in the price of risk. In all such regressions, we find a strong relationship between excess movement and the first set of proxies, and no detectable relationship between excess movement and volatility in the price of risk. These results suggest that overreaction to information by the marginal investor is likely necessary to match the data.[4]

Given that we conduct our estimation using variation in index option prices, we must also account for the effect of non-fundamental or microstructure noise. To do so, we estimate the variance of the noise component of observed RN beliefs. We use a sample of intraday option prices and apply the microstructure noise variance estimator proposed by Li and Linton (2022), which consistently estimates this variance under quite general dependence in the noise process. We can then construct an empirical noise correction, removing the effect of noise from X^* before we conduct our estimation. All of our statistics are noise-corrected in this way, and our tests are therefore constructed to be robust to idiosyncrasies specific to the option market.

Relation to previous literature. In addition to Shiller (1981), we follow, among others, LeRoy and Porter (1981), West (1988), and Stein (1989) in testing for excess volatility in asset prices relative to measures of fundamental value. Marsh and Merton (1986) emphasize non-stationarity in accounting for apparent excess volatility; much of the literature since then has emphasized time variation in discount rates (Cochrane, 2011). By contrast, our test allows for variation in discount rates and does not require any measure of fundamental value.

While our framework requires significantly weaker theoretical assumptions than classic volatility tests, one cost of this generality is that we rely on option prices rather than the behavior of the underlying index directly. In doing so, we follow a long line of work using options for information

[4] In follow-up work (Augenblick, Lazarus, and Thaler, 2023), we provide a positive explanation for our results using a model of non-Bayesian updating for which we find consistent support in a variety of settings.

about more general expectations or quantities of interest.[5] Our work particularly complements Giglio and Kelly (2018), who document excess volatility in long-maturity claims on volatility, inflation, commodities, and interest rates. They achieve identification by parameterizing the DGP for cash flows on the underlying, whereas we restrict the SDF. Their parameterization — an affine model under the RN measure — applies well to the term-structure-like claims they consider, but not to claims on the equity index itself, to which our framework does apply.[6]

Our results also complement evidence obtained from survey data, as, for example, in Greenwood and Shleifer (2014) and De la O and Myers (2021), as well as the results of Augenblick and Rabin (2021) for settings with directly observable beliefs. Another set of related literature endeavors to measure physical probabilities indirectly from asset prices. Aït-Sahalia, Wang, and Yared (2001) test whether option-implied return distributions are well-calibrated; Ross (2015) provides assumptions under which physical beliefs can be recovered from options; Polkovnichenko and Zhao (2013) consider the probability weighting functions consistent with option-price data given an assumption on the form of the weighting function. Our approach differs from this and related work in that we need not measure physical beliefs at all or know the true DGP for returns to conduct our tests. This semi-parametric approach loosely ties our theoretical contribution to a line of work including, among many others, Hansen and Jagannathan (1991) and Alvarez and Jermann (2005), which consider the identification of structural parameters from different moments of the observable data than the ones we consider here.

Organization. Section 2 introduces our theory in a two-state setting, which allows for clear derivations and intuition for our main results. Section 3 extends these results to a general asset-pricing setting. Section 4 discusses our main identifying assumption; Section 5 provides additional robustness results. We implement our bounds in Section 6, which describes our data and presents our empirical results. Section 7 concludes. Proofs of our main results are provided in Appendix A, and an Internet Appendix contains the remaining proofs and additional technical material.

2. Theoretical Framework: Introduction in a Simple Setting

To introduce our framework, we first examine risk-neutral (RN) belief movement in a simple setting with a single individual and two terminal states. This setting helps clarify three issues: (i) the economics underlying restrictions on belief movement under RE when the individual is risk-neutral; (ii) how risk aversion complicates this analysis; and (iii) how we can nonetheless bound RN belief movement. This step-by-step discussion sets the stage for our generalized framework in Section 3.

[5] A non-representative recent sample includes Backus, Chernov, and Martin (2011) regarding disaster risk, Martin (2017) and Chabi-Yo and Loudis (2020) on the equity premium, Beason and Schreindorfer (2022) on how to decompose the equity premium, and Haddad, Moreira, and Muir (2023) on the impact of policy promises.

[6] See also Gandhi, Gormsen, and Lazarus (2023) for recent evidence on the term structure of the equity premium.

2.1 Setup and Initial Results

Time is discrete and indexed by $t = 0, 1, 2, \ldots, T$. At the beginning of each period, a person observes a signal $s_t \in S$ regarding two mutually exclusive and exhaustive states $\theta \in \{0, 1\}$. The data-generating process (DGP) is general: signals are drawn from the discrete signal distribution $DGP(s_t \mid \theta, H_{t-1})$, where H_t is the history of signal realizations through t. Define $\mathbb{P}(H_T)$ to be the probability of observing history H_T induced by the DGP, and write $\mathbb{E}[\cdot] \equiv \mathbb{E}^{\mathbb{P}}[\cdot]$ for the expectation under $\mathbb{P}$. The person's (*physical* or *subjective*) *belief* in state 1 (vs. state 0) at time t given the DGP and history H_t is denoted by $\pi_t(H_t)$. The *belief stream* $\boldsymbol{\pi}(H_t) = [\pi_0, \pi_1(s_1), \pi_2(\{s_1, s_2\}), \ldots]$ is the collection of beliefs given H_t. We often suppress the dependence of these objects on H_t to simplify notation. Given our empirical setting, we focus on *resolving* streams in which the person achieves certainty about the true state by period T with probability 1: $\pi_T(H_T) = \theta \in \{0, 1\}$ for all H_T.

Throughout the paper, we maintain the assumption that the person's beliefs over the terminal state satisfy rational expectations (RE).

ASSUMPTION 1 (*RE*)**.** Beliefs satisfy $\pi_t(H_t) = \mathbb{E}[\theta \mid H_t]$ for any H_t.

This assumption states that the agent's beliefs coincide period by period with the true conditional probability of realizing state $\theta = 1$, and the assumption will be satisfied by a person with a correct prior who updates using Bayes' rule according to the true DGP. The assumption is in fact stronger than necessary for our main results: we could instead assume the weaker martingale restriction that $\pi_t = \mathbb{E}[\pi_{t+1} \mid \pi_t]$, which is implied by Assumption 1. (Under this weaker condition, the person could, for example, ignore some periods' signals.) Assuming RE directly, though, helps streamline our exposition.

Given our asset-pricing setting, we assume that the DGP and the person's physical beliefs cannot be observed directly. Instead, we assume that the econometrician can observe, period by period, the person's willingness to pay for an Arrow-Debreu security that pays \$1 (one unit of the numeraire consumption good) in period T if state θ is realized. Denote this valuation by $q_t(\theta|H_t)$ for each $\theta \in \{0, 1\}$. An object analogous to $q_t(\theta|H_t)$ will be empirically observable using options data for suitably defined states, but we postpone this additional formalism to Section 3.

We start by considering the simple case in which the person values consumption at all periods and in all states equally (i.e., she is risk-neutral and does not discount future consumption). In this risk-neutral case, beliefs are in fact directly inferable from asset values: $q_t(1|H_t) = \pi(H_t)$ and $q_t(0|H_t) = 1 - \pi(H_t)$. Testable restrictions on asset values are thus equivalent in this case to restrictions on physical beliefs.

We keep track of the following objects related to the physical belief stream, and we discuss shortly how these objects are restricted under RE. First, total *belief movement* of $\boldsymbol{\pi}$ is defined as the sum of squared changes (or quadratic variation) in beliefs across all periods:

$$\mathsf{m}(\boldsymbol{\pi}) \equiv \textstyle\sum_{t=0}^{T-1} (\pi_{t+1} - \pi_t)^2. \tag{1}$$

Second, *initial uncertainty* of $\boldsymbol{\pi}$ is defined as the variance of the Bernoulli random variable $\mathbb{1}\{\theta = 1\}$ as of $t = 0$:

$$\mathsf{u}_0(\boldsymbol{\pi}) \equiv (1 - \pi_0)\pi_0. \tag{2}$$

Given that we focus on resolving belief streams for which $\pi_T \in \{0, 1\}$, final uncertainty is always zero ($\mathsf{u}_T = (1 - \pi_T)\pi_T = 0$). Initial uncertainty u_0 is therefore equal to the total amount of uncertainty reduction for $\boldsymbol{\pi}$, $\mathsf{u}_0 - \mathsf{u}_T$, which is helpful in interpreting some of the following results.

Our main variable of interest will be the difference between movement and initial uncertainty, which — for reasons that will become clear — we call *excess movement*:

$$X(\boldsymbol{\pi}) \equiv \mathsf{m}(\boldsymbol{\pi}) - \mathsf{u}_0(\boldsymbol{\pi}). \tag{3}$$

Belief movement and initial uncertainty are related under RE according to the following result, which restates a main result in Augenblick and Rabin (2021).

Lemma 1 (Augenblick and Rabin, 2021)**.** *Under Assumption 1, for any DGP, expected total belief movement must equal initial uncertainty. Expected excess movement in beliefs must therefore be zero:*

$$\mathbb{E}[X] = 0.$$

Lemma 1 is a straightforward implication of the assumption of martingale beliefs.[7] The result formalizes a notion of the "correct" amount of belief volatility under RE, and it motivates referring to X as *excess movement*. Given a set of observed belief streams, one can straightforwardly calculate the sample average of the empirical excess movement statistic and statistically test if it differs from zero. The restriction reflects the intuition that if the person's beliefs are moving, this movement must on average correspond to learning about the true terminal state (in the sense that uncertainty is resolved from its initial value to 0). Rewriting $\mathbb{E}[X] = 0$ as $\mathbb{E}[\sum_{t=0}^{T-1}(1 - 2\pi_t)(\pi_{t+1} - \pi_t)] = 0$ (see footnote 7), it is apparent that expected belief movements toward 0.5 (the point of highest uncertainty) lead to a positive $\mathbb{E}[X]$ statistic, and vice versa. So it could be the case that $\mathbb{E}[\pi_{t+1} - \pi_t] = 0$ unconditionally, but a test based on the lemma would still reject the null of RE if, for instance, low values of π_t ($\pi_t < 0.5$) tend to be revised upward ($\pi_{t+1} - \pi_t > 0$), and high values tend to be revised downward.

To clarify our setting and the above lemma, Figure 1 plots belief streams under a two-period DGP. Two fair coins are flipped sequentially at $t = 1$ and 2, generating two possible signals (H or T) at each of these dates. If two heads occur (HH), then state $\theta = 1$ is realized; otherwise, $\theta = 0$ is realized. As the figure shows, the person's prior π_0 is equal to 0.25 under RE (equal to the probability of two heads). If the first coin flip is tails (shown in the red path), then $\pi_1 = \pi_2 = 0$; if heads then tails are flipped, then $\pi_1 = 0.5$, $\pi_2 = 0$ (light blue); if two heads are flipped, then $\pi_1 = 0.5$, $\pi_2 = 1$ (dark blue). The accompanying table shows belief movement $\mathsf{m} = (\pi_1 - \pi_0)^2 + (\pi_2 - \pi_1)^2$ for each possible stream. Weighting the paths by their relative frequencies, expected belief movement

[7] To see this, rewrite X as $\sum_{t=0}^{T-1}(2\pi_t - 1)(\pi_t - \pi_{t+1})$. Using the law of iterated expectations on each term in the sum, $\mathbb{E}[(2\pi_t - 1)(\pi_t - \pi_{t+1})] = \mathbb{E}[(2\pi_t - 1)(\pi_t - \mathbb{E}[\pi_{t+1}|\pi_t])]$, which must be zero under the martingale assumption. This result has appeared in other forms in past literature; for one example, see Barndorff-Nielsen and Shephard (2001).

Figure 1: Physical Beliefs and Excess Movement: Two-Period Example

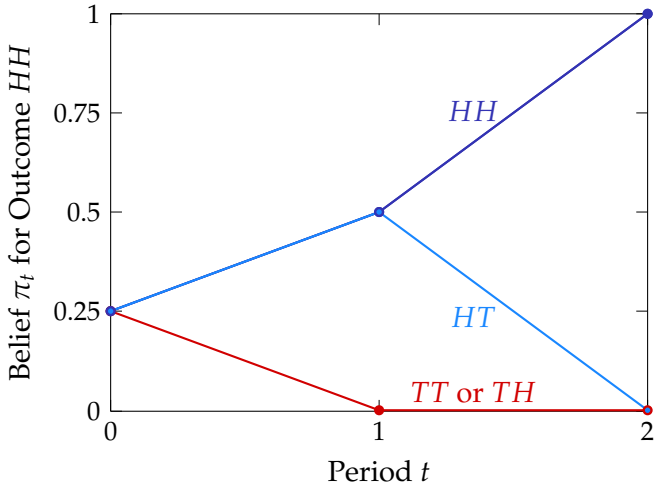

STATISTICS

Signals (s_1, s_2)	Frequency $\mathbb{P}(s_1, s_2)$	Movement m
HH	0.25	0.3125
HT	0.25	0.3125
TT or TH	0.5	0.0625

$$\mathbb{E}[\mathsf{m}] = 0.1875 = \mathsf{u}_0$$
$$\Longrightarrow \mathbb{E}[X] = 0$$

Notes: Signals (s_1, s_2) are generated by sequential fair coin flips. State $\theta = 1$ is realized if two heads occur: $(s_1, s_2) = (H, H)$, labeled HH; otherwise $\theta = 0$. Each path in the figure corresponds to a possible belief stream over $\theta = 1$ for a person with RE. In the table, m, u_0, and X are as defined in (1)–(3), and $\mathbb{E}[\mathsf{m}] = 0.25 \times 0.3125 \times 2 + 0.5 \times 0.0625$.

is $\mathbb{E}[\mathsf{m}] = 0.1875$. This is exactly equal to initial uncertainty $\mathsf{u}_0 = (1 - 0.25) \times 0.25 = 0.1875$, illustrating the restriction that $\mathbb{E}[X] = 0$. This applies beyond this two-period example: the lemma implies that *any* DGP for which $\pi_0 = 0.25$ would generate expected movement of 0.1875 under RE.

2.2 Risk-Neutral Beliefs: Setup and Identification Challenge

Lemma 1 shows that one can make statements about excess belief movement under RE when beliefs are directly observable or inferrable from asset prices. But identifying excess movement in asset valuations becomes significantly more complicated when the person is risk averse, as valuations no longer correspond directly to beliefs in this more general case. To see this, assume now that the agent has time-separable utility, with concave period utility function $U(C_t)$, and that she exponentially discounts future consumption with discount factor β. Assume that the state θ determines period-T consumption $C_{T,\theta}$. Valuations for the two Arrow-Debreu securities at time t are now

$$q_t(1|H_t) = \frac{\beta^{T-t} U'(C_{T,1})}{U'(C_t)} \pi_t, \qquad q_t(0|H_t) = \frac{\beta^{T-t} U'(C_{T,0})}{U'(C_t)} (1 - \pi_t). \tag{4}$$

Valuations thus no longer directly reveal beliefs. Instead, they are distorted by the relative value of a marginal dollar in state θ in period T versus one in period t. As $q_t(1|H_t)$ and $q_t(0|H_t)$ are similarly distorted by β^{T-t} and $U'(C_t)$, it is useful to focus on their relative valuations. This logic leads to the consideration of *risk-neutral (RN)* beliefs,

$$\pi_t^*(H_t) \equiv \frac{q_t(1|H_t)}{q_t(0|H_t) + q_t(1|H_t)} = \frac{U'(C_{T,1})}{\mathbb{E}_t[U'(C_T)]} \pi_t(H_t) = \frac{\phi \pi_t(H_t)}{1 + (\phi - 1)\pi_t(H_t)}, \tag{5}$$

$$\text{where } \phi \equiv \frac{U'(C_{T,1})}{U'(C_{T,0})}. \tag{6}$$

The definition in (5) follows the usual convention for RN beliefs, and the remaining expressions follow from (4). Like π_t, the RN belief π_t^* corresponds to state $\theta = 1$. The RN belief for $\theta = 0$ can be similarly defined as $\frac{q_t(0|H_t)}{q_t(0|H_t)+q_t(1|H_t)} = 1 - \pi_t^*$, so the two states' RN beliefs are positive and sum to 1 by construction. We define the RN belief stream $\boldsymbol{\pi}^*(H_t)$, RN belief movement $\mathsf{m}^*(\boldsymbol{\pi}^*)$, RN initial uncertainty $\mathsf{u}_0^*(\boldsymbol{\pi}^*)$, and RN excess movement $X^*(\boldsymbol{\pi}^*)$ as in Section 2.1, but with RN beliefs π_t^* in the place of physical beliefs π_t.

Risk-neutral beliefs are so named because they can be interpreted as the subjective beliefs for a fictitious risk-neutral agent. In general, they represent a pseudo-belief distribution, reflecting a combination of the person's physical beliefs π_t and risk preferences as indexed by ϕ. This object ϕ will be particularly important in our environment. It represents the (constant) marginal rate of substitution across primitive states, as can be seen in (6). Up to a scaling constant, it also serves as an index of relative risk aversion: conducting a Taylor expansion of $U'(C_{T,0})$ around $C_{T,1}$ gives $U'(C_{T,0}) = U'(C_{T,1}) + U''(C_{T,1})(C_{T,0} - C_{T,1}) + \mathcal{O}\big((C_{T,0} - C_{T,1})^2\big)$, and thus, to first order,

$$\gamma(C_{T,1}) \equiv -\frac{C_{T,1}U''(C_{T,1})}{U'(C_{T,1})} = \frac{\phi - 1}{(C_{T,0} - C_{T,1})/C_{T,1}}. \tag{7}$$

Relative risk aversion γ thus depends on the ratio of marginal utilities across states ϕ relative to the percent consumption gap across states. Finally, in asset-pricing terms, ϕ is equivalent to the ratio of *stochastic discount factor (SDF)* realizations $M_{t,T}(\theta)$ across the two states:

$$\phi = \frac{M_{t,T}(1)}{M_{t,T}(0)}, \text{ where } M_{t,T}(1) \equiv \frac{q_t(1|H_t)}{\pi_t(H_t)}, \; M_{t,T}(0) \equiv \frac{q_t(0|H_t)}{1 - \pi_t(H_t)}.$$

This SDF-based representation of ϕ will be discussed in detail in the general setting in Section 3.

To complete the setup for the current consumption-based setting, we assume that consumption in state 1 is weakly less than in state 0, $C_{T,1} \leqslant C_{T,0}$. This is without loss of generality for now, as the states can be relabeled arbitrarily. With concave utility, this labeling of state 1 as the low-consumption state implies that $U'(C_{T,1}) \geqslant U'(C_{T,0})$ and thus $\phi \geqslant 1$. Given $\phi \geqslant 1$, the RN belief π_t^* in general exceeds the subjective belief π_t: the person is willing to pay relatively more for a bad-state consumption claim given her high marginal utility in that state, upwardly biasing the bad-state RN belief relative to π_t.

We wish to make statements similar to Lemma 1, but applicable to observable RN beliefs rather than physical beliefs. Under a risk-neutral expectation $\mathbb{E}^*[\cdot]$ defined such that $\pi_t^*(H_t) = \mathbb{E}^*[\pi_{t+1}(H_{t+1}) \mid H_t]$, one could in fact apply Lemma 1 directly, as $\mathbb{E}^*[X^*] = 0$. But the frequency of observed RN belief streams is determined by the physical measure rather than the RN measure; that is, we can only observe an empirical counterpart to $\mathbb{E}[X^*]$ rather than $\mathbb{E}^*[X^*]$. And even under the maintained assumption that physical beliefs π_t satisfy RE, the distortion in π_t^* relative to π_t can cause RN movement to differ from RN initial uncertainty on average, so $\mathbb{E}[X^*] \neq 0$. This is the fundamental identification challenge.

For an illustration of this issue, Figure 2 returns to the coin-flip example from Figure 1. In

Figure 2: RN Beliefs and Excess Movement: Two-Period Example

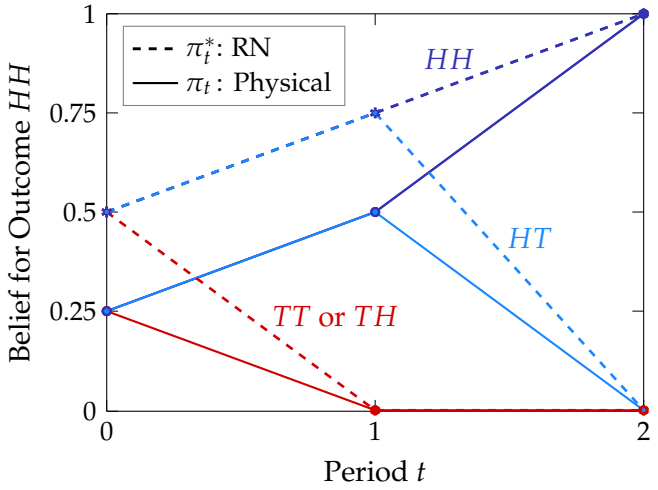

STATISTICS

Signals (s_1, s_2)	Frequency $\mathbb{P}(s_1, s_2)$	RN Movement m^*
HH	0.25	0.125
HT	0.25	0.625
TT or TH	0.5	0.25

$$\mathbb{E}[\mathsf{m}^*] = 0.3125 > 0.25 = \mathsf{u}_0^*$$
$$\Longrightarrow \mathbb{E}[X^*] = 0.0625 > 0$$

Notes: See Figure 1 for description of signals and physical beliefs. Observed RN beliefs are calculated using (5), with the assumption that $\phi = 3$. In the table, m^*, u_0^*, and X^* are calculated as in (1)–(3), with RN beliefs π_t^* in place of π_t.

addition to physical beliefs, this figure now shows RN belief streams with $\phi = 3$.[8] From (5), the physical prior $\pi_0 = 0.25$ corresponds to an RN prior of $\pi_0^* = 0.5$. Intuitively, the person perceives state $\theta = 0$ as three times as likely as $\theta = 1$ (HH), but values a marginal dollar in $\theta = 1$ three times more than in $\theta = 0$, so $q_0(0) = q_0(1)$ and $\pi_0^* = 0.5$. The same calculations are then applied to obtain π_1^* and π_2^* for each stream shown in the figure. The accompanying table shows RN movement m^* for each stream. Comparing this to the table in Figure 1, it is apparent that $\mathsf{m}^* > \mathsf{m}$ for streams in which the RN belief has large downward revisions (HT, TT, and TH): π_t^* is biased upward relative to π_t, so these large downward revisions generate more RN movement than physical movement. These streams cause RN excess movement to be positive on average: $\mathbb{E}[X^*] = 0.0625 > 0$.

As this example illustrates, even with rational physical beliefs, one can observe what appears to be excess movement in RN beliefs implied by valuations. So if we naively test for RE using Lemma 1 on observed RN (rather than actual) beliefs, we may spuriously conclude that beliefs are excessively volatile.

2.3 Risk-Neutral Beliefs: Results

The fact that there can be excess movement in RN beliefs even under RE would seem to pose an intractable challenge. But this turns out not to be the end of the story. RN beliefs are not arbitrarily distorted relative to physical beliefs: as in (5), they are linked through the single unobserved parameter ϕ. And regardless of the value of ϕ, RN beliefs must lie between 0 and 1 by definition. These insights will allow us to bound $\mathbb{E}[X^*]$ over all possible DGPs for a given value of ϕ, and over all possible values of ϕ. Because our main results are most straightforwardly stated in the current section's two-state setting, we state them here before discussing how they generalize in Section 3.

[8] Under risk neutrality, $\phi = 1$. This was implicitly assumed to be the case for Figure 1.

Main Results

Before turning to the results, it will be useful to define two additional objects. First, we invert (5) to solve for π_t as a function of π_t^* and ϕ, the solution to which we denote by $\pi_t(\pi_t^*, \phi)$:

$$\pi_t(\pi_t^*, \phi) = \frac{\pi_t^*}{\phi + (1-\phi)\pi_t^*}. \tag{8}$$

Second, it will be helpful to define the difference in conditional expected X^* across states as

$$\triangle \equiv \mathbb{E}[X^*|\theta = 0] - \mathbb{E}[X^*|\theta = 1]. \tag{9}$$

Given these definitions, we can now provide a number of expressions and bounds for $\mathbb{E}[X^*]$. We assume throughout that Assumption 1 holds.

PROPOSITION 1. *For any DGP,*

$$\begin{aligned}\mathbb{E}[X^*] &= (\pi_0^* - \pi_0)\triangle \\ &= \left(\pi_0^* - \frac{\pi_0^*}{\phi + (1-\phi)\pi_0^*}\right)\left(\mathbb{E}[X^*|\theta = 0] - \mathbb{E}[X^*|\theta = 1]\right).\end{aligned}$$

PROPOSITION 2. *For any DGP and any value for* $\triangle$*,*

$$\begin{aligned}\mathbb{E}[X^*] &\leqslant (\pi_0^* - \pi_0)\pi_0^* \\ &\leqslant \left(1 - \frac{1}{\phi + (1-\phi)\pi_0^*}\right)\pi_0^{*2}.\end{aligned} \tag{10}$$

Proofs for this section's main results are provided in Appendix A. Proposition 1 starts from the fact that $\mathbb{E}^*[X^*] = 0$. We then connect $\mathbb{E}^*[X^*]$ to $\mathbb{E}[X^*]$. The key step is to show that *conditional* expectations of X^* under both measures are equal, $\mathbb{E}^*[X^*|\theta] = \mathbb{E}[X^*|\theta]$ for $\theta = 0, 1$, which leads to the stated result. Note that if $\phi = 1$, then $\pi_0^* = \pi_0$ and therefore $\mathbb{E}[X^*] = 0$, as in Lemma 1. As ϕ rises, π_0 drops further below π_0^*, and $\mathbb{E}[X^*]$ departs from 0: the greater is risk aversion, the more one can observe excess RN movement differ from zero on average under RE. The sign and magnitude of this deviation depend on $\triangle$, as explored in more detail later in this section.

Across all DGPs, $\triangle$ is bounded above by π_0^*, from which Proposition 2 follows. The version of the bound in (10) is one of our main results. It gives a bound for $\mathbb{E}[X^*]$ as a function of π_0^* and ϕ, regardless of $\triangle$. Under risk neutrality ($\phi = 1$), this upper bound again becomes zero. But the bound is otherwise positive, and the *admissible excess movement* in RN beliefs given by the right side of the inequality increases monotonically in ϕ. This result thus formalizes a more general notion of the admissible amount of belief volatility under rationality, this time as an increasing function of risk aversion across the two states.

Intuitively, movement in RN beliefs must still correspond on average to the agent learning something about the true terminal state, but the bias in RN relative to subjective beliefs induced

by risk aversion allows for positive excess movement in those observed beliefs under RE. This is reflected in the first term in the bound, $(\pi_0^* - \pi_0)$, as this difference increases in ϕ. For the second term (π_0^*), higher RN priors yield more "room" for downward RN belief movement. This increases admissible excess movement along the lines of the example considered in Figure 2. The bound in Proposition 2 is conservative, as it holds under a "worst-case" DGP with an extreme value for $\triangle$.

Because of the monotonicity of the bound in ϕ, the inequality can equivalently be read as providing a *lower* bound for the unobserved structural parameter ϕ as a function of observables. The observed excess movement in RN belief streams thus provides information on the minimal value of risk aversion necessary for the data to be consistent with RE. But more still can be said: taking $\phi \to \infty$ in (10) generates the following maximally conservative bound for $\mathbb{E}[X^*]$, which applies for *any* ϕ.

COROLLARY 1. *For any DGP and any values* $\triangle$ *and* ϕ*,*

$$\mathbb{E}[X^*] \leqslant \pi_0^{*2}.$$

Corollary 1 exploits that RN beliefs are bounded between 0 and 1 by construction: there is only so far that RN beliefs can be distorted relative to subjective beliefs, so the bound is well-defined even for arbitrarily high risk aversion.[9] It states that price movements for which $\mathbb{E}[X^*] > \pi_0^{*2}$ simply cannot be rationalized under RE given constant ϕ. Despite its maximal conservatism, this bound still imposes a meaningful limit on admissible RN excess movement, especially for low π_0^*. For example, with $\pi_0^* = 0.2$, RN excess movement is at most 0.04, regardless of ϕ or the DGP.

Taken together, Proposition 2 and Corollary 1 characterize the maximal admissible excess movement in RN beliefs as a function of ϕ for any RN prior. Figure 3 provides a graphical illustration of these bounds. Starting from the bottom of the chart, the thick purple line corresponds to the bound for $\phi = 1$: in this case, $\mathbb{E}[X^*] = \mathbb{E}[X] = 0$ regardless of the prior or DGP, from Lemma 1. The thin dashed gray lines correspond to arbitrarily selected DGPs in the case of $\phi = 3$. While there can be positive RN excess movement, this is not necessarily the case for all possible DGPs. Taking the envelope over all of these processes for $\phi = 3$ yields the bound from Proposition 2, which is shown in the thick blue line. It is asymmetric around 0.5 as well as non-monotonic in π_0^*.[10] Finally, the thick red line shows the bound for the limiting case $\phi \to \infty$, which is equal to the squared RN prior from Corollary 1.

When should we expect to see *negative* RN excess movement — as observed in the lowest dashed gray line in Figure 3 — even with risk aversion? If one is willing to make an assumption on the sign of $\triangle$ (discussed shortly), the following stronger bound applies as a corollary of Proposition 1.

[9] In the limit as $\phi \to \infty$, $\pi_0 \to 0$ for any π_0^*, so $\pi_0^* - \pi_0 \to \pi_0^*$.

[10] The second term in the bound (π_0^*) of course increases monotonically, generating asymmetry in the bound around $\pi_0^* = 0.5$ for $\phi > 1$. But the first term in the bound $(\pi_0^* - \pi_0)$ does not increase monotonically for $1 < \phi < \infty$, exerting a countervailing force that generates the observed non-monotonicity.

Figure 3: RN Excess Belief Movement vs. Prior by ϕ Under RE

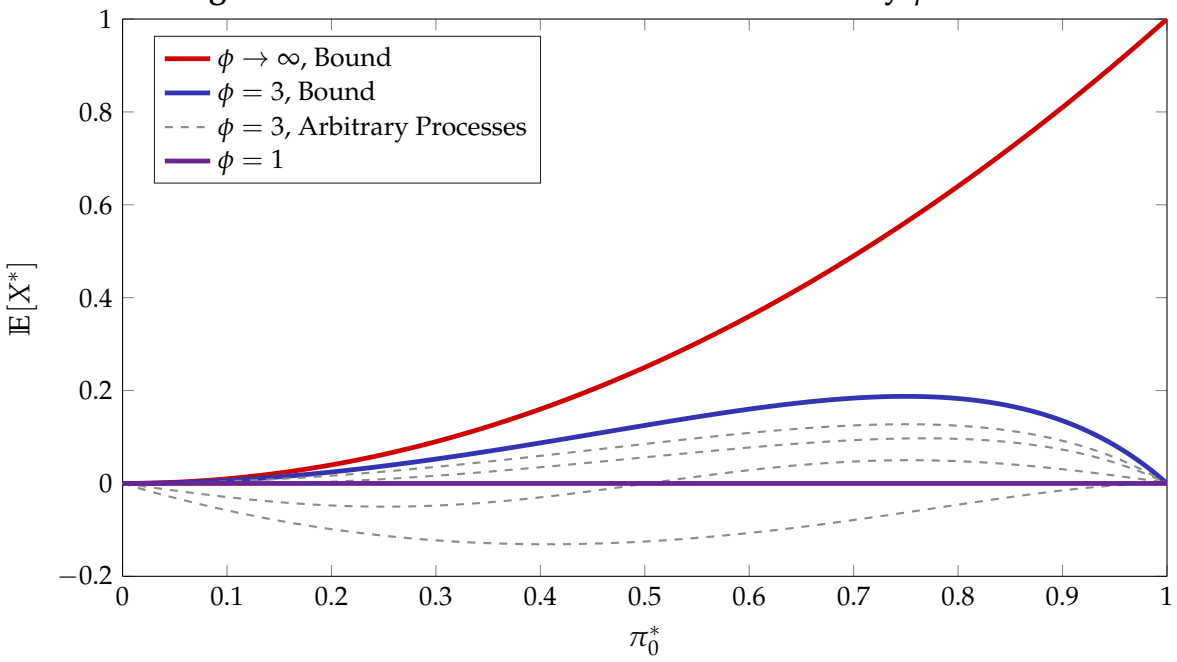

Note: Theoretical bounds are obtained from the formulas in Proposition 2 and Corollary 1.

COROLLARY 2. *If* $\mathbb{E}[X^*|\theta = 0] \leqslant \mathbb{E}[X^*|\theta = 1]$, *for any DGP and any value for* ϕ,

$$\mathbb{E}[X^*] \leqslant 0.$$

When $\triangle < 0$, $\mathbb{E}[X^*]$ is decreasing in ϕ and therefore $\mathbb{E}[X^*] < 0$ for any $\phi > 1$. Consequently, as formalized in Corollary 2, the highest excess movement is $\mathbb{E}[X^*] = 0$. While most of our focus is on the conservative positive upper bounds for $\mathbb{E}[X^*]$, this corollary shows that asset-pricing settings with risk aversion do not necessarily entail positive excess movement in observed beliefs. We now further explore the statistical features of the DGP that are informative about the degree of RN excess movement to be expected under RE.

How the DGP Determines $\mathbb{E}[X^*]$

Proposition 1 says that the deviation of $\mathbb{E}[X^*]$ from 0 depends on the product of $\pi_0^* - \pi_0$ and $\triangle \equiv \mathbb{E}[X^*|\theta = 0] - \mathbb{E}[X^*|\theta = 1]$. The difference $\pi_0^* - \pi_0$ is always positive and increases in ϕ. But how are the sign and magnitude of $\triangle$ related to the DGP? To answer this question, we provide two theoretical results and briefly summarize a set of simulations discussed in detail in Internet Appendix C.1. These results will then be useful in interpreting the empirical results to come.

First, given the arbitrary labeling of the two states, there is no reason to expect under RE that $\triangle$ should take a particular sign:

PROPOSITION 3. *Fixing* ϕ, *for every RN prior and DGP that leads to a given* $\triangle$, *there exists a different RN prior and DGP that leads to* $-\triangle$.

For any RN prior π_0^* and DGP with some $\triangle$, the RN prior $1-\pi_0^*$ with the "reversed" DGP will necessarily lead to $-\triangle$. Consequently, there is no reason to assume that $\mathbb{E}[X^*]$ is more likely to be positive than negative given $\phi > 1$.

Next, we summarize numerical simulations for a large set of DGPs as described in Internet Appendix C.1. First, when the DGP is symmetric (with equal movements up or down, as is likely to roughly apply for option prices), $\triangle < 0$ if $\pi_0^* < .5$, $\triangle = 0$ if $\pi_0^* = .5$, and $\triangle > 0$ if $\pi_0^* > .5$. This suggests, for example, that low π_0^* should lead to a negative $\triangle$ unless the DGP is asymmetric. As we show later, the empirical DGPs in our setting appear largely symmetric, so that we estimate $\triangle < 0$ for $\pi_0^* < .5$. Second, the numerical results also suggest that extreme values of $\triangle$ only occur in highly asymmetric DGPs where movements in one direction are large and movements in the other direction are tiny. In fact, our upper bound in (10) is attainable asymptotically given the most asymmetric DGP possible:

PROPOSITION 4. *There exists a sequence of DGPs, indexed by T, for which $\mathbb{E}[X^*]$ approaches the bound in Proposition 2 as $T \to \infty$. For each DGP in this sequence, downward movements ($\pi_{t+1}^* < \pi_t^*$) are resolving ($\pi_{t+1}^* = 0$) and thus as large as possible, while upward movements are small ($\pi_{t+1}^* - \pi_t^* \to 0$ as $T \to \infty$). Meanwhile, the bound holds with strict inequality for any $T < \infty$ as long as $\phi > 1$ and $\pi_0^* \in (0,1)$.*

One implication of this result is that the bound in Proposition 2 is approximately tight, as one can construct a DGP for which $\mathbb{E}[X^*]$ is close to the bound for large T. Perhaps more important, though, is that it points to the bound's conservatism: it holds under a somewhat perverse DGP that can be thought of as a "rare bonanzas" process, where with small probability the person receives news that the bad state ($\theta = 1$) will not be realized (so $\pi_{t+1}^* = 0$), and otherwise there is mostly uninformative bad news that increases π_{t+1}^* slightly. More reasonable DGPs, or $T \ll \infty$, will give lower $\mathbb{E}[X^*]$. That said, the conservative bound has the advantage of being very simple and not requiring any estimation of $\triangle$. And as we show below, empirical excess movement is in fact so high that even these conservative bounds are often violated for reasonable values of ϕ.

3. Generalized Theoretical Results for Equilibrium Asset Prices

While the binary-state setting considered in the previous section is useful for exposition, it is also artificial: one cannot obtain a single person's valuation of Arrow-Debreu claims in observational data alone; there are more than two possible states; and the realized state determines more than just consumption. We thus now consider a general many-state framework for equilibrium asset prices and show how our results extend to this empirically relevant case.

3.1 Setup and Notation

Preliminaries: Probability Space, Prices, and Risk-Neutral Probabilities

Time is again indexed by $t \in \{0, 1, 2, \ldots\}$, and we consider a discrete probability space $(\Omega, \mathcal{F}, \mathbb{P})$ with filtration $\{H_t\}$.[11] A realization of the elementary state is denoted by $\omega \in \Omega$. To make our results empirically implementable, we will be concerned with the ex-dividend value of the market index, $V_t^m : \Omega \to \mathbb{R}_+$, on some option expiration date T. (We will later extend the notation to allow for multiple option expiration dates.) A European call option on the index with strike price K has date-T payoff $(V_T^m - K)^+ = \max(V_T^m - K, 0)$, and its time-$t$ price is $q_{t,K}^m$. These option prices are observable for some set of strike prices $\mathcal{K} \subseteq \mathbb{R}_+$ beginning at date 0. Assuming the absence of arbitrage, there exists a strictly positive *stochastic discount factor (SDF)* $M_{t,T}$ such that option prices satisfy $q_{t,K}^m = \mathbb{E}_t[M_{t,T}(V_T^m - K)^+]$, where $\mathbb{E}_t[\cdot] \equiv \mathbb{E}^{\mathbb{P}}[\cdot \mid H_t]$. The SDF can equivalently be written as $M_{t,T} = M_T / M_t$ for strictly positive $\{M_t\}$, with $M_0 = 1$.

Option prices will be of interest for inferring a distribution over the change in value of the market index from 0 to T (rather than consumption, for which options are not directly traded). We say that *return state* $\theta \in \Theta \subset \mathbb{R}_+$ is realized for the market as of date T if $R_T^m \equiv V_T^m / V_0^m = \theta$. The measure $\mathbb{P} : \mathcal{F} \to [0, 1]$ governs the *objective* or *physical* probabilities of these return states. In this general case, the *risk-neutral (RN) measure* is defined by the change of measure

$$\left.\frac{d\mathbb{P}^*}{d\mathbb{P}}\right|_{H_t} = \frac{M_{t,T}}{\mathbb{E}_t[M_{t,T}]} = \frac{M_T}{\mathbb{E}_t[M_T]}, \tag{11}$$

and expectations under $\mathbb{P}^*$ are denoted by $\mathbb{E}^*[\cdot]$.[12] Using this definition of $\mathbb{P}^*$, the RN probability of return state θ is

$$\mathbb{P}_t^*(R_T^m = \theta) = \frac{\mathbb{E}_t[M_T \mid R_T^m = \theta]}{\mathbb{E}_t[M_T]} \mathbb{P}_t(R_T^m = \theta). \tag{12}$$

The RN pricing equation $q_{t,K}^m = \mathbb{E}_t^*[(V_T^m - K)^+] / R_{t,T}^f$ can be used to show that the date-t option prices $\{q_{t,K}^m\}_{K \in \mathcal{K}}$ reveal the set of RN probabilities $\{\mathbb{P}_t^*(R_T^m = \theta)\}_{\theta \in \Theta}$. Assume that the set of return states Θ is ordered such that $\theta_1 < \theta_2 < \cdots < \theta_J$, and assume for notational simplicity that the set of traded option strikes $\mathcal{K}$ coincides with the set of possible date-T index values (i.e., $\mathcal{K} = \{K_j\}_{j=1}^J$, with $K_j = V_0^m \theta_j$). We can then back out RN probabilities from option prices as follows:

$$\mathbb{P}_t^*(R_T^m = \theta_j) = R_{t,T}^f \left[\frac{q_{t,K_{j+1}}^m - q_{t,K_j}^m}{K_{j+1} - K_j} - \frac{q_{t,K_j}^m - q_{t,K_{j-1}}^m}{K_j - K_{j-1}} \right]. \tag{13}$$

[11] We could consider continuous states with additional technicalities, but do not do so as empirical implementation requires discretization. We note as well that objects analogous to those in Section 2 are given the same denotation here.

[12] As $\text{Price}_t = \mathbb{E}_t[M_{t,T}\text{Payoff}_T]$ for any asset, we have $R_{t,T}^f = \mathbb{E}_t[M_{t,T}]^{-1}$, where $R_{t,T}^f$ is the gross risk-free rate from t to T, and $\text{Price}_t = \mathbb{E}_t^*[\text{Payoff}_T] / R_{t,T}^f$. Thus $\mathbb{P}^*$ incorporates the risk adjustment needed to discount T-payoffs at $R_{t,T}^f$. This $\mathbb{P}^*$ is sometimes referred to as the T-forward measure (e.g., Geman, El Karoui, and Rochet, 1995).

See Internet Appendix B.1 for a derivation of this result, which follows from a discrete-state application of the classic result of Breeden and Litzenberger (1978). As in Section 2.2, the above RN probabilities are a more convenient object of analysis than raw option prices.

Beliefs

Aside from assuming no arbitrage, we have not yet taken a stance on the market structure or subjective beliefs underlying prices and RN probabilities. We could in principle pursue a strict mapping from Section 2 to the current case, by assuming a setting in which all individual traders have common beliefs satisfying RE. The assumptions required to generate such an equilibrium are well studied in the literature on information and asset prices following Radner (1979) and Milgrom and Stokey (1982).[13] But rather than strictly focusing on the rationality of individual beliefs, we prefer an interpretation in which the "agent" in question is the market as a whole (or alternatively, the marginal trader); this interpretation requires no auxiliary assumptions, and our resultant tests are informative about the efficiency of market valuations.[14]

We therefore assume prices correspond to valuations for an agent ("the market") who, at the beginning of each period, observes a signal vector $s_t \in \mathcal{S}$ drawn from the distribution $DGP(s_t \mid \theta, H_{t-1}) = \mathbb{P}_{t-1}(s_t|\theta)$, where θ is the return state realized at T and $H_t = \sigma(s_\tau, 0 \leqslant \tau \leqslant t)$ is the Borel σ-algebra representing the history of signal realizations. The agent's subjective belief distribution over return states is denoted by $\Pi_{t,T} = \{\pi_t(R^m_T = \theta)\}_{\theta\in\Theta}$, where $\pi_t(R^m_T = \theta) \geqslant 0 \ \forall\theta \in \Theta$ and $\sum_{\theta\in\Theta} \pi_t(R^m_T = \theta) = 1$. More generally, for any random variable $Y(\omega)$, the agent attaches subjective probability $\pi_t(Y = y)$ to the outcome $Y = y$. We generalize Assumption 1 as:

ASSUMPTION 2 (*RE*)**.** For any random variable Y, beliefs satisfy $\pi_t(Y = y) = \mathbb{P}_t(Y = y)$ with probability 1 for all t.

This assumption again implies that beliefs satisfy $\pi_t(R^m_T = \theta) = \mathbb{E}[\pi_{t+1}(R^m_T = \theta) \mid \pi_t(R^m_T = \theta)]$ for all $\theta \in \Theta$. As in Section 2, this martingale condition for beliefs over returns is all that is required for our main results to carry through. The full-RE generalization stated in Assumption 2 is useful for streamlining some of the remaining discussion, as it further implies that *all* conditional expectations — including over the SDF — are martingales with respect to H_t.

Given Assumption 2, we can define the RN belief distribution without explicitly restricting the agent's utility or constraint set by applying the same change of measure as in (11). This yields the RN belief-distribution $\Pi^*_{t,T} = \{\pi^*_t(R^m_T = \theta)\}_{\theta\in\Theta}$ such that $\pi^*_t(R^m_T = \theta) = \frac{\mathbb{E}_t[M_T \mid R^m_T=\theta]}{\mathbb{E}_t[M_T]}\,\pi_t(R^m_T = \theta)$ as in (12), and thus (13) tells us that option prices reveal the agent's RN beliefs as given here.

[13] Complete markets and a common-prior assumption, for example, are sufficient: prices in general reveal information (including private signals) in a rational expectations equilibrium, giving common posteriors. Results under alternative conditions have also been studied extensively (to take one example, see Blume, Coury, and Easley, 2006).

[14] Belief heterogeneity, for example, is one plausible channel underlying our results, at least in part.

Localization: Conditional Beliefs, SDF Ratio, and Excess Movement

To align with the analysis in Section 2, we consider the behavior of *conditional* RN beliefs over adjacent pairs of return states. That is, rather than directly considering the full distribution $\Pi^*_{t,T}$, we instead consider restrictions on the behavior of the individual entries in $\{\widetilde{\pi}^*_{t,j}\}_{j=1}^{J-1}$, defined by

$$\widetilde{\pi}^*_{t,j} \equiv \pi^*_t(R^m_T = \theta_j \mid R^m_T \in \{\theta_j, \theta_{j+1}\}) = \frac{\pi^*_t(R^m_T = \theta_j)}{\pi^*_t(R^m_T = \theta_j) + \pi^*_t(R^m_T = \theta_{j+1})},$$

for $\pi^*_t(R^m_T = \theta_j) + \pi^*_t(R^m_T = \theta_{j+1}) > 0$. In words, $\widetilde{\pi}^*_{t,j}$ is the RN belief that return state θ_j will be realized, conditional on either θ_j or θ_{j+1}. This binary localization will be useful for two reasons: (i) it will allow us to apply results from the two-state setting of Section 2, and (ii) the main identifying assumption used to derive our tests is less restrictive than it would be without such a transformation (as discussed in Section 4.1 below). Conditional physical beliefs $\widetilde{\pi}_{t,j}$ are defined analogously, and the expectation under the conditional physical measure $\widetilde{\mathbb{P}}_t$ is $\widetilde{\mathbb{E}}_t[\,\cdot\,] \equiv \mathbb{E}_t[\,\cdot \mid R^m_T \in \{\theta_j, \theta_{j+1}\}]$.

In this context, the analogue to ϕ as defined in Section 2 is

$$\phi_{t,j} \equiv \frac{\mathbb{E}_t[M_T \mid R^m_T = \theta_j]}{\mathbb{E}_t[M_T \mid R^m_T = \theta_{j+1}]}, \tag{14}$$

which encodes the slope of the SDF across the adjacent return states θ_j, θ_{j+1}. In a representative-agent economy with SDF $M_{t,T} = \beta^{T-t}\frac{U'(C_T)}{U'(C_t)}$, the above definition implies $\phi_{t,j} = \frac{\mathbb{E}_t[U'(C_T) \mid R^m_T = \theta_j]}{\mathbb{E}_t[U'(C_T) \mid R^m_T = \theta_{j+1}]}$, akin to (6). But (14) is general and does not require a representative-agent structure (though we make periodic reference to such an economy for interpretation). This SDF slope can also be thought of loosely as the local price of risk around index return state θ_j.

Using this definition of $\phi_{t,j}$, RN beliefs satisfy $\frac{\widetilde{\pi}^*_{t,j}}{1-\widetilde{\pi}^*_{t,j}} = \phi_{t,j}\frac{\widetilde{\pi}_{t,j}}{1-\widetilde{\pi}_{t,j}}$ and thus $\widetilde{\pi}^*_{t,j} = \frac{\phi_{t,j}\widetilde{\pi}_{t,j}}{1+(\phi_{t,j}-1)\widetilde{\pi}_{t,j}}$, as in (5). Given a resolving RN belief stream $\boldsymbol{\pi}^*_j = [\widetilde{\pi}^*_{0,j}, \ldots, \widetilde{\pi}^*_{T,j}]$, RN belief movement m^*_j, RN initial uncertainty $\mathsf{u}^*_{0,j}$, and RN excess movement X^*_j are as defined in (1)–(3), with $\widetilde{\pi}^*_{t,j}$ in place of π_t. We often suppress the dependence on j (writing, e.g., X^*) when considering an arbitrary state pair.

3.2 Identifying Assumptions on ϕ

The analysis in Section 2 considered Arrow-Debreu claims on primitive states (in that case, consumption states). This section's analysis instead considers claims on index-return states, with an eye toward empirical implementation. We must thus confront the joint hypothesis problem. The additional identifying assumptions to be tested jointly with Assumption 2 take the form of two restrictions on $\phi_{t,j}$. We introduce these assumptions here, and we discuss them in much greater detail in the following sections after presenting our main results below.

We first impose an ordering assumption on the states. Return state θ_j here corresponds to state 1 in Section 2 (vs. state 0 for θ_{j+1}). We thus maintain the convention of labeling θ_j as the "bad" state, so that $\phi_{t,j} \geqslant 1$. While this is an innocuous labeling convention in theory, empirical implementation

requires taking a stand on how to distinguish θ_j from θ_{j+1}. We make the intuitive assumption that the bad state θ_j corresponds to the lower return:

Assumption 3 (*Positive Risk Aversion in Index Return*)**.** $\phi_{t,j} \geqslant 1$ with probability 1 for all t, j, where the set of return states Θ is ordered such that $\theta_1 < \theta_2 < \cdots < \theta_J$.

We discuss the empirical plausibility of this assumption, and how our results can be modified if it is violated (as might be a concern given the so-called pricing kernel puzzle), in Section 5.

Second, and more substantively, we must impose an assumption on the evolution of the unobserved parameter $\phi_{t,j}$. In Section 2's setting, ϕ is naturally constant over t: the terminal states index consumption and thus marginal utility, so the marginal rate of substitution across these primitive states is fixed. For our main analysis, we impose an analogous assumption on $\phi_{t,j}$:

Assumption 4 (*Constant SDF Ratio*, or *Conditional Transition Independence*)**.** We say the SDF satisfies *conditional transition independence (CTI)* for return-state pair (θ_j, θ_{j+1}) if $\phi_{t,j}$ is constant with probability 1 for all t. We assume CTI is satisfied for all *interior* state pairs, $j = 2, 3, \ldots, J-2$, and we write $\phi_{t,j} = \phi_j$ for these states.

This assumption imposes that the *relative* expected "severity" of the adjacent return states is constant over a contract, so that the expected SDF (or marginal utility) realization in the low return state θ_j is a constant multiple of that of θ_{j+1}. This is akin to assuming a constant local price of risk, as discussed further in the following section. It corresponds to a notion of transition or path independence because it implies that the expected relative SDF realizations depend only on the return state pair and not on the path of variables realized between t and T.[15] Note that we exclude the extreme state pairs (θ_1, θ_2) and (θ_{J-1}, θ_J) from the constant-ϕ requirement: thinking of θ_1 and θ_J as tail return states, we are allowing for time-varying disaster (or positive jump) risk.

As discussed below in Section 4, this assumption is weaker than the joint assumptions imposed in past volatility tests, and we view it as a reasonable starting point for our analysis. But it is unlikely to hold perfectly in reality, so that section also provides results characterizing RN excess movement when the assumption is violated.

3.3 Main Results in the General Setting

Having completed the formal setup and description of our main assumptions, we turn now to our main results in this more general asset-pricing setting. The bulk of the work in this case is, it turns out, in the setup and notation, as all our main results apply with appropriate relabeling.

Proposition 5. *Under no arbitrage and Assumptions 2–4, for $j = 2, 3, \ldots, J-2$, Lemma 1, Propositions 1–4, and Corollaries 1–2 continue to hold, with $\widetilde{\pi}^*_{t,j}$ replacing π^*_t, $\widetilde{\pi}_{t,j}$ replacing π_t, X^*_j replacing X^*, ϕ_j replacing ϕ, $\widetilde{\mathbb{E}}_0[\cdot]$ replacing $\mathbb{E}[\cdot]$, and with $\triangle_j \equiv \widetilde{\mathbb{E}}_0[X^*_j \mid R^m_T = \theta_{j+1}] - \widetilde{\mathbb{E}}_0[X^*_j \mid R^m_T = \theta_j]$ replacing $\triangle$.*

[15] This is formalized in Lemma A.3 in Appendix A.2.

The main theoretical complication in applying the results in Section 2 to this setting is in proving that $\widetilde{\mathbb{E}}^*[X_j^* \mid R_T^m = \theta_j] = \widetilde{\mathbb{E}}[X_j^* \mid R_T^m = \theta_j]$. The economic intuition for these results is largely identical to the intuition discussed in Section 2. And while the results above are convenient to express in terms of the SDF slope ϕ_j given that this allows for closed-form solutions that can be applied regardless of the origin of the SDF, the results also admit an interpretation in terms of the approximate required risk aversion for a fictitious representative agent who consumes the market index (analogous to (7)). To avoid repetition, for the remaining results we will continue to assume no arbitrage and that Assumptions 2–4 hold for $j = 2, 3, \ldots, J-2$, unless stated otherwise.

PROPOSITION 6. *Assume additionally that there is a representative agent with (indirect) utility over time-T wealth, with wealth equal to the market index value, and denote $V_j^m \equiv V_0^m \theta_j$. Then local relative risk aversion $\gamma_j \equiv -V_j^m U''(V_j^m)/U'(V_j^m)$ is given to a first order around return state θ_j by*

$$\gamma_j = \frac{\phi_j - 1}{(V_{j+1}^m - V_j^m)/V_j^m}.$$

This result formalizes the sense in which ϕ_j reflects the local price of risk, as it corresponds to the market's effective relative risk aversion in a neighborhood around return θ_j. As in Section 2, γ_j is proportional to $\phi_j - 1$, as this gives the percent decrease in marginal utility in moving from low-return state θ_j to high-return state θ_{j+1}. To calculate relative risk aversion, this change in marginal utility must be normalized by the percent wealth increase $(V_{j+1}^m - V_j^m)/V_j^m$ in moving from θ_j to θ_{j+1}, which is also equal to the percent return deviation $(\theta_{j+1} - \theta_j)/\theta_j$ between the two states. If, for example, $\theta_j = 1$, $\theta_{j+1} = 1.05$, then a value $\phi_j = 1.5$ implies $\gamma_j = 10$.

4. Interpreting and Relaxing the CTI Assumption

The analysis thus far has proceeded under the joint null implied by Assumptions 2–4. We now discuss these assumptions in more detail. What do they entail specifically? If the joint null is rejected in the data, how informative is such a rejection, and how should it be interpreted? We begin by considering CTI, which we consider the most important assumption imposed alongside RE. We first discuss settings in which it does (and doesn't) hold, and how it relates to assumptions imposed in past work. We then provide a set of robustness results when the assumption is relaxed, before turning to the other assumptions in the following section.

4.1 CTI Generates an Informative Test

We note first that the constant-ϕ assumption is significantly weaker than the assumption of constant discount rates. Our framework allows for any variation in the physical distribution of R_T^m, which can be thought of as changes in the *quantity* of risk. Further, by considering RN beliefs implied by options, we allow arbitrary variation in risk-free discount rates (since risk-free discounting affects all option prices proportionally). Both sources of variation are ruled out in tests with constant

discount rates. We formalize these statements and discuss the relationship between RN beliefs and discount rates further in Internet Appendix C.2.

That said, the assumption of constant ϕ is substantively restrictive in one way: the price of risk is assumed to be locally constant over the life of a given option contract. We are assuming, for example, that the market's effective risk aversion over whether the return will be 0% or 5% is fixed over a span of weeks or months. Thus a violation of our bounds can be interpreted as reflecting either excessive volatility in the marginal investor's beliefs, or variation in this local price of risk. Assuming a constant local price of risk, though, does not require that the *aggregate* price of risk is constant. For example, if risk aversion is decreasing with R_T^m, then bad news about the return distribution can increase aggregate risk aversion without affecting *local* risk aversion in a neighborhood of a 0% return.

More generally, CTI is satisfied in a range of theoretical settings, with a few notable exceptions. We make this point not to assert that CTI must hold in reality, but instead to demonstrate that a violation of our bounds is informative in ruling out a range of well-studied frameworks:[16]

1. Any shocks that affect the expectation of M_T proportionally in all return states (e.g., multiplying $\mathbb{E}_t[M_T \mid R_T^m = \theta_j]$ by 1.2 for all j) are trivially ruled in by the definition of CTI. For example, if a shock to M_t is permanent in the sense that it increases the expectation of M_T proportionally in all return states, then such a shock is admissible. As Alvarez and Jermann (2005) show, permanent shocks appear to be important empirically for SDF variation.[17]

2. If a representative agent's utility depends only on the maturity value of the market index, then CTI holds. Similarly, if there is *some* agent whose indirect utility can be written as a function only of the terminal index value — for example, an unconstrained investor with horizon T (i.e., Utility $= f(\text{Wealth}_T)$) who is fully invested in the market — then CTI holds. This encompasses a setting in which an unconstrained log investor holds the market, which is the leading case considered by Martin (2017) for measuring the equity premium, and by Gandhi, Gormsen, and Lazarus (2023) for studying the term structure of return expectations.

3. In the variable rare disasters model of Gabaix (2012), CTI holds for all market return-state pairs (θ_j, θ_{j+1}) for which there is negligible probability of having realized a disaster conditional on reaching θ_j.[18] This illustrates the usefulness of the localization provided by considering conditional beliefs: if we are concerned that time-varying disaster risk may affect $\phi_{t,j}$ for states in the tail of the return distribution, we can ignore these states and confine attention to the center of the return distribution, where $\phi_{t,j}$ can be expected to be approximately constant.

4. If a representative agent has Epstein–Zin (1989) recursive utility and holds the market, then CTI holds if any of the following apply: (i) relative risk aversion is $\gamma = 1$, and the elasticity of

[16] Derivations for statements 3–6 are in Internet Appendix B.2; statements 1–2 are immediate.

[17] Meanwhile, Borovička, Hansen, and Scheinkman (2016) show that permanent SDF shocks are ruled out in the framework proposed by Ross (2015) for recovering physical probabilities from state prices.

[18] Formally, for any δ, there exists a $\underline{\theta}$ such that $\forall\, \theta_j \geqslant \underline{\theta}$, $\mathbb{P}_0\big(\sum_{t=1}^{T} \mathbb{1}\{\text{disaster}_t\} > 0 \,\big|\, R_T^m \geqslant \underline{\theta}\big) < \delta$, so the conditional probability of having realized a disaster before T is negligible. For all $\theta_j \geqslant \underline{\theta}$, CTI holds for the state pair (θ_j, θ_{j+1}) up to a negligible error, as $\phi_{t,j} = \phi_j + \eta_t$ for ϕ_j constant and $\eta_t = o_p(1)$ as $\delta \to 0$. Again see Internet Appendix B.2 for detail.

intertemporal substitution (EIS) ψ and DGP are arbitrary; (ii) γ is arbitrary, the EIS is $\psi = 1$, and log consumption growth follows an AR(1) process; or (iii) γ and ψ are arbitrary, and consumption growth is i.i.d. (a less interesting case). As Martin (2017, Example 4b) notes, case (i) is "considered (and not rejected) by Epstein and Zin (1991) and Hansen and Jagannathan (1991)." Case (ii) is an approximation to the Bansal and Yaron (2004) long-run risks model, with $\psi = 1$ and common shocks to current and expected future consumption (as in Bansal and Yaron, 2000). While $\psi = 1$ often allows for a reasonable approximation to the full model with $\psi \neq 1$ (Dew-Becker and Giglio, 2016), the approximation degrades given highly persistent growth or volatility processes, and CTI will not hold in this case. Finally, case (iii) is considered by Martin (2013).

These examples illustrate further that the assumption of CTI is significantly weaker than the assumption of constant discount rates. This should again not be taken as evidence *in favor* of CTI in fact holding; instead, it allows for an informative joint test whose null includes a range of models that have been advanced as rationalizations of the excess-volatility puzzle.

That said, there are also well-known models under which CTI does *not* hold. Such models are also useful for illustrating the content of the assumption:

5. In the habit-formation model of Campbell and Cochrane (1999), CTI fails to hold: the path of consumption matters in a manner not fully accounted for by conditioning on the return state.
6. In the Basak (2000) model with heterogeneous beliefs and extraneous (non-fundamental) risk, CTI fails to hold as long as extraneous risk is priced.

Habit-like models, in other words, feature a time-varying local price of risk. We view the fact that CTI rules out these models to be a downside of the current framework, which we address below by means of robustness results and simulations. The fact that we rule out models of belief volatility induced by dynamic belief heterogeneity, though, is by design: if ϕ is time-varying due to changing weights being assigned to different individual agents — and therefore the as-if representative agent has excessively volatile beliefs — then this represents a meaningful alternative to our null.

4.2 Relaxing CTI Theoretically

While CTI allows for an informative null in our main analysis, it is also a knife-edge restriction that is unlikely to hold exactly. We thus now investigate how such a violation affects RN excess movement. One might worry that even small fluctuations in ϕ could generate dramatic violations of our bounds. For example, suppose that π_t is constant at 0.5 and ϕ_t changes back and forth from 1 to 1.5 repeatedly. Without any movement in physical beliefs, π_t^* will vary repeatedly between 0.5 and 0.6, leading to unbounded movement as $T \to \infty$. But this argument overlooks a core insight: this repeated oscillation is *also* inconsistent with RE as long as the variance of ϕ_t is bounded, because it implies predictable mean reversion in the expected marginal value of \$1. That is, the fact that ϕ_t is itself a function of martingale conditional expectations restricts its evolution under RE. We pursue this logic more formally here and in the following subsection.

Dropping the constant-ϕ_t assumption comes at the cost of much of the parsimony in our

previous analysis: SDF expectations non-linearly map to ϕ_t, which then non-linearly combines with π_t to determine π_t^*, which is then non-linearly mapped into X. Perhaps surprisingly, though, we can still make theoretical statements for a meaningful subset of DGPs. Consider ϕ_t as defined in (14) (continuing to suppress j subscripts). The agent now also receives signals $s_{\phi_t} \in \mathcal{S}_{\phi_t}$ to learn about ϕ_t over time. For simplicity, assume that uncertainty over ϕ_t evolves on a binomial tree ($|S_{\phi_t}| = 2$), though this is not necessary for the following statements. We also assume that π_t and ϕ_t do not change (relative to their $t-1$ values) together in the same period.[19] Then the following holds.

PROPOSITION 7. *If ϕ_t evolves as a martingale or supermartingale ($\mathbb{E}_t[\phi_{t+1}] \leqslant \phi_t$) and $Var(\phi_t) < \infty$, then the bounds in Proposition 2 and Corollary 1 (and their counterparts in Proposition 5) continue to apply, with ϕ_0 replacing ϕ.*

The proof of Proposition 7 demonstrates that the variation in π_0^* arising when ϕ_t is a non-degenerate (super)martingale always *strictly lowers* excess RN belief movement, rendering the main bound in (10) even more conservative. Changes in ϕ_t do cause π_t^* to change, which adds movement. But when ϕ_t is a supermartingale, this movement works *against* the upward bias in RN beliefs themselves and decreasing $\pi_t^* - \pi_t$ in expectation. This reduces potential *future* excess movement more than enough to offset the increase in period t.

As for the interpretation of the supermartingale restriction, from the definition of covariance, $\phi_{t,j}$ is a supermartingale if and only if $\text{Cov}_t(\phi_{t+1,j}, \mathbb{E}_t[M_T \mid R_T^m = \theta_{j+1}]) \geqslant 0$. Interpreting the SDF M_T as proportional to $U'(C_T)$, this requires that risk aversion (encoded in $\phi_{t+1,j}$) be positively correlated with expected marginal utility (MU) in the high-consumption state. This is an intuitively reasonable restriction, as it implies bad news (higher expected MU) generally arrives at the same time for both states, with the expected low-consumption MU increasing more than its high-consumption counterpart.[20] The converse ($\text{Cov}_t(\phi_{t+1,j}, \mathbb{E}_t[M_{t,T} \mid R_T^m = \theta_{j+1}]) < 0$), by contrast, requires risk aversion to increase in general in response to *good* news about MU in the good state.

4.3 Relaxing CTI in Numerical Simulations

Given the complexity of the setting, it is difficult to make analytical statements when the local price of risk ϕ_t does not satisfy the assumptions of Proposition 7. Instead, we numerically simulate DGPs in which ϕ_t can vary with more freedom. The agent learns about the terminal state, and the SDF realization in both the j and $j+1$ states, over time, under binary DGPs with different combinations of signal strengths and uncertainty for all three objects. We describe the setting more fully in Internet Appendix C.3, and we outline the results of these simulations here.

Figure 4 plots distributions for the estimated $\mathbb{E}[\mathsf{m}^*]$ (rather than $\mathbb{E}[X^*]$, as $\mathbb{E}[\mathsf{m}^*]$ is what changes with the DGP here) across these simulations. Each DGP is simulated repeatedly to obtain an estimated $\mathbb{E}[\mathsf{m}^*]$ for that DGP. Each line represents a different $\mathbb{E}[\mathsf{m}^*]$ distribution given variation

[19] In a previous version of this manuscript (Augenblick and Lazarus, 2022), we prove the result for arbitrary $|S_{\phi_t}|$. For the second assumption, one can split each period into two sub-periods, with ϕ_t changing in the first half and π_t in the second. The proof becomes intractable without this assumption, but we provide simulation evidence relaxing it below.

[20] For further discussion of such a restriction in a different context, see Lazarus (2022).

Figure 4: RN Belief Movement Distributions with Time-Varying ϕ_t

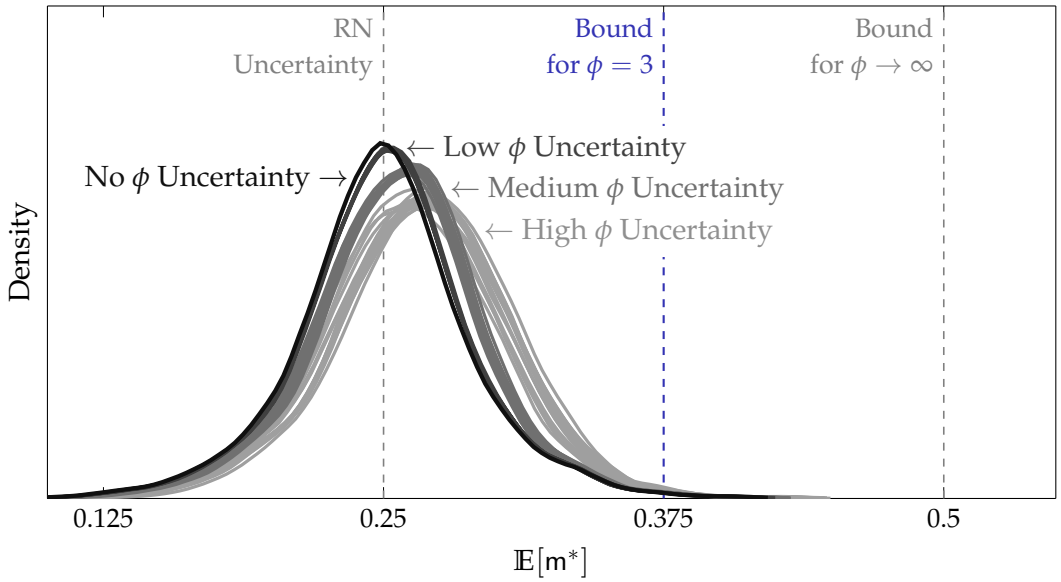

Notes: This figure shows the results of simulations studying the impact of time-varying ϕ_t on the distribution of $\mathbb{E}[m^*]$ given different DGPs with possibly asymmetric signal strengths about θ and ϕ_T over time. The dark black line ("No ϕ Uncertainty") shows the distribution when there is no uncertainty about ϕ. Each line in the slightly lighter dark gray set ("Low ϕ Uncertainty") represents the equivalent distribution for a DGP that also contains uncertainty about the SDF in both states. In this case, $\phi_0 = 3$, but ϕ_T can vary from 2.14 to 4.2. The set of gray lines ("Medium ϕ Uncertainty") allow ϕ_T to vary from 1.5 to 6, and the set of light-colored lines ("High ϕ Uncertainty") allow ϕ_T to vary from 1 to 9.

in the signal strengths for θ, with the different lines showing different signal strengths for learning about the conditional values of M_T (and thus ϕ). In all cases, $\pi_0^* = 0.5$ and $\phi_0 = 3$.

The black line ("No ϕ Uncertainty") shows a baseline with $\phi_t = \phi = 3$ for all t. As in Section 2.3, when signals are symmetric, $\mathbb{E}[m^*] = u_0^* = 0.25$, and very asymmetric DGPs produce the tails. Up to smoothing noise, $\mathbb{E}[m^*]$ never crosses the theoretical upper bound of 0.375 from (10). In the dark gray lines ("Low ϕ Uncertainty"), $\phi_0 = 3$ as before, but ϕ_t now varies such that the ex ante standard deviation of ϕ_T is $\sigma_\phi \equiv \text{SD}_0(\phi_T) = 0.36$. Using Proposition 6, if return states θ_j and θ_{j+1} differ by 5% (as in our empirical setting), this corresponds to relative risk aversion of $\gamma_0 = 40$ and standard deviation for γ_T of $\sigma_\gamma = 7.2$. Changing ϕ has virtually no effect regardless of the signal structure: average $\mathbb{E}[m^*]$ rises by 0.0012, and the number of DGPs for which $\mathbb{E}[m^*]$ exceeds the bound rises by just 0.00007 percentage points (pp). In the medium gray lines ("Medium ϕ Uncertainty"), $\sigma_\phi = 1.62$ (or $\sigma_\gamma = 32.4$). Even with such sizable variation, average $\mathbb{E}[m^*]$ rises by 0.006, and DGPs above the bound by 0.0003 pp. In the light gray lines ("High ϕ Uncertainty"), $\sigma_\phi = 3.0$ ($\sigma_\gamma = 60$). Average $\mathbb{E}[m^*]$ still only increases by 0.015, and DGPs above the bound by 0.0012 pp. In all cases, the bound in Corollary 1 for $\phi \to \infty$ holds for 100 percent of the simulations.

We conclude, somewhat surprisingly, that even significant uncertainty in the local price of risk ϕ_T has limited impact on our bounds in these DGPs. When the agent updates her SDF expectations, these updates must still respect RE. Thus even large values for σ_ϕ do not allow for arbitrary oscillations of ϕ_t, as information about ϕ_T is revealed gradually over time. While there may exist

DGPs in which time-varying ϕ_t generates large effects in an otherwise standard rational setting, we suspect given our results that they would require rather perverse time-varying structures. Instead, for variation in the price of risk to explain our results, such variation is likely to require departures from RE for expected terminal marginal utility.

Finally, to test the effects of variation in ϕ_t in a less abstract environment, we proceed to solve and simulate the Campbell and Cochrane (1999) habit formation model using that paper's baseline calibration. We find in this case that for the interior state pairs, ϕ_t is closely approximated by a martingale and therefore does not generate additional $\mathbb{E}[X^*]$. Our bounds thus continue to hold and continue to be conservative. See Internet Appendix C.4 for details.[21]

4.4 Aggregating Over Belief Streams

The previous subsection considers the effect of time variation in ϕ_j *within* a given RN belief stream (i.e., within a single option contract, lasting weeks or months). But even if the effects of such higher-frequency variation are small, it may be less palatable to assume that ϕ_j is constant *across* belief streams, given the possibility of lower-frequency variation over the span of years. We now ask how such variation affects our bounds when considering multiple belief streams.

Answering this question is also important for empirical implementation. The bounds in Proposition 5 are stated as date-0 expectations conditional on the RN prior, but we observe only one draw X_j^* per expiration date rather than the expectation of this statistic for a given $\widetilde{\pi}_{0,j}^*$. Estimation thus requires aggregating over multiple streams with different $\widetilde{\pi}_{0,j}^*$ and, as above, potentially different ϕ_j. Thus, generalizing slightly, assume now that we can observe index options for N expiration dates $\mathcal{T} \equiv \{T_i\}_{i=1}^N$, so i indexes belief streams (and their DGPs). We use $\phi_{i,j}$ for the SDF ratio for expiration date T_i and state pair (θ_j, θ_{j+1}); RN beliefs are $\widetilde{\pi}_{t,i,j}^*$; and RN excess movement is $X_{i,j}^*$. We again often suppress j for an arbitrary state pair. Due to Jensen's inequality, we cannot simply use $\mathbb{E}[\phi_i]$ in place of ϕ_i or $\mathbb{E}[\pi_{0,i}^*]$ in place of $\pi_{0,i}^*$ when taking the expectation of both sides of the results in Propositions 1, 2 and 5 over all i. However, the following generalizations do hold:

PROPOSITION 8. *Define* $\overline{\phi} \equiv \max_{\pi_{0,i}^*} \mathbb{E}[\phi_i \mid \pi_{0,i}^*]$. *We have:*

(i) GENERALIZATION OF PROPOSITION 1: *If* $\mathrm{Cov}(\pi_{0,i}, \triangle_i) = 0$, *and* $\pi_{0,i}^*$ *is constant across* i *(i.e., fixing a given* $\pi_{0,i}^*$*), then over all streams,*

$$\mathbb{E}[X_i^*] \leqslant \max\left\{0, \left(\pi_{0,i}^* - \frac{\pi_{0,i}^*}{\mathbb{E}[\phi_i] + (1 - \mathbb{E}[\phi_i])\pi_{0,i}^*}\right)\mathbb{E}[\triangle_i]\right\}. \tag{15}$$

(ii) GENERALIZATION OF PROPOSITION 2: *Over all streams, without any additional assumptions,*

$$\mathbb{E}[X_i^*] \leqslant \mathbb{E}\left[\left(\pi_{0,i}^* - \frac{\pi_{0,i}^*}{\overline{\phi} + (1 - \overline{\phi})\pi_{0,i}^*}\right)\pi_{0,i}^*\right], \tag{16}$$

[21] One might reasonably argue that the habit model is the wrong place to start when looking for plausible alternatives, as it is designed to match low-frequency variation. This is in fact the point of the exercise: it shows that to generate bounds violations, alternative models are needed to produce the high- and medium-frequency variation that we measure.

or, fixing a given $\pi^*_{0,i}$, $\mathbb{E}[X^*_i] \leqslant \left(\pi^*_{0,i} - \frac{\pi^*_{0,i}}{\mathbb{E}[\phi_i]+(1-\mathbb{E}[\phi_i])\pi^*_{0,i}}\right)\pi^*_{0,i}$.

(iii) GENERALIZATION OF COROLLARY 1: *Over all streams, without any additional assumptions,*

$$\mathbb{E}[X^*_i] \leqslant \mathbb{E}\left[\pi^{*\,2}_{0,i}\right].$$

(iv) GENERALIZATION OF COROLLARY 2: *If* $\triangle_i \leqslant 0$ *for all* i*, then over all streams,*

$$\mathbb{E}[X^*_i] \leqslant 0.$$

Only the analogue to Proposition 1 requires an additional assumption. The original formula includes the product of $\pi^*_0 - \pi_0$ and $\triangle$, so the covariance between $\pi_{0,i}$ and $\triangle_i$ across DGPs affects the generalized bound. For simplicity, we set this covariance to zero, which is equivalent to assuming no relationship between the asymmetry of the DGP and ϕ. This part also holds fixing $\pi^*_{0,i}$; this is sufficient for our purposes, as our empirical results for this less-conservative bound will generally be conditional on a given $\pi^*_{0,i}$.[22] Part (ii), meanwhile, generalizes (10) by applying Jensen's inequality for one of several variables, as the second partial derivative of that bound in $\phi_{i,j}$ is negative. The bound in (16) is thus even more conservative than the original bound for a single stream. The bounds that do not depend on $\phi_{i,j}$ (parts (iii)–(iv)) apply as previously stated.

These bounds are now empirically implementable, and the minimum $\overline{\phi}$ that solves (16) is a conservative estimate of the maximal conditional-mean SDF slope for the return-state pair in question. Finally, reintroducing dependence on the state pair j, it is likely that the values $\overline{\phi}_j$ vary over j. But the same steps used for Proposition 8 to take expectations over i can also be applied to take expectations over j, thereby obtaining a single estimate $\overline{\boldsymbol{\phi}}$ aggregated over both streams *and* return states (for all states meeting CTI) when desired.

5. Robustness to Additional Assumptions

Having considered Assumption 4 in detail, we turn to the other two assumptions to continue our discussion on how to interpret a rejection of the joint null. We consider Assumption 2 first, as the robustness result in this case will be a useful stepping stone in discussing Assumption 3. Finally, we provide a result accounting for possible mismeasurement or market microstructure noise.

5.1 RE and the Interpretation of Bound Violations

We have assumed throughout that Assumption 2 holds, which in general requires both (i) a correct subjective prior and (ii) rational updating using the true signal distribution as the likelihood. One natural question is whether an incorrect prior by itself can generate violations of the upper bound for X^*, or whether excessive movement in general requires incorrect updating. The following straightforward proposition makes clear that the latter is likely to be necessary for a bound violation.

[22] The constant-$\pi^*_{0,i}$ bounds can also be read as bounds for the conditional expectation $\mathbb{E}[X^*_i \mid \pi^*_{0,i}]$ given $\mathbb{E}[\phi_i \mid \pi^*_{0,i}]$.

We continue to adopt the notation from Section 2 for clarity, but the following should be understood to apply for conditional beliefs for some state j.[23] Assume that Assumptions 3–4 continue to hold.

PROPOSITION 9. *In place of Assumption 2, assume that the agent has an incorrect prior, $\pi_0 \neq \mathbb{P}_0(\theta)$, but updates correctly, in the sense that $\pi_t \propto \pi_{t-1} DGP(s_t \mid \theta, H_{t-1})$. Define $\check{\phi} \equiv \phi L$, where $L \equiv \frac{\pi_0/(1-\pi_0)}{\mathbb{P}_0(\theta)/(1-\mathbb{P}_0(\theta))}$ indexes the prior belief distortion, with $0 < L < \infty$. Then:*

(i) For all H_t, the agent's RN beliefs π_t^* are equivalent to the RN beliefs of a fictitious agent whose physical beliefs $\check{\pi}_t$ satisfy Assumption 2 but who has $\check{\phi}$ in place of ϕ.

(ii) If $\check{\phi} \geqslant 1$, then all previously stated restrictions on $\mathbb{E}[X^*]$ continue to hold, with $\check{\phi}$ in place of ϕ and $\check{\pi}_0$ in place of π_0. In particular, one cannot in this case have $\mathbb{E}[X^*] > \pi_0^{*2}$.

(iii) If $\check{\phi} < 1$ so that $\pi_0^* < \mathbb{P}_0(\theta) = \check{\pi}_0$, then the bound expressed in Proposition 2 becomes $\mathbb{E}[X^*] \leqslant (\check{\pi}_0 - \pi_0^*)(1 - \pi_0^*)$, and Corollary 1 becomes $\mathbb{E}[X^*] \leqslant (1 - \pi_0^*)^2$. Thus regardless of $\check{\phi}$, it must be the case that $\mathbb{E}[X^*] \leqslant \max(\pi_0^{*2}, (1 - \pi_0^*)^2)$.

Part (i) formalizes that risk aversion is isomorphic to an incorrect prior, in that both have the same effect on π_t^* relative to the objective $\mathbb{P}_t(\theta)$. Thus with a suitably altered value of ϕ, the bounds generally cover the case of an incorrect prior, as in part (ii). The only case in which this argument requires slight amendment is when the prior is so downwardly distorted that $\pi_0^* < \mathbb{P}_0(\theta)$. Even in this case, though, a slightly altered version of Corollary 1 still applies, as in part (iii). An incorrect prior acts as a one-time belief distortion; while reverting to the correct belief in this case does require some excess movement, this is generally not sufficient for a full violation of the bound in Proposition 2. In general, then, incorrect updating behavior must be present in such a violation.[24]

5.2 Robustness to $\phi < 1$

We now turn to Assumption 3, which imposes that $\phi_j \geqslant 1$ with return states ordered such that $\theta_j < \theta_{j+1}$. This requires that the expected SDF realization in the low-return state be greater than its expected realization in the high-return state. A line of work beginning with Jackwerth (2000) and Aït-Sahalia and Lo (2000), however, argues that the SDF does not decrease monotonically with the index return in options data. This finding, often referred to as the "pricing kernel puzzle," would imply a violation of Assumption 3 for at least some subset of the return space. How should our results be interpreted in light of this possibility?

Given such a violation, it turns out that one can still make theoretical statements providing an upper bound for RN excess movement. As shown in Proposition 9(i), assuming a different value for ϕ is formally equivalent to assuming a distortion in the agent's prior belief. The case with $\phi < 1$ is equivalent to a large downward distortion in the prior, as in part (iii) of that proposition. This equivalence leads to the following corollary, which holds under Assumptions 2 and 4.

[23] For example, the incorrect prior is $\tilde{\pi}_{0,j} \neq \mathbb{P}_0(R_T^m = \theta_j \mid R_T^m \in \{\theta_j, \theta_{j+1}\})$, and $L \equiv \frac{\tilde{\pi}_{0,j}/(1-\tilde{\pi}_{0,j})}{\tilde{\mathbb{P}}_0(R_T^m=\theta_j)/(1-\tilde{\mathbb{P}}_0(R_T^m=\theta_j))}$.

[24] Note that even if ϕ is constant under the agent's subjective belief, incorrect updating will induce a probability distortion such that the *actual* SDF (assessed under $\mathbb{P}$) will feature a time-varying ϕ_t.

COROLLARY 3. *If $\phi < 1$ rather than $\phi \geqslant 1$ in Assumption 3, then the bound from Proposition 2 becomes*

$$\mathbb{E}[X^*] \leqslant (\pi_0 - \pi_0^*)(1 - \pi_0^*) = \left(1 - \frac{1}{\phi^{-1} + (1 - \phi^{-1})(1 - \pi_0^*)}\right)(1 - \pi_0^*)^2,$$

and Corollary 1 becomes $\mathbb{E}[X^*] \leqslant (1 - \pi_0^*)^2$. For any ϕ, therefore, $\mathbb{E}[X^*] \leqslant \max(\pi_0^{*2}, (1 - \pi_0^*)^2)$.

The main bounds thus apply with minor modification, effectively flipping the role of the two states when $\phi < 1$. This entails replacing π_0^* with $1 - \pi_0^*$, and for Proposition 2, replacing ϕ with ϕ^{-1} as well. Thus it is *not* the case that anything goes when Assumption 3 is violated: excess movement is bounded no matter what, and its upper bound is a function of $\max(\phi, \phi^{-1})$, which in both cases indexes risk aversion across the two states. Bounds violations, meanwhile, retain their interpretation regardless of ϕ.

While Corollary 3 shows that one can still make statements about excess movement when $\phi < 1$, the bound in this case would have to be estimated separately from our main bounds derived for the $\phi \geqslant 1$ case. So for the sake of simplicity, we empirically estimate only the main bounds. We do so in part because we estimate the bounds separately for multiple points in the return space. Thus even if one is concerned about the pricing kernel puzzle affecting our results, one can confine empirical attention to our estimates for return ranges for which the puzzle does *not* emerge. For example, within this literature, it is a robust finding that the estimated SDF declines monotonically for the range of negative index returns; see, for example, Driessen, Koëter, and Wilms (2022, Figure 4) or Schreindorfer and Sichert (2022, p. 4). And as will be seen in Section 6, our empirical estimates for ϕ_j for these negative return states are just as high (in fact somewhat higher) than for positive return states, indicating that the results are unlikely to be driven by violations of Assumption 3.

5.3 Robustness to Measurement Error

The robustness results above speak to the possibility of theoretical misspecification. As the final step in making our bounds implementable, we now consider how to account for possible *empirical* misspecification arising from mismeasurement or microstructure noise in RN beliefs. The bounds provide a minimum value of ϕ required to rationalize the observed variation in RN beliefs; if some of this variation is in fact arising due to noise, then we may overestimate this required ϕ. A simple correction can be applied to our bounds to account for this issue, as shown in the following result. Given that noise arises period-by-period, we first define one-period analogues for our statistics: denote RN movement between t and $t+1$ by $\mathsf{m}_{t,t+1}^* \equiv (\pi_t^* - \pi_{t+1}^*)^2$, RN uncertainty at t by $\mathsf{u}_t^* \equiv (1 - \pi_{t+1}^*)\pi_t^*$, and RN excess movement between t and $t+1$ as $X_{t,t+1}^* \equiv \mathsf{m}_{t,t+1}^* - (\mathsf{u}_t^* - \mathsf{u}_{t+1}^*)$. Similar to Augenblick and Rabin (2021, Section II.E), we then have the following:

PROPOSITION 10. *Assume that the observed $\widehat{\pi}_t^*$ is measured with error with respect to the true π_t^*:*

$$\widehat{\pi}_t^* = \pi_t^* + \epsilon_t, \tag{17}$$

where $\mathbb{E}[\epsilon_t] = 0$, $\mathbb{E}[\epsilon_t\, \epsilon_{t+1}] = 0$, and $\mathbb{E}[\epsilon_{t+k}\, \pi_{t+k'}^*] = 0$ for $k, k' \in \{0, 1\}$. Denoting the observed

one-period RN excess movement statistic by $\widehat{X}^*_{t,t+1}$*, its relation to the true value* $X^*_{t,t+1}$ *in expectation is*

$$\mathbb{E}\left[\widehat{X}^*_{t,t+1} - X^*_{t,t+1}\right] = 2\text{Var}(\epsilon_t).$$

We can thus subtract $2\text{Var}(\epsilon_{t,j})$ from each period's observed excess-movement statistic to obtain an unbiased true excess movement value, which can then be used in our bounds. If measurement error is positively correlated over time rather than uncorrelated, this will reduce the upward bias in measured X^*. We discuss estimation of $\text{Var}(\epsilon_t)$, and autocovariance statistics for ϵ_t, in Section 6.2.

6. Empirical Estimation and Results

Our theory leads to bounds on the variation in RN beliefs over the market index return, which we proceed now to measure in the data. We begin by describing how we map from theory to data and how we estimate microstructure noise; we then summarize the data before turning to our main results. We conclude with a discussion of the predictors of RN excess movement.

6.1 Data and Risk-Neutral Distribution

Data. Our main source for S&P 500 index options data is the OptionMetrics database, which provides end-of-day prices for European call and put options for all strike prices and option expiration dates traded on the Chicago Board Options Exchange (CBOE). The sample runs from January 1996 through December 2018.[25] We augment this data with intraday price quotes obtained directly from the CBOE for a subset of trading days in our sample, in order to account for market microstructure noise; this additional data is described further in Section 6.2.

We apply standard filters to remove outliers and options with poor trading liquidity from the OptionMetrics data, with details provided in Internet Appendix C.5.[26] Two aspects of this data cleaning bear mention here. First, while our bounds apply for belief streams of arbitrary length, we follow past literature (e.g., Christoffersen, Heston, and Jacobs, 2013; Martin, 2017) and consider options with maturity of at most one year. Second, after transforming the filtered prices to RN beliefs (described below), we keep only conditional RN belief observations $\widetilde{\pi}^*_{t,i,j}$ for which the non-conditional beliefs satisfy $\pi^*_t(R^m_{T_i} = \theta_j) + \pi^*_t(R^m_{T_i} = \theta_{j+1}) \geqslant 5\%$, as conditional beliefs are likely to be particularly susceptible to mismeasurement when the underlying beliefs are close to zero.

Empirical return space. For our baseline estimation, we define the return state space Θ in terms of log excess return intervals:

$$\Theta = R^f_{0_i,T_i} \exp\big\{(-\infty, -0.2], (-0.2, -0.15], (-0.15, -0.1], \ldots, (0.1, 0.15], (0.15, 0.2], (0.2, \infty)\big\},$$

[25] We use the same sample as in an earlier version of the paper (Augenblick and Lazarus, 2022), as it aligns with our intraday data for noise estimation. The 2018 cutoff precludes the volatility observed in 2020 from affecting our estimates.

[26] There are 12.4 million option prices in the raw data, and 4.3 million (for 5,537 trading dates and 991 expiration dates) after filtering. The bulk of the difference is attributable to our use of only out-of-the-money call and put strikes.

where $R^f_{0_i,T_i}$ is the gross risk-free rate from 0_i to T_i.[27] In words, return state 1 is realized if the log excess S&P return from 0_i to T_i is less than -0.2 $\approx$ -20%; state 2 is realized if the excess return is in the five-percentage-point bin between -0.2 and -0.15; and so on. Abusing notation slightly, we often refer to states by the right end of their associated excess-return bin: $\theta_1 = -0.2$, $\theta_2 = -0.15, \ldots, \theta_9 = 0.2$, $\theta_{10} = \infty$. The binary conditional beliefs to be used in our tests are $\widetilde{\pi}^*_{t,i,j} \equiv \pi^*_t(R^m_{T_i} = \theta_j \,|\, R^m_{T_i} \in \{\theta_j, \theta_{j+1}\})$, so $\widetilde{\pi}^*_{t,i,j}$ again corresponds to the probability that the low state j (e.g., $\theta_2 = -15\%$) will be realized, conditional on j or $j+1$ (in this case, conditional on an excess return between -20% and -10%). We again use the right end of the return bin for j in referencing statistics for pair (θ_j, θ_{j+1}), corresponding to the midpoint of the two return bins.

This five-percentage-point partition of the return space reflects a desire to balance (i) measurement accuracy for the RN beliefs and (ii) plausibility of our assumption of constant ϕ_j (CTI). Wider bins lead to greater measurement accuracy, but make it less likely that there are no changes in the expected SDF realization conditional on a given return state θ_j relative to θ_{j+1}. We report empirical estimates below for all adjacent state pairs for completeness, but as discussed after Assumption 4, it is unlikely that CTI is met for the extreme state pairs (θ_1 relative to θ_2, and $\theta_9 = \theta_{J-1}$ vs. $\theta_{10} = \theta_J$). Our focus is thus on the interior state pairs with low-return states $\theta_2, \ldots, \theta_8$; in particular, when we aggregate our state-by-state estimates of ϕ_j required to rationalize the data into a single average value $\overline{\boldsymbol{\phi}}$ across states, we use only these interior states.[28]

Risk-neutral beliefs. To extract a risk-neutral distribution over the return states in Θ from the observed option cross-sections, we use standard tools from the option-pricing literature. Our starting point is equation (13), which tells us how to map from option prices to RN beliefs. We use this to construct a smooth RN distribution for returns, largely following the technique proposed by Malz (2014); Appendix C.5 provides a detailed description. With the RN beliefs $\pi^*_{t,i,j}$ in hand, we can then calculate conditional beliefs straightforwardly as $\widetilde{\pi}^*_{t,i,j} = \pi^*_{t,i,j}/(\pi^*_{t,i,j} + \pi^*_{t,i,j+1})$. We then use the resulting conditional RN belief streams to calculate the excess movement statistics $X^*_{i,j}$ needed to implement our bounds. Our general results in Section 3 restrict the expectation of $X^*_{i,j}$ conditional on state θ_j or θ_{j+1} being realized — in particular, Propositions 5 and 8 give bounds for $\widetilde{\mathbb{E}}[X^*_{i,j}]$ — and we accordingly keep only observations for which $\widetilde{\pi}^*_{T_i,i,j} = 0$ or 1 ex post; for example, if the total excess return on the market over the life of option contract i is -14%, then we keep only $X^*_{i,2}$ (θ_2 ranges from -20% to -15% return, so $\widetilde{\pi}^*_{T_i,i,2} = 0$) and $X^*_{i,3}$ ($\widetilde{\pi}^*_{T_i,i,3} = 1$).

Simplifying notation. Having clarified how the relevant empirical objects ($\widetilde{\pi}^*_{t,i,j}$, $X^*_{i,j}$) depend on the contract i and state pair j, in what follows we generally drop the cumbersome use of i, j, and $\widetilde{\cdot}$, and again write π^*_t for $\widetilde{\pi}^*_{t,i,j}$, X^* for $X^*_{i,j}$, and so on. Similarly, we often drop the "conditional" qualifier when referring to conditional RN belief statistics.

[27] We use excess returns for convenience of interpretation. Following van Binsbergen, Diamond, and Grotteria (2022), we measure $R^f_{0_i,T_i}$ directly from the options prices by applying the put-call parity relationship; again see Appendix C.5.

[28] This yields an additional de facto data filter, as we are effectively considering only option strikes with moneyness between 0.8 and 1.2 (following, e.g., Constantinides, Jackwerth, and Savov, 2013).

6.2 Noise Estimation

As in Proposition 10, we also wish to account for measurement error stemming from possible non-fundamental or microstructure noise in risk-neutral beliefs. With noise described by $\widehat{\pi}_t^* = \pi_t^* + \epsilon_t$ as in (17), Proposition 10 tells us that we must estimate $\text{Var}(\epsilon_t)$ in order to eliminate the bias in X^* arising from any such non-fundamental noise. We turn to a sample of high-frequency option prices to estimate this noise variance in our RN beliefs data.

Specifically, we obtain minute-by-minute price quotes on S&P index options for a subset of trading days directly from the CBOE. For each available option expiration date on each such trading day, we recalculate the RN belief distribution at the end of each minute using exactly the same procedure as described in Section 6.1. As this requires calculating 390 sets of RN beliefs for each trading day (9:30 AM–4:00 PM), this procedure would be computationally infeasible if applied to our entire sample of 5,537 trading days (each of which has an average of 11 available option expiration dates, generating 60,543 (t, T) combinations). We accordingly select 30 trading days at random from within our available sample period, and use the minute-by-minute quotes to calculate intraday RN distributions for these days.[29]

We then use tools from the literature on microstructure noise to estimate $\text{Var}(\epsilon_t)$ using these intraday data. The intuition for this strategy — as described, for example, by Zhang, Mykland, and Aït-Sahalia (2005) — is best understood by assuming temporarily that the noise ϵ_t in (17) is i.i.d., while the true π_t^* changes smoothly over time. Given high-frequency option data, imagine calculating movement using the observed beliefs, $(\widehat{\pi}_{t+h}^* - \widehat{\pi}_t^*)^2$, with less and less time h between consecutive observations. As one decreases h to 0, the noise swamps the true variation: since $(\pi_{t+h}^* - \pi_t^*)^2 \to 0$, we have $\mathbb{E}[(\widehat{\pi}_{t+h}^* - \widehat{\pi}_t^*)^2] \to 2\text{Var}(\epsilon_t)$. Thus in this simple example, $\text{Var}(\epsilon_t)$ can be estimated by calculating the quadratic variation in RN beliefs sampled at a high frequency.

In practice, one would expect the data to contain both non-i.i.d. noise ϵ_t and jumps in the true process π_t^*, and it is desirable to use a noise estimation method that is robust to these features. One such estimator for $\text{Var}(\epsilon_t)$ is the ReMeDI ("Realized moMents of Disjoint Increments") estimator proposed by Li and Linton (2022). This estimator takes the average product of *disjoint increments* of the observed process, $(\widehat{\pi}_t^* - \widehat{\pi}_{t-h}^*)(\widehat{\pi}_t^* - \widehat{\pi}_{t+h}^*)$.[30] The idea is that even if the true process features jumps so that $\mathbb{E}[(\pi_{t+h}^* - \pi_t^*)^2] > 0$, its increments over non-overlapping windows are still approximately uncorrelated. Li and Linton (2022, Theorem 4.1) show that this estimator is consistent for $\text{Var}(\epsilon_t)$ for quite general dependent noise processes and for π_t^* in a general class of semimartingales. It also performs well in simulations and empirical applications.

Using this ReMeDI estimator on our minute-by-minute data, we estimate $\text{Var}(\epsilon_t) = \text{Var}(\epsilon_{t,i,j})$ separately for each combination of trading day t, expiration date T_i, and state pair j in our intraday sample. We then match the noise estimates (which are obtained for a subsample of days) to the

[29] This yields an intraday data set roughly twice as large as the original one, as $30 \times 390 \times 11 \approx 130{,}000$.

[30] More formally, the estimator is $\widehat{\text{Var}}(\epsilon_t) = \frac{1}{N_{\epsilon,n}} \sum_{i=2k_n}^{N_{\epsilon,n}-k_n} (\widehat{\pi}_{t_i}^* - \widehat{\pi}_{t_i-2k_n}^*)(\widehat{\pi}_{t_i}^* - \widehat{\pi}_{t_i+k_n}^*)$, where $N_{\epsilon,n}$ is the number of observations over a fixed span (in our case, one trading day) and k_n is a tuning parameter.

X^* observations in our original data.[31] Finally, we subtract $2\widehat{\text{Var}}(\epsilon_{t,i,j})$ from $\widehat{X}^*_{t,t+1,i,j}$ to obtain a *noise-adjusted* estimate of one-day excess movement following Proposition 10, and we sum these noise-adjusted one-day values over the full stream to obtain noise-adjusted $X^*_{i,j}$.

We discuss the magnitude of the noise estimates in the next subsection. The ReMeDI procedure also allows for estimation of the intraday autocovariances of the noise ϵ_t. These autocovariances are estimated to be positive for small lag values, but they die out quickly and are precisely estimated near zero for noise observations more than an hour apart. This justifies the assumption in Proposition 10 that end-of-day noise observations are uncorrelated, $\mathbb{E}[\epsilon_t \epsilon_{t+1}] = 0$, as ultimately we care about noise only to the extent that it affects our excess movement statistics at a daily frequency.

Our main results in Section 6.4 use the noise-adjusted excess movement data. All standard errors and confidence intervals are based on a bootstrap procedure (detailed in Section 6.4) that accounts for the sampling uncertainty in the above noise estimation and averaging procedure.

6.3 Excess Movement: Descriptive Statistics and Figures

Table 1 summarizes the average RN excess movement $\overline{X}^*$ overall (across all interior state pairs and expiration dates) and by subsample. Excess movement is difficult to interpret without some normalization. The first two columns thus divide $\overline{X}^*$ by average initial uncertainty $\bar{u}_0$. As in Augenblick and Rabin (2021), this normalized statistic can be interpreted as the percent by which movement exceeds initial uncertainty and thus uncertainty resolution. These values are quite high in our data: for the noise-adjusted statistics, there is on average 123% more movement than initial uncertainty. These values decrease for return states in the middle of the distribution. The early sample has high but noisy X^* statistics,[32] but these averages remain high until the most recent subsample. And higher priors π^*_0 correspond with greater X^*, in line with our bounds given $\phi \geqslant 1$.

The next two columns of Table 1 instead normalize $\overline{X}^*$ by the average contract length $\overline{T}$, so the resulting statistics can be interpreted as excess movement per day.[33] Under this normalization, there is now no clear pattern for average excess movement across bins: longer average contract lengths tend to coincide with more excess movement, as RN beliefs bounce up and down over the length of a contract. This is inconsistent with RE, under which excess movement in subjective beliefs should not depend at all on the horizon at which uncertainty is resolved. For the splits by date and by prior, the basic patterns discussed above are still present here.

Comparing the raw and noise-adjusted values makes clear that despite the substantial excess movement in the noise-adjusted statistics, noise does represent a meaningful portion (about 1/3) of the raw X^* data. The raw and noise-adjusted mean for $\overline{X}^*/\overline{T}$ differ by about 0.002, so $\widehat{\text{Var}}(\epsilon_t) \approx 0.002/2 = 0.001$. The standard deviation of ϵ_t is thus roughly 0.03 per day. For the return-state

[31] We match these observations using the two best predictors of $\widehat{\text{Var}}(\epsilon_t)$ in our data: the state pair j and the sum $\pi^*_t(R^m_T = \theta_j) + \pi^*_t(R^m_T = \theta_{j+1})$. Further explanation and technical details can be found in Internet Appendix C.6.

[32] Excess movement peaks in this subsample during the 1998 Russian debt crisis.

[33] For a rough idea of the actual variation in RN beliefs given these values, consider a pair $(t, t+1)$ for which $\pi^*_{t+1} = 1 - \pi^*_t$. One-day X^* and m^* then coincide (there is no uncertainty resolution), so, for example, the noise-adjusted mean of 0.0038 corresponds to a raw change of $\sqrt{0.0038} \approx 0.06$ (or $\pi^*_t = 0.47$, $\pi^*_{t+1} = 0.53$).

Table 1: Descriptive Statistics for Excess Movement

	$\overline{X}^*/\overline{u}_0$		$\overline{X}^*/\overline{T}$				
	Raw	Noise-Adj.	Raw	Noise-Adj.	$\overline{u}_0$	$\overline{T}$	N (Obs.)
Overall mean:	1.89	1.23	0.0059	0.0038	0.18	56	1,809
[Bootstrapped SE]	[0.25]	[0.22]	[0.0015]	[0.0013]	[0.00]	[2]	
By return state:							
1 (-20%)	5.83	4.83	0.0049	0.0041	0.17	200	26
	[1.18]	[1.05]	[0.0027]	[0.0024]	[0.01]	[20]	
2 (-15%)	11.61	5.70	0.0180	0.0088	0.22	141	19
	[3.32]	[3.06]	[0.0096]	[0.0083]	[0.01]	[25]	
3 (-10%)	5.76	2.37	0.0151	0.0062	0.21	81	49
	[0.99]	[1.07]	[0.0059]	[0.0051]	[0.01]	[12]	
4 (-5%)	2.67	1.39	0.0088	0.0046	0.14	42	272
	[0.59]	[0.50]	[0.0038]	[0.0029]	[0.01]	[5]	
5 (0%)	0.70	0.47	0.0045	0.0030	0.23	37	700
	[0.16]	[0.14]	[0.0019]	[0.0017]	[0.00]	[2]	
6 (+5%)	1.71	1.14	0.0039	0.0026	0.11	49	567
	[0.35]	[0.34]	[0.0015]	[0.0014]	[0.01]	[3]	
7 (+10%)	3.87	2.92	0.0053	0.0040	0.18	129	144
	[1.00]	[1.03]	[0.0023]	[0.0023]	[0.01]	[9]	
8 (+15%)	5.65	5.26	0.0060	0.0056	0.21	200	58
	[1.48]	[1.48]	[0.0027]	[0.0027]	[0.01]	[11]	
9 (+20%)	3.44	2.09	0.0032	0.0020	0.22	232	36
	[0.89]	[1.27]	[0.0015]	[0.0020]	[0.01]	[9]	
By date:							
1996–2000	10.89	9.67	0.0211	0.0187	0.21	107	109
	[2.24]	[2.17]	[0.0074]	[0.0072]	[0.01]	[11]	
2001–2005	1.75	0.55	0.0042	0.0013	0.22	90	112
	[0.51]	[0.40]	[0.0021]	[0.0015]	[0.01]	[11]	
2006–2010	1.25	0.68	0.0065	0.0035	0.17	32	502
	[0.22]	[0.19]	[0.0026]	[0.0021]	[0.00]	[4]	
2011–2015	1.75	1.09	0.0050	0.0031	0.19	67	530
	[0.36]	[0.28]	[0.0024]	[0.0019]	[0.00]	[5]	
2016–2018	0.36	-0.11	0.0011	-0.0003	0.16	50	556
	[0.21]	[0.14]	[0.0017]	[0.0009]	[0.00]	[3]	
By π_0^**:*							
0–0.25	1.01	0.30	0.0055	0.0017	0.09	16	185
	[0.60]	[0.55]	[0.0048]	[0.0047]	[0.01]	[2]	
0.25–0.5	1.58	0.91	0.0067	0.0039	0.23	55	883
	[0.21]	[0.17]	[0.0017]	[0.0014]	[0.00]	[3]	
0.5–0.75	2.84	2.19	0.0053	0.0041	0.23	123	284
	[0.61]	[0.58]	[0.0020]	[0.0019]	[0.00]	[7]	
0.75–1	2.54	1.88	0.0048	0.0036	0.06	31	457
	[0.95]	[0.90]	[0.0031]	[0.0029]	[0.00]	[2]	

Notes: Empirical conditional means of risk-neutral excess movement $\overline{X}^* \equiv \widehat{\mathbb{E}}[X^*_{i,j}]$ are calculated over all interior state pairs $j = 2, \ldots, 8$, aside from averages by bin, which are calculated for each state pair separately. Standard errors are estimated using a block bootstrap for the normalized statistic $\overline{X}^*/\overline{u}_0$ or $\overline{X}^*/\overline{T}$, with a block size of one month (where contracts are classified by the month in which they expire) and 10,000 draws.

splits, noise tends to be lowest for returns near the center of the distribution, as is intuitive.

Next, Figure 5 provides a visual summary of the X^* statistics relative to the bounds. The blue curves describe the raw and noise-adjusted local-average X^* statistics as one varies the RN prior π_0^*; these curves are the same in both panels. As one would expect, there is very little excess movement for RN priors near 0 or 1, but excess movement is positive for intermediate π_0^* values for which there is greater initial uncertainty. We compare these values to the theoretical bounds under different levels of ϕ for each value of π_0^*, as shown in gray. Panel (a) uses the tighter bound from Proposition 8(i), with $\triangle$ estimated using local averages for the conditional expectations $\mathbb{E}[X^* \mid \theta, \pi_0^*]$ in (9) over π_0^*.[34] Panel (b) uses the conservative bound from the second inequality in Proposition 8(ii), so the gray lines in this panel align with the solid bound lines in Figure 3.

Across the two panels, the X^* values observed in the data exceed both sets of bounds, other than for high RN priors π_0^* and for high ϕ. For panel (a), we estimate $\widehat{\triangle} = 0$ for $\pi_0^* \approx 0.5$, $\widehat{\triangle} < 0$ for π_0^* below this cutoff, and $\widehat{\triangle} > 0$ above it, as is evident from the bounds crossing zero at $\pi_0^* \approx 0.5$. As discussed in Section 2.3, this indicates that the DGP is close to symmetric, with equally informative signals for the two states (θ_j, θ_{j+1}) on average (and thus roughly equal-sized upward and downward movements of π_t^*). As the bounds in Proposition 8 apply for each possible π_0^*, the positive point estimates for $\mathbb{E}[X^* \mid \pi_0^*]$ clearly violate the bounds for $\pi_0^* < 0.5$, which are (at most) 0 for all ϕ. And while the empirical curves are closer to the more-conservative bounds in panel (b), the noise-adjusted estimates still exceed ${\pi_0^*}^2$ (the bound for $\phi = \infty$) for π_0^* less than about $2/3$.

These figures do not, however, integrate over π_0^*, nor do they include any measures of statistical uncertainty necessary to make inferential statements or conduct hypothesis tests. To address these issues, we move on to our main estimation and results.

6.4 Main Results

We turn now to the empirical implementation of our theoretical bounds. Given our sample of noise-adjusted excess movement statistics and corresponding RN priors, each possible value of $\overline{\phi}$ leads to a *residual* excess movement value $e_i(\overline{\phi}) = X_i^* - \text{bound}(\pi_{0,i}^*, \overline{\phi})$ for contract i. We calculate two versions of this residual corresponding to the bound in part (i) and the unconditional bound in part (ii) of Proposition 8 (equations (15) and (16), respectively):

$$\begin{aligned} e_i^{\triangle}(\overline{\phi}) &= X_i^* - \max\left\{0, \left(\pi_{0,i}^* - \frac{\pi_{0,i}^*}{\overline{\phi} + (1-\overline{\phi})\pi_{0,i}^*}\right)\widehat{\triangle}_i\right\}, \\ e_i^{\text{main}}(\overline{\phi}) &= X_i^* - \left(\pi_{0,i}^* - \frac{\pi_{0,i}^*}{\overline{\phi} + (1-\overline{\phi})\pi_{0,i}^*}\right)\pi_{0,i}^*. \end{aligned} \tag{18}$$

The first version corresponds to the tighter bound from Proposition 1, which requires a smoothed estimate of $\triangle_i$ as calculated for Figure 5. This version accounts for the estimated DGP (through $\widehat{\triangle}_i$) and thus conveys some useful preliminary information, but strictly speaking, part (i) of the

[34] To emphasize that $\widehat{\triangle} < 0$ for $\pi_0^* < 0.5$, the figure does not cut the bounds off at 0.

Figure 5: Excess Movement vs. RN Prior: Data and Theoretical Bounds

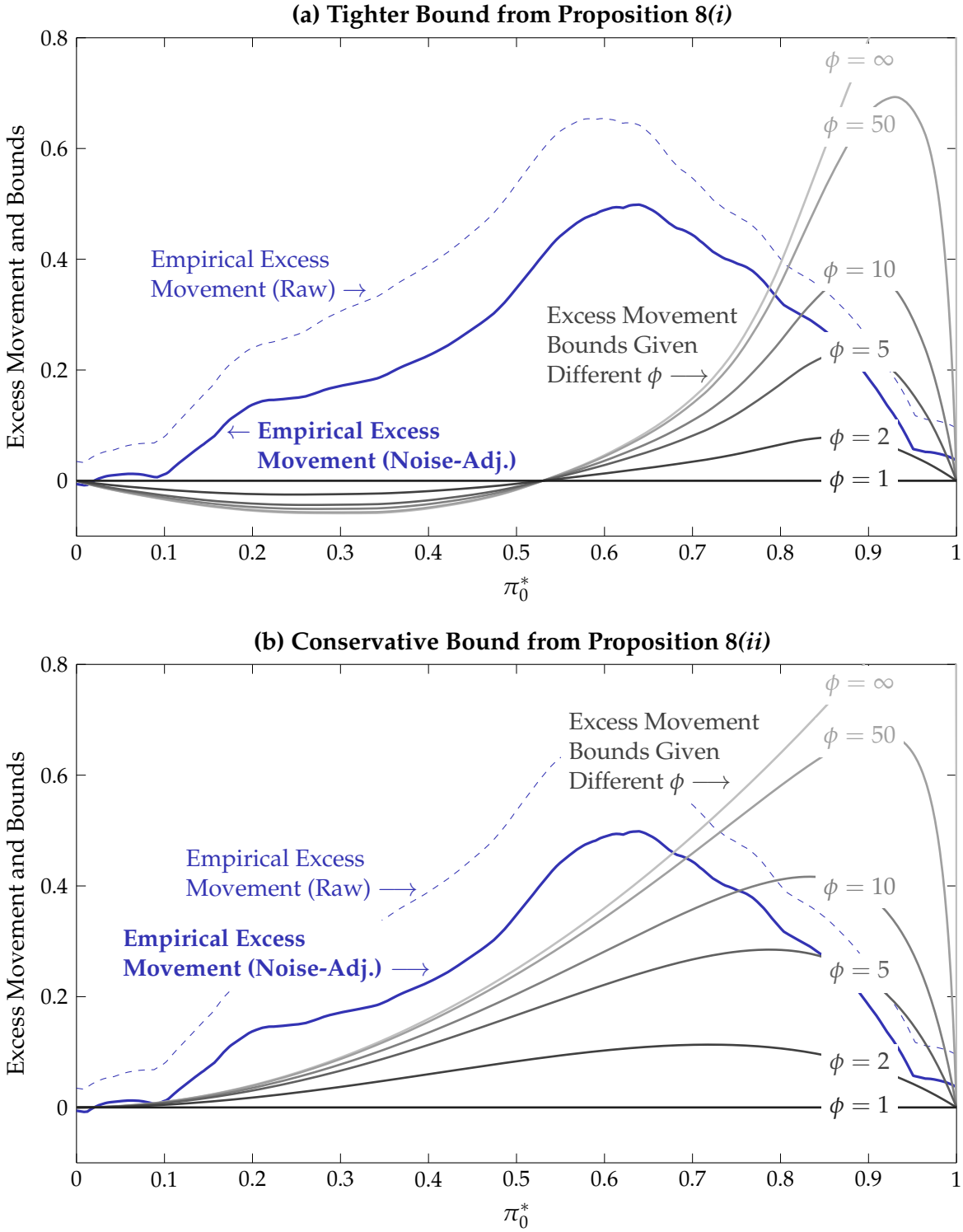

Notes: Empirical excess movement curves are kernel-weighted local averages (Epanechnikov kernel, bandwidth for π_0^* of 0.08) over all interior state pairs $j = 2, \ldots, 8$. All statistics are estimates of conditional means $\widetilde{\mathbb{E}}[\cdot]$ for RN beliefs $\widetilde{\pi}^*_{t,i,j}$, and theoretical curves correspond to $\phi \equiv \widetilde{\mathbb{E}}[\phi_{i,j}]$, with notation simplified for clarity. Bounds for (a) obtain $\widehat{\triangle}$ using a kernel-weighted local average over π_0^* for each of the two terms in (9), with $\widehat{\triangle}$ then plugged into the inequality in Proposition 8(i). Bounds for (b) use only the second inequality in Proposition 8(ii).

Table 2: Residual Excess Movement *t*-Statistics for Different $\overline{\phi}$

	(a) *Tighter Lower Bound from Proposition 8(i)*						(b) *Conservative Lower Bound from Proposition 8(ii)*					
$\overline{\phi}$:	1	2	5	10	50	∞	1	2	5	10	50	∞
Overall *t*-stat.:	5.19	5.15	4.98	4.64	3.03	0.78	5.19	4.08	2.68	1.75	0.07	-1.48
By return state:												
1 (-20%)	4.06	3.69	3.04	2.57	1.94	1.72	4.06	3.58	2.79	2.22	1.47	1.21
2 (-15%)	2.13	2.13	2.13	2.13	2.14	2.14	2.13	2.03	1.94	1.90	1.87	1.86
3 (-10%)	2.23	2.23	2.23	2.23	2.23	2.23	2.23	2.03	1.86	1.79	1.72	1.70
4 (-5%)	2.78	2.78	2.77	2.77	2.76	2.76	2.78	2.51	2.28	2.18	2.09	2.06
5 (0%)	3.09	3.09	3.08	3.08	3.06	3.06	3.09	1.86	0.74	0.26	-0.19	-0.31
6 (+5%)	3.26	2.66	1.27	0.04	-1.71	-2.42	3.26	1.96	-0.12	-1.77	-5.22	-8.39
7 (+10%)	2.82	2.73	2.51	2.29	1.70	1.23	2.82	2.38	1.73	1.28	0.50	0.06
8 (+15%)	3.53	3.49	3.42	3.37	3.29	3.25	3.53	3.20	2.77	2.51	2.21	2.10
9 (+20%)	1.63	1.58	1.52	1.48	1.44	1.43	1.63	1.36	1.05	0.89	0.72	0.68

Notes: This table shows *t*-statistics for the average residuals $\overline{e_i(\phi)}$ in (18) for different values of $\overline{\phi}$. The columns for (a) use $e_i^{\triangle}(\overline{\phi})$, with $\triangle_i$ estimated as in panel (a) of Figure 5. The columns for (b) use $e_i^{\text{main}}(\overline{\phi})$. Standard errors are estimated using a block bootstrap with block size of one month and 10,000 draws. All statistics are calculated using conditional means of noise-adjusted X^*.

proposition applies only conditional on a given $\pi^*_{0,i}$ and only under the unverifiable condition that $\text{Cov}(\pi_{0,i}, \triangle_i) = 0$. Thus the second version, which implements the more conservative bound from Proposition 2 and which applies unconditionally, is the basis for our main set of results. Both residuals can be directly calculated using our noise-adjusted data for each possible value of $\overline{\phi}$.

We first present sample averages of these residual statistics for a range of values of $\overline{\phi}$, both for each individual state pair j and aggregated over all interior states. As these values have no natural scaling, we present them as *t*-statistics, $t_{\bar{e}} = \overline{e_i(\phi)} / \widehat{SE}_{\bar{e}}$, where $\overline{e_i(\phi)}$ is the sample average of $e_i(\overline{\phi})$ and $\widehat{SE}_{\bar{e}}$ is its standard error. We calculate these standard errors using a block bootstrap with a block length of one month, with each block containing (i) raw excess movement statistics and priors for all contracts expiring in a given month, and (ii) noise variance estimates for any trading days in our intraday sample that fall in the same month. For each resampled data set, we use the set of $(X_i^*, \widetilde{\pi}^*_{0,i}, \{\widehat{\text{Var}}(\epsilon_{t,i})\})$ values to recalculate noise-adjusted excess movement and residual values $e_i(\overline{\phi})$.[35] The bootstrap accordingly accounts for sampling uncertainty in all statistics used to calculate noise-adjusted X_i^* and $e_i(\overline{\phi})$. We conduct 10,000 such draws, from which we calculate standard errors as the standard deviation of $\overline{e_i(\phi)}$ across draws.

These residual *t*-statistics are presented in Table 2 for the two versions of the residual in (18), both overall and by state pair. Since $\mathbb{E}[e_i(\overline{\phi})] = 0$ under RE given a correctly specified $\overline{\phi}$, these

[35] For the residual $e_i^{\triangle}(\overline{\phi})$ corresponding to the tighter bound, we also re-estimate $\widehat{\triangle}_i$ in each bootstrap draw by calculating the same local average (with respect to $\pi^*_{0,i}$) as in Figure 5(a), and then evaluating it at the observed $\pi^*_{0,i}$.

t-statistics tell us how far the residuals are from being consistent with any hypothesized null for the SDF slope. Positive numbers correspond to the data exhibiting too much excess movement to be consistent with a given value of $\overline{\phi}$. In the first six columns, the only negative t-statistics for the tighter bound are for RN beliefs over $(\theta_j, \theta_{j+1}) = ([0\%, 5\%], [5\%, 10\%])$ (i.e., $j = 6$) for $\overline{\phi} > 10$; all other t-statistics, including the overall values, are positive (and mostly large in magnitude), indicating no value of $\overline{\phi}$ is consistent with the degree of observed excess RN movement. In the remaining columns, the conservative bound t-statistics are somewhat smaller in magnitude but also generally positive, other than for large $\overline{\phi}$ and for returns in the middle of the distribution.

As admissible excess movement $\mathbb{E}[X_i^*]$ is monotonically increasing in the unobserved parameter $\overline{\phi}$, our main empirical exercise is to estimate the lower bound for this SDF slope such that the bound for $\mathbb{E}[X_i^*]$ is satisfied. This lower bound for $\overline{\phi}$ is estimated as the minimal value for which the average residual $\overline{e_i(\phi)}$ is zero, so that we are effectively finding the root of the function traced out in Table 2. Given that the tighter bound is generally not satisfied even for $\overline{\phi} = \infty$ (and since it holds only under restrictive assumptions), we now confine attention to the conservative bound from Proposition 8(ii). The estimated $\overline{\phi}$ is the minimal SDF slope for which the amount of observed excess movement in RN beliefs can be rationalized; it is thus an index of the restrictiveness of Assumptions 2–4 (or, given Proposition 7, Assumptions 2–3 and supermartingale ϕ_t). As above, we estimate this SDF slope both for each individual state pair ($\overline{\phi} = \overline{\phi}_j$) and overall ($\overline{\phi} = \overline{\boldsymbol{\phi}}$). To make the estimates for $\overline{\phi}$ more interpretable, we also use Proposition 6 to translate them into local relative risk aversion values $\overline{\gamma} = \frac{(\overline{\phi}-1)}{0.05} = 20(\overline{\phi} - 1)$ for a representative agent who consumes the market.

Table 3 presents our main results. Whenever there is *no* value of $\overline{\phi}$ for which the bound for $\mathbb{E}[X_i^*]$ is satisfied — i.e., from Proposition 8(iii), when we estimate $\mathbb{E}[X_i^*] > \mathbb{E}[{\pi_{0,i}^*}^2]$ — we write $\overline{\phi} = \infty$. In brackets below each point estimate, we provide the lower bound of a one-sided 95% confidence interval (CI) for the parameter in question.[36] Starting from the same bootstrap resampling procedure as described just above, we obtain these CIs by inverting a one-sided test. The CI lower bound $\widehat{\phi}_{LB}$ is the minimal $\overline{\phi}$ such that $\overline{e_i^{\text{main}}(\phi)} = 0$ is not rejected at the 5% level using the bootstrapped data (see Internet Appendix C.7 for further details).

Starting with the overall estimates in the first row, the point estimate for the conservative lower bound for $\overline{\boldsymbol{\phi}}$ is slightly greater than 50, in line with the t-statistic of 0.07 in Table 2(b) for $\overline{\boldsymbol{\phi}} = 50$. This translates to an extraordinarily high estimated lower bound for $\overline{\gamma}$ of 1,075. Values of $\overline{\boldsymbol{\phi}}$ below 9.8 (for $\overline{\gamma}$, below 175) are rejected at the 5% level. This is our main empirical result: under our maintained assumptions, extremely high risk aversion is needed to rationalize the large degree of excess movement in RN beliefs observed in the data.

For the individual return-state pairs, all but two of the point estimates are infinite, indicating that no amount of utility curvature (or SDF slope) can rationalize the observed excess movement such that the bounds are satisfied. For many of the states ($j = 2, 3, 4, 8$), their confidence intervals also have lower bounds of ∞ (or more precisely, are empty), indicating outright model rejection. Only for RN beliefs over state pairs in the middle of the distribution — i.e., for $j = 5$ and 6, with return

[36] The set identification implied by our theoretical bound motivates our use of these one-sided intervals.

Table 3: Main Estimation Results

	Conservative Lower Bound for:	
	SDF Slope $\overline{\phi}$	RRA $\overline{\gamma}$
Overall bound:	54.7	1,075
[95% CI Lower Bound]	[9.8]	[175]
By return state:		
1 (-20%)	∞ [24.2]	∞ [464]
2 (-15%)	∞ [∞]	∞ [∞]
3 (-10%)	∞ [∞]	∞ [∞]
4 (-5%)	∞ [∞]	∞ [∞]
5 (0%)	19.4 [2.1]	368 [22]
6 (+5%)	4.8 [2.2]	75 [24]
7 (+10%)	∞ [4.6]	∞ [73]
8 (+15%)	∞ [∞]	∞ [∞]
9 (+20%)	∞ [1.0]	∞ [1]

Notes: The first column reports estimates for the minimal value of $\overline{\phi}$ satisfying the conservative bound for excess movement in Proposition 8(ii). These estimates are translated to relative risk aversion $\overline{\gamma}$ using Proposition 6, as shown in the second column. Point estimates are obtained by finding the value $\overline{\phi}$ such that $\overline{e_i^{\text{main}}(\phi)} = 0$ in (18). Confidence interval lower bounds are obtained by inverting a test for $\overline{\phi}$ using bootstrapped data; see Online Appendix C.7 for details. All estimates use conditional means of noise-adjusted excess movement.

midpoints of 0% and 5%, respectively — are there finite point estimates and confidence intervals that contain reasonable risk-aversion values of about 20. RN beliefs over these intermediate return states are thus comparatively well-behaved; for all other states, there is so much mean-reverting variation in RN beliefs that the bounds are only met for implausibly large values of $\overline{\phi}_j$, if at all.

As discussed in Section 5.2, the pricing kernel puzzle tends to emerge only in the range of positive returns. One can thus focus attention on the interior states with negative returns, $j = 2$–5, for estimates that are unlikely to be affected by the possibility that $\phi < 1$. For all four of these states, the null is fully rejected. It is thus unlikely that Assumption 3 is driving our results. Similarly, by Proposition 9, our findings cannot in general be produced solely by miscalibrated priors. This indicates that our rejection must be arising either from excessively volatile physical belief revisions, or a strong violation of CTI arising from changes in the local price of risk.

Table 4: Regressions for Monthly Average of RN Excess Movement

	(1)	(2)	(3)	(4)	(5)	(6)
Option Bid-Ask Spread	0.24					-0.03
	[0.15]					[0.11]
Option Volume	0.07					-0.05
	[0.09]					[0.10]
RN Belief Stream Length		0.28			0.16	0.18
		[0.14]			[0.05]	[0.07]
VIX^2			0.33		0.58	0.62
			[0.16]		[0.32]	[0.36]
Variance Risk Premium			0.38			
			[0.24]			
Volatility of Risk-Aversion Proxy			0.06			
			[0.10]			
Repurchase-Adjusted $\left\|pd_t - \overline{pd}\right\|$				0.37	0.17	0.18
				[0.12]	[0.05]	[0.06]
12-Month S&P 500 Return				0.30	0.53	0.53
				[0.16]	[0.22]	[0.21]
R^2	0.08	0.08	0.28	0.14	0.37	0.37
Obs.	264	264	264	264	264	264

Notes: Heteroskedasticity- and autocorrelation-robust standard errors are in brackets, calculated using the equal-weighted periodogram estimator with $0.4\,\text{Obs.}^{2/3} = 16$ degrees of freedom following Lazarus et al. (2018) and Lazarus, Lewis, and Stock (2021). Dependent variable in all regressions is the mean noise-adjusted $X^*_{t,t+1,i,j}$, for all available expiration dates and interior state pairs, over trading dates within a given month. All variables are normalized to have unit standard deviation, and all regressions include a constant. See Internet Appendix C.8 for variable construction details.

6.5 Predictors of RN Excess Movement

Our results suggest there must either be significant mean reversion in the marginal investor's beliefs, or large variation in the local price of risk, in order to make sense of the observed excess movement without resorting to implausibly large risk aversion. While we have provided some theoretical results and simulations suggesting that it is difficult to rationalize the data from variation in the price of risk alone, this is ultimately an empirical question that we consider here.

More generally, we ask what variables comove strongly with observed RN excess movement. This exercise is meant to provide preliminary guidance on the ingredients a model would need in order to get closer to explaining the data. Table 4 shows results from a set of time-series regressions to this end. The dependent variable in all cases is the monthly average of noise-adjusted RN excess movement $X^*_{t,t+1,i,j}$, and all variables are normalized to have unit standard deviation. See Internet Appendix C.8 for details on variable construction.

The first column shows that proxies for option illiquidity and trading activity — namely, volume-weighted average monthly bid-ask spread in our options sample, and exponentially detrended option trading volume — are insignificant as predictors of X^*, which provides further evidence that option-market frictions are unlikely to be the main drivers of our results. Column (2) shows,

however, that one economically meaningful factor specific to the option market *does* robustly predict excess movement: the average length of RN belief streams (i.e., $\overline{T_i}$ for contracts i traded in the given month). As in Section 6.3, excess volatility seems to be concentrated at longer horizons, suggesting the possibility of overreaction to weak signals about events resolving relatively far in the future.

Column (3) considers volatility-related predictors. Excess movement has a significant positive relationship with the (squared) VIX; a weak positive relationship with the variance risk premium, calculated as VIX^2 minus realized variance following Bollerslev, Tauchen, and Zhou (2009); and essentially no relationship with the volatility of Bekaert, Engstrom, and Xu's (2022) high-frequency risk-aversion proxy.[37] This suggests that X^* comoves strongly with the quantity of market uncertainty; slightly less strongly with the price of this uncertainty; and not at all with the volatility of risk aversion, which can be thought of as a proxy for $\text{Var}(\phi_t)$. We thus find no evidence, at least with this set of predictors, for meaningful comovement between variation in the price of risk and our measured RN excess movement.

Column (4) considers proxies for (mis)valuation and return reversals, in the form of the absolute deviation of the log repurchase-adjusted price-dividend ratio (from Nagel and Xu, 2022) and the trailing 12-month S&P return. Both are significantly positively related to X^*. As noted by Greenwood and Shleifer (2014), the trailing 12-month return predicts Gallup survey-based return expectations well, suggesting a plausible role here for similar survey expectations to predict excess movement. Column (5) considers all four predictors from (1)–(4) that are significant separately at the 10% level and shows that they remain significant jointly, and explain 37% of the variation in X^*. Column (6) adds back the illiquidity and volume predictors; they remain insignificant, while the other predictors from (5) retain their significance.

Taken together, these results suggest again that RN excess movement is a real phenomenon: it is not attributable to option-specific frictions, and it comoves strongly with variables that are intuitively related to aggregate equity valuations and excess volatility in expectations. While we find no evidence that variation in ϕ_t contributes substantially to X^*, it is of course possible that alternative models for time variation in ϕ_t are capable of generating significant excess movement, alongside alternative models of belief formation.

7. Conclusion

We derive new bounds on the admissible rational variation in risk-neutral beliefs as expressed in asset prices. Unlike in much of the previous literature, these results do not require any restrictions on the data-generating process, and they allow for meaningful time variation in discount rates. Further, by using asset prices, we do not require direct measures of physical beliefs over future outcomes, and our bounds exploit intertemporal consistency requirements of rational beliefs without the need for the econometrician to know what agents' beliefs "should" be under RE.

[37] Using daily data, they estimate time-varying relative risk aversion ra_t^{BEX} for a representative agent with habit-like preferences and preference shocks. We then take the sum of squared daily changes in ra_t^{BEX} in a given month.

When taken to the data using risk-neutral beliefs over the return on the S&P 500 index, we find that these RN beliefs are so volatile that our bounds are routinely violated. This implies a violation of our joint assumptions. We provide evidence suggesting that RE violations by the marginal investor are likely to be at least partly responsible for this violation, though we remain open to alternative forms of variation in the local price of risk playing a part. But our framework allows us to rule out other explanations for the excess volatility we document, providing a meaningful improvement in understanding the restrictions implied by the observed volatility in prices.

We believe that there are numerous feasible ways to make additional progress in identifying the specific causes of our bound violations. Largely missing from our analysis is a positive explanation for the underlying drivers of excess movement in beliefs. We begin to take up this question in a follow-up paper (Augenblick, Lazarus, and Thaler, 2023), in which we show that a model of overreaction to strong signals and underreaction to weak signals helps explain a range of experimental and observational data (including our option-price data). But in the current paper's setting, conducting additional tests on the empirical correlates of excess movement, as well as generalizing our analysis to alternative asset classes, may provide useful additional information. Further, detailed data on changes in individual portfolios could allow for tests on the rationality of individual beliefs, which would help distinguish between micro and macro explanations for the observed excess movement in RN beliefs.

Appendix A. Proofs of Main Results

This appendix contains proofs for the main results in Sections 2–3. The remaining proofs can be found in the Internet Appendix, along with additional technical materials and discussions.

A.1. Proofs for Section 2

See Internet Appendix B.1 for a rederivation of Lemma 1. Some preliminaries are useful before proceeding to the main proofs. Start by defining the *RN measure* as

$$\mathbb{P}^*(H_T) \equiv \begin{cases} \mathbb{P}(H_T)\frac{\pi_0^*}{\pi_0} & \text{if } \pi_T(H_T) = 1 \\ \mathbb{P}(H_T)\frac{1-\pi_0^*}{1-\pi_0} & \text{if } \pi_T(H_T) = 0, \end{cases} \tag{A.1}$$

where $\mathbb{P}(H_T)$ is the probability of observing history H_T under DGP. As shown in Lemma A.3 below, (A.1) follows from the usual definition of the RN measure in a general asset-pricing setting. It suffices to think of $\mathbb{P}^*$ as representing the change of measure that adjusts the frequency of each path of signal realizations such that a person with RN beliefs has RE.

Lemma A.1. *Define $\mathbb{E}^*[\cdot]$ to be the expectation under $\mathbb{P}^*$. Under Assumption 1 (RE):*

(i) For any H_T and θ, $\mathbb{P}^*(H_T|\theta) = \mathbb{P}(H_T|\theta)$.

(ii) For any H_t, $\pi_t^*(H_t) = \mathbb{E}^*[\pi_{t+1}^*(H_{t+1})|H_t]$.

(iii) For any DGP, $\mathbb{E}^*[X^*] = 0$.

Proof of Lemma A.1. For the physical measure,

$$\begin{aligned}\mathbb{P}(H_T) &= \mathbb{P}(\theta = 1) \cdot \mathbb{P}(H_T|\theta = 1) + \mathbb{P}(\theta = 0) \cdot \mathbb{P}(H_T|\theta = 0) \\ &= \pi_0 \cdot \mathbb{P}(H_T|\theta = 1) + (1 - \pi_0) \cdot \mathbb{P}(H_T|\theta = 0), \end{aligned} \tag{A.2}$$

where the second line uses that $\pi_0 = \mathbb{E}[\theta] = \mathbb{P}(\theta = 1)$ by RE. For the RN measure, (A.1)–(A.2) give

$$\begin{aligned}\mathbb{P}^*(H_T) &= \frac{\pi_0^*}{\pi_0} \cdot \pi_0 \cdot \mathbb{P}(H_T|\theta = 1) + \frac{1 - \pi_0^*}{1 - \pi_0} \cdot (1 - \pi_0) \cdot \mathbb{P}(H_T|\theta = 0) \\ &= \pi_0^* \cdot \mathbb{P}(H_T|\theta = 1) + (1 - \pi_0^*) \cdot \mathbb{P}(H_T|\theta = 0). \end{aligned} \tag{A.3}$$

For any H_T such that $\pi_T = 1$, (A.1) gives that $\mathbb{P}^*(H_T) = \frac{\pi_0^*}{\pi_0}\mathbb{P}(H_T)$, so $\mathbb{P}^*(\theta = 1) = \frac{\pi_0^*}{\pi_0}\mathbb{P}(\theta = 1)$. Thus from the definition of conditional probability, $\mathbb{P}^*(H_T|\theta = 1) = \mathbb{P}(H_T|\theta = 1)$. Similarly, $\mathbb{P}^*(H_T|\theta = 0) = \mathbb{P}(H_T|\theta = 0)$, proving part (i).

Given this, (A.3) becomes $\mathbb{P}^*(H_T) = \pi_0^* \cdot \mathbb{P}^*(H_T|\theta = 1) + (1 - \pi_0^*) \cdot \mathbb{P}^*(H_T|\theta = 0)$. Summing over all H_T for which $\theta = 1$ gives $\pi_0^* = \mathbb{P}^*(\theta = 1)$, so $\mathbb{P}^*$ is a valid distribution for which the law of iterated expectations holds. Part (ii) then follows from $\mathbb{P}^*(\theta = 1) = \mathbb{E}^*[\theta] = \mathbb{E}^*[\pi_T] = \mathbb{E}^*[\pi_T^*]$.

Finally, given (ii), the same proof for Lemma 1 (see Appendix B.1) gives $\mathbb{E}^*[X^*] = 0$, as expected RN movement under the RN measure must equal RN initial uncertainty. This proves part (iii). □

Part (i) says that compared to the physical measure, the RN measure places higher likelihood of all signal histories resolving in state 1, but does so proportionally, so that likelihoods of signal histories *conditional on state 1* do not change. This implies that conditional expectations under the two respective measures are equal. Therefore, $\mathbb{E}^*[X^*|\theta] = \mathbb{E}[X^*|\theta]$ (see Lemma A.4 below for the analogue of this result in the general asset-pricing setting). This implies

$$\begin{aligned}\mathbb{E}^*[X^*] &= \pi_0^* \cdot \mathbb{E}^*[X^*|\theta = 1] + (1 - \pi_0^*) \cdot \mathbb{E}^*[X^*|\theta = 0] \\ &= \pi_0^* \cdot \mathbb{E}[X^*|\theta = 1] + (1 - \pi_0^*) \cdot \mathbb{E}[X^*|\theta = 0] = 0, \end{aligned} \tag{A.4}$$

where the last equality applies part (iii) of the lemma. For $\mathbb{E}[X^*]$, it is useful to similarly write

$$\mathbb{E}[X^*] = \pi_0 \cdot \mathbb{E}[X^*|\theta = 1] + (1 - \pi_0) \cdot \mathbb{E}[X^*|\theta = 0]. \tag{A.5}$$

Now, recall that $\triangle \equiv \mathbb{E}[X^*|\theta = 0] - \mathbb{E}[X^*|\theta = 1]$. It will be useful to bound $\triangle$:

LEMMA A.2. *For any DGP,* $\triangle \leqslant \pi_0^*$.

Proof of Lemma A.2. First write:

$$\begin{aligned}\triangle &\equiv \mathbb{E}^*[X^*|\theta=0] - \mathbb{E}^*[X^*|\theta=1] \\ &= \mathbb{E}^*[\mathsf{m}^*|\theta=0] - \mathsf{u}_0^* - (\mathbb{E}^*[\mathsf{m}^*|\theta=0] - \mathsf{u}_0^*) = \mathbb{E}^*[\mathsf{m}^*|\theta=0] - \mathbb{E}^*[\mathsf{m}^*|\theta=1]. \end{aligned} \tag{A.6}$$

Further, using (A.4),

$$\begin{aligned}0 &= \pi_0^* \cdot \mathbb{E}[X^*|\theta=1] + (1-\pi_0^*) \cdot \mathbb{E}[X^*|\theta=0] \\ &= \pi_0^* \cdot (\mathbb{E}[\mathsf{m}^*|\theta=1] - \mathsf{u}_0^*) + (1-\pi_0^*) \cdot (\mathbb{E}[\mathsf{m}^*|\theta=0] - \mathsf{u}_0^*),\end{aligned}$$

so from the definition of u_0^*,

$$\pi_0^* \cdot \mathbb{E}[\mathsf{m}^*|\theta=1] + (1-\pi_0^*) \cdot \mathbb{E}[\mathsf{m}^*|\theta=0] = \pi_0^*(1-\pi_0^*). \tag{A.7}$$

Solving for $\mathbb{E}[\mathsf{m}^*|\theta=0]$ gives $\mathbb{E}[\mathsf{m}^*|\theta=0] = \pi_0^* - \frac{\pi_0^*}{1-\pi_0^*} \cdot \mathbb{E}[\mathsf{m}^*|\theta=1]$. Using this in (A.6),

$$\triangle = \pi_0^* - \frac{\pi_0^*}{1-\pi_0^*} \cdot \mathbb{E}[\mathsf{m}^*|\theta=1] - \mathbb{E}^*[\mathsf{m}^*|\theta=1] = \pi_0^* - \frac{1}{1-\pi_0^*} \cdot \mathbb{E}[\mathsf{m}^*|\theta=1]. \tag{A.8}$$

Given that $\frac{1}{1-\pi_0^*} \geqslant 0$ and $\mathbb{E}[\mathsf{m}^*|\theta=1] \geqslant 0$, $\triangle$ is bounded above by π_0^*. □

Proof of Proposition 1. Start from equation (A.5) and apply equation (A.4):

$$\begin{aligned}\mathbb{E}[X^*] &= \pi_0 \cdot \mathbb{E}[X^*|\theta=1] + (1-\pi_0) \cdot \mathbb{E}[X^*|\theta=0] - 0 \\ &= \pi_0 \cdot \mathbb{E}[X^*|\theta=1] + (1-\pi_0) \cdot \mathbb{E}[X^*|\theta=0] - (\pi_0^* \cdot \mathbb{E}[X^*|\theta=1] + (1-\pi_0^*) \cdot \mathbb{E}[X^*|\theta=0]) \\ &= (\pi_0^* - \pi_0)(\mathbb{E}[X^*|\theta=0] - \mathbb{E}[X^*|\theta=1]) = (\pi_0^* - \pi_0)\triangle, \end{aligned} \tag{A.9}$$

as stated. Then the second equality holds using equation (8) and the definition of $\triangle$. □

Proof of Proposition 2. From Lemma A.2 above, we have $\triangle \leqslant \pi_0^*$. Further, equation (8) implies

$$\begin{aligned}\pi_0^* - \pi_0 &= \pi_0^* - \frac{\pi_0^*}{\pi_0^* + \phi(1-\pi_0^*)} \\ &= \pi_0^* \left(1 - \frac{1}{\pi_0^* + \phi(1-\pi_0^*)}\right) \geqslant 0, \end{aligned} \tag{A.10}$$

where the last inequality uses $\pi_0^* + \phi(1-\pi_0^*) \geqslant 0$ since $\phi \geqslant 1$. Using these two inequalities in the expression for $\mathbb{E}[X^*]$ in (A.9),

$$\mathbb{E}[X^*] = (\pi_0^* - \pi_0)\triangle \leqslant (\pi_0^* - \pi_0)\pi_0^*. \tag{A.11}$$

Plugging in the expression for $\pi_0^* - \pi_0$ in (A.10) then gives equation (10). □

Proof of Corollary 1. This is an immediate implication of (A.11) and $\pi_0 \geqslant 0$. □

Proof of Corollary 2. As in (A.10), we have $\pi_0^* - \pi_0 \geqslant 0$. Using this in the equality in (A.11) alongside the assumption that $\triangle = \mathbb{E}^*[\mathsf{m}^*|\theta = 0] - \mathbb{E}^*[\mathsf{m}^*|\theta = 1] \leqslant 0$ gives $\mathbb{E}[X^*] \leqslant 0$. □

Proof of Proposition 3. Consider a given ϕ, RN prior π_0^*, and signal DGPs $DGP(s_t|\theta = 0, H_{t-1})$ and $DGP(s_t|\theta = 1, H_{t-1})$ that lead to some $\mathbb{E}[X^*|\theta = 0]$, $\mathbb{E}[X^*|\theta = 1]$, and $\triangle$. Now consider the "reversed" DGP $\widehat{DGP}$ in which we modify the DGP by relabeling state 1 as state 0 and state 0 as state 1. That is, $\widehat{DGP}(s_t|\theta = 0, H_{t-1}) \equiv DGP(s_t|\theta = 1, H_{t-1})$ and $\widehat{DGP}(s_t|\theta = 1, H_{t-1}) \equiv DGP(s_t|\theta = 0, H_{t-1})$. Similarly, we consider the "reversed" RN prior $\widehat{\pi}_0^* = 1 - \pi_0^*$ implied by the physical prior $\widehat{\pi}_0 = \frac{1-\pi_t^*}{\phi+(1-\phi)(1-\pi_t^*)}$.

With this relabeling, if the RN belief in the original DGP given history H_t is $\pi_t^*(H_t)$, then the RN belief in the reversed $\widehat{DGP}$ with RN prior $1 - \pi_0^*$ must be $\widehat{\pi}_t^*(H_t) = 1 - \pi_t^*(H_t)$. Thus $\mathbb{E}^*[\widehat{X}^*|\theta = 0] = \mathbb{E}^*[X^*|\theta = 1]$ and $\mathbb{E}^*[\widehat{X}^*|\theta = 1] = \mathbb{E}^*[X^*|\theta = 0]$. And since $\mathbb{E}^*[X^*|\theta] = \mathbb{E}[X^*|\theta]$ by Lemma A.1(i), $\mathbb{E}[\widehat{X}^*|\theta = 0] = \mathbb{E}[X^*|\theta = 1]$ and $\mathbb{E}[\widehat{X}^*|\theta = 1] = \mathbb{E}[X^*|\theta = 0]$. Thus for $\widehat{DGP}$, $\widehat{\triangle} \equiv \mathbb{E}[\widehat{X}^*|\theta = 0] - \mathbb{E}[\widehat{X}^*|\theta = 1] = -\triangle$. □

Proof of Proposition 4. Consider a sequence of binary resolving DGPs indexed by T. There are two possible signals in each period, l and h, and assume that for any history,

$$DGP(s_t = h|\theta = 1) = 1, \tag{A.12}$$

$$DGP(s_t = h|\theta = 0) = \frac{\pi_{t-1}^*(1 - \pi_{t-1}^* - \epsilon)}{(1 - \pi_{t-1}^*)(\pi_{t-1}^* + \epsilon)}, \quad \text{with } \epsilon \equiv \frac{1 - \pi_0^*}{T}. \tag{A.13}$$

Since $DGP(s_t = l|\theta = 1) = 0$ from (A.12), beliefs (both physical and RN) update to 0 given any l signal. Meanwhile, after seeing h (and assuming no l through $t - 1$), Bayes' rule gives that physical beliefs update to

$$\pi_t(\{s_1 = h, \ldots, s_t = h\}) = \frac{\pi_{t-1}}{\pi_{t-1} + (1 - \pi_{t-1})DGP(s_t = h|\theta = 0)}.$$

Applying the transformation (8) to the π_{t-1} values on the right side of this equation,

$$\pi_t(\{s_1 = h, \ldots, s_t = h\}) = \frac{\pi_{t-1}^*}{\pi_{t-1}^* + (1 - \pi_{t-1}^*)\phi DGP(s_t = h|\theta = 0)}.$$

Now applying the transformation (5), we obtain that π_t^* given an only-h signal history (suppressing the dependence on this history for simplicity) is, after additional algebra,

$$\pi_t^* = \frac{\pi_{t-1}^*}{\pi_{t-1}^* + (1 - \pi_{t-1}^*)DGP(s_t = h|\theta = 0)}.$$

Now using (A.13), we obtain after further algebra that $\pi_t^* - \pi_{t-1}^* = \epsilon$. Given the definition of ϵ, this DGP is resolving for any T: given any l signal at any t, beliefs resolve to 0, while given only h

signals, beliefs increase slowly ($\pi_t^* = \pi_0^* + t\epsilon$) and resolve to 1 at period T. We thus have

$$\mathbb{E}[\mathsf{m}^*|\theta = 1] = T\epsilon^2 = T\left(\frac{1-\pi_0^*}{T}\right)^2 = \frac{(1-\pi_0^*)^2}{T} \xrightarrow{T\to\infty} 0.$$

Thus for such a sequence, using equation (A.8),

$$\triangle = \pi_0^* - \frac{1}{1-\pi_0^*} \cdot \mathbb{E}[\mathsf{m}^*|\theta = 1] \xrightarrow{T\to\infty} \pi_0^*.$$

Using this in equation (A.9) gives $\mathbb{E}[X^*] \to (\pi_0^* - \pi_0)\pi_0^*$ as $T \to \infty$, as stated. And as further stated, the sequence of DGPs is constructed such that any downward movement is resolving and any upward movement is small ($\pi_t^* - \pi_{t-1}^* = \epsilon \to 0$). We have thus proven the first two statements.

For the final statement, given $\phi > 1$ and $0 < \pi_0^* < 1$, the inequality in (A.10) is strict, so that $\pi_0^* - \pi_0 > 0$. Further, the only way to obtain $\mathsf{m}^* = 0$ for finite T is if $\pi_0^* = \pi_1^* = \ldots = \pi_T^*$, which is ruled out by $0 < \pi_0^* < 1$ since $\pi_T^* = 0$ or 1 with probability 1, so $\mathbb{E}[\mathsf{m}^*|\theta = 1] > 0$. Thus in (A.8), we have the strict inequality $\triangle < \pi_0^*$ for fixed $T < \infty$. Combining these in (A.9) gives $\mathbb{E}[X^*] < (\pi_0^* - \pi_0)\pi_0^*$ for fixed T, as stated. □

A.2. Proofs for Section 3

Again see Internet Appendix B.1 for a derivation of equation (13). A pair of preliminary lemmas will also be useful in proving this section's main results. As usual, assume throughout that Assumptions 2–4 hold.

Lemma A.3. *For some return-state pair (θ_j, θ_{j+1}), with $\widetilde{\mathbb{P}} \equiv \mathbb{P}(\cdot \,|\, R_T^m \in \{\theta_j, \theta_{j+1}\})$, define a new pseudo-risk-neutral measure $\widetilde{\mathbb{P}}^\diamond$ by*

$$\left.\frac{d\widetilde{\mathbb{P}}^\diamond}{d\widetilde{\mathbb{P}}}\right|_{H_t} = \frac{\widetilde{\pi}_{t,j}^*}{\widetilde{\pi}_{t,j}} \mathbb{1}\{R_T^m = \theta_j\} + \frac{1-\widetilde{\pi}_{t,j}^*}{1-\widetilde{\pi}_{t,j}} \mathbb{1}\{R_T^m = \theta_{j+1}\}. \tag{A.14}$$

Denote the conditional expectation under $\widetilde{\mathbb{P}}^\diamond$ by $\widetilde{\mathbb{E}}_t^\diamond[\,\cdot\,]$. If conditional transition independence holds for the return-state pair (θ_j, θ_{j+1}), and $\mathbb{P}_t(R_T^m \in \{\theta_j, \theta_{j+1}\}) > 0$, we have that $\widetilde{\mathbb{P}}^\diamond$ serves as a martingale measure for the risk-neutral belief in the sense that

$$\widetilde{\pi}_{t,j}^* = \widetilde{\mathbb{E}}_t^\diamond[\widetilde{\pi}_{t+1,j}^*]. \tag{A.15}$$

We conclude from Lemma 1 that

$$\widetilde{\mathbb{E}}_0^\diamond[X_j^*] = 0. \tag{A.16}$$

Proof of Lemma A.3. Following the discussion after equation (14), we have that

$$\frac{\widetilde{\pi}^*_{t,j}}{\widetilde{\pi}_{t,j}} = \frac{\phi_j}{1+\widetilde{\pi}_{t,j}(\phi_j-1)}, \tag{A.17}$$

$$\frac{1-\widetilde{\pi}^*_{t,j}}{1-\widetilde{\pi}_{t,j}} = \frac{1}{1+\widetilde{\pi}_{t,j}(\phi_j-1)}. \tag{A.18}$$

Note therefore that $\widetilde{\mathbb{P}}^\diamond$ is absolutely continuous with respect to $\widetilde{\mathbb{P}}$.

Recall that $H_t = \sigma(s_\tau, 0 \leqslant \tau \leqslant t)$, where $\sigma(s_\tau, 0 \leqslant \tau \leqslant t)$ is the σ-algebra generated by $\{s_t\}$, with signals $s_t \in \mathcal{S}$. Denote $N_\mathcal{S} \equiv |\mathcal{S}|$, so $s_t \in \{s_1, s_2, \ldots, s_{N_\mathcal{S}}\}$, and further denote $\mathfrak{p}_{t,k} \equiv \widetilde{\mathbb{P}}_t(s_{t+1} = \theta_k)$, $\varrho_{t,k} \equiv \widetilde{\mathbb{P}}_t(R^m_T = \theta_j \mid s_{t+1} = s_k)$, and $\varrho^*_{t,k} \equiv \mathbb{P}^*_t(R^m_T = \theta_j \mid s_{t+1} = s_k, R^m_T \in \{\theta_j, \theta_{j+1}\})$, so that $\widetilde{\pi}_{t+1,j} = \varrho_{t,k}$ if $s_{t+1} = s_k$, and similarly $\widetilde{\pi}^*_{t+1,j} = \varrho^*_{t,k}$ if $s_{t+1} = s_k$. Combining (A.14), (A.17), (A.18), and these definitions:

$$\begin{aligned}
\widetilde{\mathbb{E}}^\diamond_t[\widetilde{\pi}^*_{t+1,j}] &= \frac{\widetilde{\pi}^*_{t,j}}{\widetilde{\pi}_{t,j}} \sum_{k=1}^{N_\mathcal{S}} \mathfrak{p}_{t,k}\, \varrho^*_{t,k}\, \widetilde{\mathbb{E}}_t\big[\mathbb{1}\{R^m_T = \theta_j\} \mid s_{t+1} = s_k\big] \\
&\quad + \frac{1-\widetilde{\pi}^*_{t,j}}{1-\widetilde{\pi}_{t,j}} \sum_{k=1}^{N_\mathcal{S}} \mathfrak{p}_{t,k}\, \varrho^*_{t,k}\, \widetilde{\mathbb{E}}_t\big[\mathbb{1}\{R^m_T = \theta_{j+1}\} \mid s_{t+1} = s_k\big] \\
&= \frac{\phi_j}{1+\widetilde{\pi}_{t,j}(\phi_j-1)} \sum_{k=1}^{N_\mathcal{S}} \mathfrak{p}_{t,k}\, \frac{\phi_j \varrho_{t,k}}{1+\varrho_{t,k}(\phi_j-1)}\, \varrho_{t,k} \\
&\quad + \frac{1}{1+\widetilde{\pi}_{t,j}(\phi_j-1)} \sum_{k=1}^{N_\mathcal{S}} \mathfrak{p}_{t,k}\, \frac{\phi_j \varrho_{t,k}}{1+\varrho_{t,k}(\phi_j-1)}\, (1-\varrho_{t,k}) \\
&= \frac{\phi_j}{1+\widetilde{\pi}_{t,j}(\phi_j-1)} \sum_{k=1}^{N_\mathcal{S}} \mathfrak{p}_{t,k}\, \frac{\varrho_{t,k}\big(1+\varrho_{t,k}(\phi_j-1)\big)}{1+\varrho_{t,k}(\phi_j-1)} \\
&= \frac{\phi_j}{1+\widetilde{\pi}_{t,j}(\phi_j-1)} \sum_{k=1}^{N_\mathcal{S}} \mathfrak{p}_{t,k}\, \varrho_{t,k} = \frac{\phi_j \widetilde{\pi}_{t,j}}{1+\widetilde{\pi}_{t,j}(\phi_j-1)} = \widetilde{\pi}^*_{t,j},
\end{aligned}$$

where the second-to-last equality uses that $\widetilde{\pi}_{t,j} = \widetilde{\mathbb{E}}_t[\widetilde{\pi}_{t+1,j}]$, as can be seen from the law of iterated expectations (LIE) given that $\widetilde{\pi}_{t,j} = \mathbb{E}_t[\mathbb{1}\{R^m_T = \theta_j\} \mid R^m_T \in \{\theta_j, \theta_{j+1}\}] = \widetilde{\mathbb{E}}_t[\mathbb{1}\{R^m_T = \theta_j\}] = \widetilde{\mathbb{E}}_t[\widetilde{\mathbb{E}}_{t+1}[\mathbb{1}\{R^m_T = \theta_j\}]] = \widetilde{\mathbb{E}}_t[\widetilde{\pi}_{t+1,j}]$, and the last equality above again uses (A.17). Then $\widetilde{\mathbb{E}}^\diamond_0[X^*_j] = 0$ follows immediately from the proof of Lemma 1. □

Lemma A.4. *For any return-state pair (θ_j, θ_{j+1}) meeting CTI, for $j' = j, j+1$, RN movement must satisfy*

$$\widetilde{\mathbb{E}}^\diamond_0[\mathsf{m}^*_j \mid R^m_T = \theta_{j'}] = \widetilde{\mathbb{E}}_0[\mathsf{m}^*_j \mid R^m_T = \theta_{j'}]. \tag{A.19}$$

Proof of Lemma A.4. The stream of RN beliefs is $\boldsymbol{\pi}^*_j$, and denote some arbitrary realization for that

path by $\mathfrak{b}_j$. For any $\mathfrak{b}_j$ such that $\widetilde{\pi}^*_{T,j} = 1$ (i.e., $R^m_T = \theta_j$), the definition of $\widetilde{\mathbb{P}}^\diamond$ in (A.14) gives that

$$\widetilde{\mathbb{P}}^\diamond_0(\boldsymbol{\pi}^*_j = \mathfrak{b}_j) = \frac{\widetilde{\pi}^*_{0,j}}{\widetilde{\pi}_{0,j}}\,\widetilde{\mathbb{P}}(\boldsymbol{\pi}^*_j = \mathfrak{b}_j), \tag{A.20}$$

and further $\widetilde{\mathbb{P}}^\diamond_0(R^m_T = \theta_j) = (\widetilde{\pi}^*_{0,j}/\widetilde{\pi}_{0,j})\,\widetilde{\mathbb{P}}_0(R^m_T = \theta_j)$ trivially. Combining these two equations yields $\widetilde{\mathbb{P}}^\diamond_0(\boldsymbol{\pi}^*_j = \mathfrak{b}_j \mid R^m_T = \theta_j) = \widetilde{\mathbb{P}}_0(\boldsymbol{\pi}^*_j = \mathfrak{b}_j \mid R^m_T = \theta_j)$. (Intuitively, all paths ending in $\widetilde{\pi}^*_{T,j} = 1$ receive the same change of measure under $\widetilde{\mathbb{P}}^\diamond$ relative to $\widetilde{\mathbb{P}}$, so probabilities conditional on $R^m_T = \theta_j$ are preserved, and similarly for $R^m_T = \theta_{j+1}$, as was the case for the simpler version in (A.1).) Thus

$$\begin{aligned}\widetilde{\mathbb{E}}^\diamond_0[\mathsf{m}^*_j \mid R^m_T = \theta_j] &= \sum_{\mathfrak{b}_j\,:\,\widetilde{\pi}^*_{T,j}=1} \mathsf{m}^*_j(\mathfrak{b}_j)\,\widetilde{\mathbb{P}}^\diamond_0\Big(\boldsymbol{\pi}^*_j = \mathfrak{b}_j \;\Big|\; R^m_T = \theta_j\Big) \\ &= \sum_{\mathfrak{b}_j\,:\,\widetilde{\pi}^*_{T,j}=1} \mathsf{m}^*_j(\mathfrak{b}_j)\,\widetilde{\mathbb{P}}_0\Big(\boldsymbol{\pi}^*_j = \mathfrak{b}_j \;\Big|\; R^m_T = \theta_j\Big) = \widetilde{\mathbb{E}}_0[\mathsf{m}^*_j \mid R^m_T = \theta_j].\end{aligned}$$

The same applies for $R^m_T = \theta_{j+1}$: for any $\mathfrak{b}_j$ such that $\widetilde{\pi}^*_{T,j} = 0$, (A.20) now becomes $\widetilde{\mathbb{P}}^\diamond_0(\boldsymbol{\pi}^*_j = \mathfrak{b}_j) = (1-\widetilde{\pi}^*_{0,j})/(1-\widetilde{\pi}_{0,j})\,\widetilde{\mathbb{P}}(\boldsymbol{\pi}^*_j = \mathfrak{b}_j)$. Further, $\widetilde{\mathbb{P}}^\diamond_0(R^m_T = \theta_{j+1}) = (1-\widetilde{\pi}^*_{0,j})/(1-\widetilde{\pi}_{0,j})\,\widetilde{\mathbb{P}}_0(R^m_T = \theta_{j+1})$, so again $\widetilde{\mathbb{P}}^\diamond_0(\boldsymbol{\pi}^*_j = \mathfrak{b}_j \mid R^m_T = \theta_{j+1}) = \widetilde{\mathbb{P}}_0(\boldsymbol{\pi}^*_j = \mathfrak{b}_j \mid R^m_T = \theta_{j+1})$. Thus $\widetilde{\mathbb{E}}^\diamond_0[\mathsf{m}^*_j \mid R^m_T = \theta_{j+1}] = \widetilde{\mathbb{E}}_0[\mathsf{m}^*_j \mid R^m_T = \theta_{j+1}]$. □

Note that the definition in (A.14) aligns with the definition of the RN measure in (A.1), so the two lemmas above prove the statements in the text connecting the RN measure in the simple case in Section 2 to the general case in Section 3 (see after (A.1) and Lemma A.1(i)). Indeed, (A.15) is the precise analogue to Lemma A.1(i); (A.16) is the analogue to Lemma A.1(iii); and (A.19) gives immediately that $\widetilde{\mathbb{E}}^\diamond_0[X^*_j \mid R^m_T] = \widetilde{\mathbb{E}}_0[X^*_j \mid R^m_T]$, which was the main implication of Lemma A.1(i) used in deriving the results in Section 2. We will thus be able to apply those results in this case using the above two lemmas, as follows.

Proof of Proposition 5. No arbitrage gives the existence of a positive SDF for which (14) and Assumption 3 are valid. We have

$$\begin{aligned}\widetilde{\pi}_{t,j} &= \mathbb{E}_t[\widetilde{\pi}_{t+1,j}], \qquad \widetilde{\pi}^*_{t,j} = \widetilde{\mathbb{E}}^\diamond_t[\widetilde{\pi}^*_{t+1,j}], \\ \widetilde{\mathbb{E}}^\diamond_0[X^*_j] &= 0, \qquad\qquad \widetilde{\mathbb{E}}^\diamond_0[X^*_j \mid R^m_T] = \widetilde{\mathbb{E}}_0[X^*_j \mid R^m_T],\end{aligned}$$

where the first equality uses LIE and the rest use Lemmas A.3–A.4. The last equation implies, using the argument applied in Lemma A.2, that $\triangle_j \leqslant \widetilde{\pi}^*_{0,j}$. Further, (5)–(8) hold for $\widetilde{\pi}_{t,j}, \widetilde{\pi}^*_{t,j}, \phi_j$. We have thus obtained all the conditions used for Lemma 1, Propositions 1–4, and Corollaries 1–2, and thus those results continue to hold, with $\widetilde{\pi}^*_{t,j}$ replacing π^*_t, $\widetilde{\pi}_{t,j}$ replacing π_t, X^*_j replacing X^*, ϕ_j replacing ϕ, $\widetilde{\mathbb{E}}_0[\cdot]$ replacing $\mathbb{E}[\cdot]$, and $\triangle_j \equiv \widetilde{\mathbb{E}}_0[X^*_j \mid R^m_T = \theta_{j+1}] - \widetilde{\mathbb{E}}_0[X^*_j \mid R^m_T = \theta_j]$ replacing $\triangle$, as stated. □

Proof of Proposition 6. The result follows immediately from equation (7), with V^m_j and V^m_{j+1} replacing $C_{T,1}$ and $C_{T,0}$, respectively. □

References

AÏT-SAHALIA, Y. AND A. W. LO (2000): "Nonparametric Risk Management and Implied Risk Aversion," *Journal of Econometrics*, 94, 9–51.

AÏT-SAHALIA, Y., Y. WANG, AND F. YARED (2001): "Do Option Markets Correctly Price the Probabilities of Movement of the Underlying Asset?" *Journal of Econometrics*, 102, 67–110.

ALVAREZ, F. AND U. J. JERMANN (2005): "Using Asset Prices to Measure the Persistence of the Marginal Utility of Wealth," *Econometrica*, 73, 1977–2016.

AUGENBLICK, N. AND E. LAZARUS (2022): "Restrictions on Asset-Price Movements Under Rational Expectations: Theory and Evidence," *Working Paper*.

AUGENBLICK, N., E. LAZARUS, AND M. THALER (2023): "Overinference from Weak Signals and Underinference from Strong Signals," *Working Paper*.

AUGENBLICK, N. AND M. RABIN (2021): "Belief Movement, Uncertainty Reduction, and Rational Updating," *Quarterly Journal of Economics*, 136, 933–985.

BACKUS, D., M. CHERNOV, AND I. MARTIN (2011): "Disasters Implied by Equity Index Options," *Journal of Finance*, 66, 1969–2012.

BANSAL, R. AND A. YARON (2000): "Risks for the Long Run: A Potential Resolution of Asset Pricing Puzzles," *NBER Working Paper 8059*.

——— (2004): "Risks for the Long Run: A Potential Resolution of Asset Pricing Puzzles," *Journal of Finance*, 59, 1481–1509.

BARNDORFF-NIELSEN, O. E. AND N. SHEPHARD (2001): "Non-Gaussian Ornstein-Uhlenbeck-Based Models and Some of Their Uses in Financial Economics," *Journal of the Royal Statistical Society, Series B*, 63, 167–241.

BASAK, S. (2000): "A Model of Dynamic Equilibrium Asset Pricing With Heterogeneous Beliefs and Extraneous Risk," *Journal of Economic Dynamics & Control*, 24, 63–95.

BEASON, T. AND D. SCHREINDORFER (2022): "Dissecting the Equity Premium," *Journal of Political Economy*, 130, 2203–2222.

BEKAERT, G., E. C. ENGSTROM, AND N. R. XU (2022): "The Time Variation in Risk Appetite and Uncertainty," *Management Science*, 68, 3975–4004.

VAN BINSBERGEN, J. H., W. F. DIAMOND, AND M. GROTTERIA (2022): "Risk-Free Interest Rates," *Journal of Financial Economics*, 143, 1–29.

BLUME, L., T. COURY, AND D. EASLEY (2006): "Information, Trade and Incomplete Markets," *Economic Theory*, 29, 379–394.

BOLLERSLEV, T., G. TAUCHEN, AND H. ZHOU (2009): "Expected Stock Returns and Variance Risk Premia," *Review of Financial Studies*, 22, 4463–4492.

BOROVIČKA, J., L. P. HANSEN, AND J. A. SCHEINKMAN (2016): "Misspecified Recovery," *Journal of Finance*, 71, 2493–2544.

BREEDEN, D. T. AND R. H. LITZENBERGER (1978): "Prices of State-Contingent Claims Implicit in Option Prices," *Journal of Business*, 51, 621–651.

CAMPBELL, J. Y. AND J. H. COCHRANE (1999): "By Force of Habit: A Consumption-Based Explanation of Aggregate Stock Market Behavior," *Journal of Political Economy*, 107, 205–251.

CHABI-YO, F. AND J. LOUDIS (2020): "The Conditional Expected Market Return," *Journal of Financial Economics*, 137, 752–786.

CHRISTOFFERSEN, P., S. HESTON, AND K. JACOBS (2013): "Capturing Option Anomalies with a Variance-Dependent Pricing Kernel," *Review of Financial Studies*, 26, 1962–2006.

COCHRANE, J. H. (2011): "Presidential Address: Discount Rates," *Journal of Finance*, 66, 1047–1108.

CONSTANTINIDES, G. M., J. C. JACKWERTH, AND A. SAVOV (2013): "The Puzzle of Index Option Returns," *Review of Asset Pricing Studies*, 3, 229–257.

DE LA O, R. AND S. MYERS (2021): "Subjective Cash Flow and Discount Rate Expectations," *Journal of Finance*, 76, 1339–1387.

DEW-BECKER, I. AND S. GIGLIO (2016): "Asset Pricing in the Frequency Domain: Theory and Empirics," *Review of Financial Studies*, 29, 2029–2068.

DRIESSEN, J., J. KOËTER, AND O. WILMS (2022): "Horizon Effects in the Pricing Kernel: How Investors Price Short-Term Versus Long-Term Risks," *Working Paper*.

EPSTEIN, L. G. AND S. E. ZIN (1989): "Substitution, Risk Aversion, and the Temporal Behavior of Consumption and Asset Returns: A Theoretical Framework," *Econometrica*, 57, 937–969.

——— (1991): "Substitution, Risk Aversion, and the Temporal Behavior of Consumption and Asset Returns: An Empirical Analysis," *Journal of Political Economy*, 99, 263–286.

FAMA, E. F. (1991): "Efficient Capital Markets: II," *Journal of Finance*, 46, 1575–1617.

GABAIX, X. (2012): "Variable Rare Disasters: An Exactly Solved Framework for Ten Puzzles in Macro-Finance," *Quarterly Journal of Economics*, 127, 645–700.

GANDHI, M., N. GORMSEN, AND E. LAZARUS (2023): "Excess Persistence in Return Expectations," *Working Paper*.

GEMAN, H., N. EL KAROUI, AND J.-C. ROCHET (1995): "Changes of Numéraire, Changes of Probability Measure and Option Pricing," *Journal of Applied Probability*, 32, 443–458.

GIGLIO, S. AND B. KELLY (2018): "Excess Volatility: Beyond Discount Rates," *Quarterly Journal of Economics*, 133, 71–127.

GREENWOOD, R. AND A. SHLEIFER (2014): "Expectations of Returns and Expected Returns," *Review of Financial Studies*, 27, 714–746.

HADDAD, V., A. MOREIRA, AND T. MUIR (2023): "Whatever It Takes? The Impact of Conditional Policy Promises," *Working Paper*.

HANSEN, L. P. AND R. JAGANNATHAN (1991): "Implications of Security Market Data for Models of Dynamic Economies," *Journal of Political Economy*, 99, 225–262.

JACKWERTH, J. C. (2000): "Recovering Risk Aversion from Option Prices and Realized Returns," *Review of Financial Studies*, 13, 433–451.

LAZARUS, E. (2022): "Horizon-Dependent Risk Pricing: Evidence from Short-Dated Options," *Working Paper*.

LAZARUS, E., D. J. LEWIS, AND J. H. STOCK (2021): "The Size-Power Tradeoff in HAR Inference," *Econometrica*, 89, 2497–2516.

LAZARUS, E., D. J. LEWIS, J. H. STOCK, AND M. W. WATSON (2018): "HAR Inference: Recommendations for Practice," *Journal of Business & Economic Statistics*, 36, 541–559.

LEROY, S. F. AND R. D. PORTER (1981): "The Present-Value Relation: Tests Based on Implied Variance Bounds," *Econometrica*, 49, 555–574.

LI, Z. M. AND O. B. LINTON (2022): "A ReMeDI for Microstructure Noise," *Econometrica*, 90, 367–389.

MALZ, A. M. (2014): "A Simple and Reliable Way to Compute Option-Based Risk-Neutral Distributions," *Federal Reserve Bank of New York Staff Report No. 677*.

MARSH, T. A. AND R. C. MERTON (1986): "Dividend Variability and Variance Bounds Tests for the Rationality of Stock Market Prices," *American Economic Review*, 76, 483–498.

MARTIN, I. (2013): "Consumption-Based Asset Pricing with Higher Cumulants," *Review of Economic Studies*, 80, 745–773.

——— (2017): "What Is the Expected Return on the Market?" *Quarterly Journal of Economics*, 132, 367–433.

MILGROM, P. AND N. STOKEY (1982): "Information, Trade, and Common Knowledge," *Journal of Economic Theory*, 26, 17–27.

NAGEL, S. AND Z. XU (2022): "Asset Pricing with Fading Memory," *Review of Financial Studies*, 35, 2190–2245.

POLKOVNICHENKO, V. AND F. ZHAO (2013): "Probability Weighting Functions Implied in Options Prices," *Journal of Financial Economics*, 107, 580–609.

RADNER, R. (1979): "Rational Expectations Equilibrium: Generic Existence and the Information Revealed by Prices," *Econometrica*, 47, 655.

ROSS, S. (2015): "The Recovery Theorem," *Journal of Finance*, 70, 615–648.

SCHREINDORFER, D. AND T. SICHERT (2022): "Volatility and the Pricing Kernel," *Working Paper*.

SHILLER, R. J. (1981): "Do Stock Prices Move Too Much to be Justified by Subsequent Changes in Dividends?" *American Economic Review*, 71, 421–436.

STEIN, J. (1989): "Overreactions in the Options Market," *Journal of Finance*, 44, 1011–1023.

WEST, K. D. (1988): "Dividend Innovations and Stock Price Volatility," *Econometrica*, 56, 37–61.

ZHANG, L., P. A. MYKLAND, AND Y. AÏT-SAHALIA (2005): "A Tale of Two Time Scales," *Journal of the American Statistical Association*, 100, 1394–1411.

Internet Appendix:

A New Test of Excess Movement in Asset Prices*

Ned Augenblick and Eben Lazarus

JULY 2023

Contents

*Contact: ned@haas.berkeley.edu and eblazarus@gmail.com.

Appendix B. Additional Derivations and Proofs of Theoretical Results

The proofs for Propositions 1–6 and Corollaries 1–2 are provided in the main paper in Appendix A. We provide proofs for the remaining theoretical statements here.

B.1 Additional Proofs for Sections 2–3

Proof of Lemma 1. Following Augenblick and Rabin (2021), it is useful to define period-by-period movement, uncertainty reduction, and excess movement, respectively, as

$$\mathsf{m}_{t,t+1}(\boldsymbol{\pi}) \equiv (\pi_{t+1} - \pi_t)^2, \qquad \mathsf{r}_{t,t+1}(\boldsymbol{\pi}) \equiv \pi_t(1-\pi_t) - \pi_{t+1}(1-\pi_{t+1}),$$
$$X_{t,t+1}(\boldsymbol{\pi}) \equiv \mathsf{m}_{t,t+1}(\boldsymbol{\pi}) - \mathsf{r}_{t,t+1}(\boldsymbol{\pi}).$$

Given the definitions of movement, initial uncertainty, and excess movement in the text, note that

$$\mathsf{m}(\boldsymbol{\pi}) = \textstyle\sum_{t=0}^{T-1} \mathsf{m}_{t,t+1}(\boldsymbol{\pi}), \quad \mathsf{u}_0(\boldsymbol{\pi}) = \textstyle\sum_{t=0}^{T-1} \mathsf{r}_{t,t+1}(\boldsymbol{\pi}), \quad X(\boldsymbol{\pi}) = \textstyle\sum_{t=0}^{T-1} x_{t,t+1}(\boldsymbol{\pi}),$$

where the second equality relies on the fact that $\pi_T \in \{0,1\}$ and therefore $\pi_T(1-\pi_T) = 0$ for any belief stream $\boldsymbol{\pi}$. We have that

$$\begin{aligned}
\mathbb{E}[X_{t,t+1}|H_t] &= \mathbb{E}[\mathsf{m}_{t,t+1} - \mathsf{r}_{t,t+1}|H_t] = \mathbb{E}[(\pi_{t+1}-\pi_t)^2 - ((\pi_t(1-\pi_t) - (\pi_{t+1}(1-\pi_{t+1}))|H_t] \\
&= \mathbb{E}[(2\pi_t - 1)(\pi_t - \pi_{t+1})|H_t] = (2\pi_t(H_t) - 1)(\pi_t(H_t) - \mathbb{E}[\pi_{t+1}|H_t]) \\
&= (2\pi_t(H_t) - 1) \cdot 0 = 0,
\end{aligned}$$

where the last line uses Assumption 1. Summing and applying the law of iterated expectations (LIE),

$$\mathbb{E}[X] = \sum_{t=0}^{T-1} \mathbb{E}[X_{t,t+1}] = \sum_{t=0}^{T-1} \mathbb{E}[\mathbb{E}[X_{t,t+1}|H_t]] = 0. \qquad \square$$

Proof of Equation (13). This follows from a discrete-state application of Breeden and Litzenberger (1978), or see Brown and Ross (1991) for a general version. To review why the stated equation holds, the risk-neutral pricing equation for options can be written

$$q^m_{t,K} = \frac{1}{R^f_{t,T}} \mathbb{E}^*_t[\max\{V^m_T - K, 0\}] = \frac{1}{R^f_{t,T}} \left[\sum_{j\,:\,K_j \geqslant K} (K_j - K) \underbrace{\mathbb{P}^*_t(V^m_T = K_j)}_{\mathbb{P}^*_t(R^m_T = \theta_j)} \right].$$

This implies that for two adjacent return states θ_{j-1} and θ_j,

$$q^m_{t,K_j} - q^m_{t,K_{j-1}} = \frac{1}{R^f_{t,T}} \left[\sum_{j' \geqslant j} (K_{j'} - K_j)\, \mathbb{P}^*_t(V^m_T = K_{j'}) - \sum_{j' \geqslant j-1} (K_{j'} - K_{j-1})\, \mathbb{P}^*_t(V^m_T = K_{j'}) \right]$$

$$= \frac{1}{R^f_{t,T}} \left[\sum_{j' \geqslant j} (K_{j-1} - K_j)\, \mathbb{P}^*_t(V^m_T = K_{j'}) \right] = \frac{1}{R^f_{t,T}} (K_{j-1} - K_j) \left[1 - \mathbb{P}^*_t(V^m_T < K_j) \right].$$

Rearranging,

$$R^f_{t,T} \frac{q^m_{t,K_j} - q^m_{t,K_{j-1}}}{K_j - K_{j-1}} = \mathbb{P}^*_t(V^m_T < K_j) - 1.$$

Repeating this for θ_j and θ_{j+1}, we obtain $R^f_{t,T} \frac{q^m_{t,K_{j+1}} - q^m_{t,K_j}}{K_{j+1} - K_j} = \mathbb{P}^*_t(V^m_T < K_{j+1}) - 1$. Subtracting the preceding equation from this equation and using $\mathbb{P}^*_t(R^m_T = \theta_j) = \mathbb{P}^*_t(V^m_T = K_j)$ yields (13). □

B.2 Proofs for Section 4

Proof of Statements 3–6 in Section 4.1. As in footnote 16 in the main text, statements 1–2 are immediate given the definition of CTI. We take the remaining statements in order:

3. The Gabaix (2012) economy features a representative agent with CRRA consumption utility, and log consumption and log dividends follow $c_{t+1} = c_t + g_c + \varepsilon^c_{t+1} + \log(B_{t+1})\mathfrak{D}_{t+1}$ and $d_{t+1} = d_t + g_d + \varepsilon^d_{t+1} + \log(F_{t+1})\mathfrak{D}_{t+1}$, respectively, where $\mathfrak{D}_{t+1} = \mathbb{1}\{\text{disaster}_{t+1}\}$; disasters in $t+1$ occur with probability p_t; B_{t+1} and F_{t+1} are possibly correlated variables with support $[0,1]$; and $(\varepsilon^c_{t+1}, \varepsilon^d_{t+1})'$ is i.i.d. bivariate normal (or a discretized approximation thereof) with mean zero and is independent of all disaster-related variables. *Resilience* is $\mathsf{H}_t = p_t \mathbb{E}_t[B^{-\gamma}_{t+1} F_{t+1} - 1 \mid \mathfrak{D}_{t+1}]$, and write $\mathsf{H}_t = \mathsf{H}_* + \widehat{\mathsf{H}}_t$. The dynamics of p_t are governed by $\widehat{\mathsf{H}}_{t+1} = \frac{1+\mathsf{H}_*}{1+\mathsf{H}_t} e^{-\phi_{\mathsf{H}}} \widehat{\mathsf{H}}_t + \varepsilon^{\mathsf{H}}_{t+1}$, where $\varepsilon^{\mathsf{H}}_{t+1}$ is mean-zero and independent of all other shocks. Gabaix (2012, Theorem 1) shows that $V^m_t = \frac{D_t}{1-e^{-\beta_m}} \left(1 + \frac{e^{-\beta_m - h_*} \widehat{\mathsf{H}}_t}{1 - e^{-\beta_m - \phi_H}} \right)$, where $h_* \equiv \log(1 + \mathsf{H}_*)$ and $\beta_m \equiv -\log\beta + \gamma g_c - g_d - h_*$. Thus for any θ and H_0, there exists some value d_θ and function $f(d_\theta, \widehat{\mathsf{H}}_T)$, which is strictly increasing in d_θ and strictly decreasing in $\widehat{\mathsf{H}}_T$, such that, by Bayes' rule,

$$\mathbb{P}_0\left(\left(\sum_{t=1}^T \mathfrak{D}_t \right) > 0 \,\middle|\, R^m_T \geqslant \theta \right) = \frac{\mathbb{P}_0\left(R^m_T \geqslant \theta \mid \sum_{t=1}^T \mathfrak{D}_t > 0 \right) \mathbb{P}_0\left(\sum_{t=1}^T \mathfrak{D}_t > 0 \right)}{\mathbb{P}_0(R^m_T \geqslant \theta)}$$
$$= \frac{\mathbb{P}_0\left(D_T \geqslant f(d_\theta, \widehat{\mathsf{H}}_T) \,\middle|\, \sum_{t=1}^T \mathfrak{D}_t > 0 \right) \mathbb{P}_0\left(\sum_{t=1}^T \mathfrak{D}_t > 0 \right)}{\mathbb{P}_0\left(D_T \geqslant f(d_\theta, \widehat{\mathsf{H}}_T) \right)}.$$

Note now that (i) the innovation to $\widehat{\mathsf{H}}_{t+1}$ is independent of $\mathfrak{D}_{t+1}$; (ii) F_{t+1} (the exponential of the disaster shock to D_t) has support $[0,1]$; and (iii) $\mathbb{P}_t(\varepsilon^d_{t+1} \geqslant \epsilon) = o(e^{-\epsilon^2})$ as $\epsilon \to \infty$.[1] Thus $\mathbb{P}_0(D_T \geqslant f(d_\theta, \widehat{\mathsf{H}}_T) \mid \sum_{t=1}^T \mathfrak{D}_t > 0) = o(\mathbb{P}_0(D_T \geqslant f(d_\theta, \widehat{\mathsf{H}}_T)))$ as $d_\theta \to \infty$, from which

[1] To see why point (iii) holds, denote $\sigma_d \equiv \text{Var}(\varepsilon^d_t)$, and then note that $\int_\epsilon^\infty \exp(-x^2/(2\sigma_d^2))/\sqrt{2\pi\sigma_d^2}\, dx < \int_\epsilon^\infty (x/\epsilon) \exp(-x^2/(2\sigma_d^2))/\sqrt{2\pi\sigma_d^2}\, dx = \sigma_d \exp(-\epsilon^2/(2\sigma_d^2))/(\sqrt{2\pi}\epsilon)$. A similar calculation can be used to derive a lower bound for the upper tail of the normal CDF. Then applying the previous upper-bound calculation to $\mathbb{P}_0(D_T \geqslant f(d_\theta, \widehat{\mathsf{H}}_T) \mid \sum_{t=1}^T \mathfrak{D}_t > 0)$ and the lower-bound calculation to $\mathbb{P}_0(D_T \geqslant f(d_\theta, \widehat{\mathsf{H}}_T))$, it follows that $\mathbb{P}_0(D_T \geqslant f(d_\theta, \widehat{\mathsf{H}}_T) \mid \sum_{t=1}^T \mathfrak{D}_t > 0)/\mathbb{P}_0(D_T \geqslant f(d_\theta, \widehat{\mathsf{H}}_T)) = o(1)$, as stated, since the distribution of the value in the denominator is shifted to the right relative to the distribution of the value in the numerator given (i)–(ii).

the statement in footnote 18 follows. Denote the value δ in that statement by $\delta = \delta_0$. It also follows immediately that for any $t > 0$ (with $t < T$), for any $\delta_t > 0$, there exists an $\underline{\theta}$ such that $\mathbb{P}_t(\sum_{\tau=1}^T \mathfrak{D}_t > 0 \mid R_T^m \geqslant \underline{\theta}) < \delta_t$ asymptotically $\mathbb{P}_0$-a.s. as $\delta_0 \to 0$. Given some $\delta_t > 0$, consider θ_j, θ_{j+1} large enough that $\mathbb{P}_t(\sum_{\tau=1}^T \mathfrak{D}_t > 0 \mid R_T^m \in \{\theta_j, \theta_{j+1}\}) < \delta_t$. We then have from (14) that

$$\begin{aligned}
\phi_{t,j} &= \frac{\begin{array}{c}\mathbb{E}_t[M_{t,T} \mid R_T^m = \theta_j, \sum_{\tau=1}^T \mathfrak{D}_\tau = 0]\,\mathbb{P}_t(\sum_{\tau=1}^T \mathfrak{D}_\tau = 0 \mid R_T^m = \theta_j) \\ + \mathbb{E}_t[M_{t,T} \mid R_T^m = \theta_j, \sum_{\tau=1}^T \mathfrak{D}_\tau > 0]\,\mathbb{P}_t(\sum_{\tau=1}^T \mathfrak{D}_\tau > 0 \mid R_T^m = \theta_j)\end{array}}{\begin{array}{c}\mathbb{E}_t[M_{t,T} \mid R_T^m = \theta_{j+1}, \sum_{\tau=1}^T \mathfrak{D}_\tau = 0]\,\mathbb{P}_t(\sum_{\tau=1}^T \mathfrak{D}_\tau = 0 \mid R_T^m = \theta_{j+1}) \\ + \mathbb{E}_t[M_{t,T} \mid R_T^m = \theta_{j+1}, \sum_{\tau=1}^T \mathfrak{D}_\tau > 0]\,\mathbb{P}_t(\sum_{\tau=1}^T \mathfrak{D}_\tau > 0 \mid R_T^m = \theta_{j+1})\end{array}} \\
&= \frac{\mathbb{E}_t[M_{t,T} \mid R_T^m = \theta_j, \sum_{\tau=1}^T \mathfrak{D}_\tau = 0](1 - \mathcal{O}(\delta_t)) + \mathcal{O}(\delta_t)}{\mathbb{E}_t[M_{t,T} \mid R_T^m = \theta_{j+1}, \sum_{\tau=1}^T \mathfrak{D}_\tau = 0](1 - \mathcal{O}(\delta_t)) + \mathcal{O}(\delta_t)} \\
&= \frac{\mathbb{E}_t[M_{t,T} \mid R_T^m = \theta_j, \sum_{\tau=1}^T \mathfrak{D}_\tau = 0]}{\mathbb{E}_t[M_{t,T} \mid R_T^m = \theta_{j+1}, \sum_{\tau=1}^T \mathfrak{D}_\tau = 0]} + \mathcal{O}(\delta_t).
\end{aligned}$$

The fraction in the last expression is constant given that $M_{t,T} = \beta^{T-t} e^{-\gamma g_c (T-t)}$ conditional on $\sum_{t=1}^T \mathfrak{D}_t = 0$, using eq. (2) of Gabaix (2012). Thus denoting $\phi_j \equiv \frac{\mathbb{E}_0[M_{t,T} \mid R_T^m = \theta_j, \sum_{t=1}^T \mathfrak{D}_\tau = 0]}{\mathbb{E}_0[M_{t,T} \mid R_T^m = \theta_{j+1}, \sum_{t=1}^T \mathfrak{D}_\tau = 0]}$, we have $\phi_{t,j} = \phi_j + \mathcal{O}(\delta_t)$. Since we can take $\delta_t \to 0$ asymptotically $\mathbb{P}_0$-a.s. as $\delta_0 \to 0$, we have $\phi_{t,j} = \phi_j + o_p(1)$ for any sequence of values $\delta = \delta_0 \to 0$, as stated.

4. The Epstein–Zin (1989) preference recursion is $U_t = \left[(1-\beta) C_t^{1-\psi^{-1}} + \beta (\mathbb{E}_t[U_{t+1}^{1-\gamma}])^{\frac{1-\psi^{-1}}{1-\gamma}}\right]^{\frac{1}{1-\psi^{-1}}}$, and it can be shown (e.g., Campbell, 2018, eq. (6.42)) that the SDF evolves in this case according to $M_{t,t+1} = \beta (C_{t+1}/C_t)^{-\vartheta/\psi} (1/R_{t,t+1}^m)^{1-\vartheta}$, where $\vartheta \equiv (1-\gamma)/(1-\psi^{-1})$. In case (i) of the statement, $\gamma = 1$ and $M_{t,t+1} = \beta / R_{t,t+1}^m$, so M_T depends only on the index return. Thus the numerator and denominator in equation (14) are constant, and CTI holds immediately. For case (ii), write $\Delta c_{t+1} = \mu_c + \rho \Delta c_t + \sigma \eta_{t+1}$, with $\eta_{t+1} \overset{\text{i.i.d.}}{\sim} \mathcal{N}(0,1)$. Given $\psi = 1$, it follows from Hansen, Heaton, and Li (2008, eq. (3)) that the log SDF follows $m_{t,t+1} = -\Delta c_{t+1} + \frac{1-\gamma}{1-\beta\rho} \sigma \eta_{t+1}$ (up to a constant, as we ignore throughout). Further, the consumption-wealth ratio C_t / V_t^m is a constant given $\psi = 1$, so $r_{t,t+1}^m = \Delta c_{t+1}$. Using this in the log SDF and summing from t to T, $m_{t,T} = -r_{t,T}^m + \frac{1-\gamma}{1-\beta\rho} \sigma \sum_{\tau=t+1}^T \eta_\tau$. The first term is known conditional on R_t^m. In addition, recursive substitution and summation for $r_{t,t+1}^m$ gives that $r_{t,T}^m = \frac{\sigma}{1-\rho} \sum_{\tau=t+1}^T (1 - \rho^{T-\tau+1}) \eta_\tau$. Thus for the second term in $m_{t,T}$, conditioning on $R_T^m = \theta_j$ is equivalent to conditioning on $\sum_{\tau=t+1}^T (1 - \rho^{T-\tau+1}) \eta_\tau = \text{const} + \log \theta_j \equiv k_j$. Denoting $w_t \equiv (1 - \rho^{T-t+1})$, it can then be shown (e.g., Vrins, 2018, eq. (2)–(3)) that $(\sum_{\tau=t+1}^T \eta_\tau \mid \sum_{\tau=t+1}^T w_\tau \eta_\tau = k_j) \sim \mathcal{N}(\mu_{t,j}, \varsigma_t)$, where $\mu_{t,j} = k_j \frac{\sum_{\tau=t+1}^T w_\tau}{\sum_{\tau=t+1}^T w_\tau^2}$ and where ς_t does not depend on k_j. Therefore,

$$\log \phi_{t,j} = \log \mathbb{E}_t \left[\sum_{\tau=t+1}^T \eta_\tau \mid R_T^m = \theta_j \right] - \log \mathbb{E}_t \left[\sum_{\tau=t+1}^T \eta_\tau \mid R_T^m = \theta_{j+1} \right] = \log \theta_j - \log \theta_{j+1},$$

so CTI holds. Case (iii) follows immediately from eq. (17) of Kocherlakota (1990), which shows that $M_T \propto (R_T^m)^{-\gamma}$ in the i.i.d. case.

5. The Campbell and Cochrane (1999) economy features a representative agent with utility $\mathbb{E}_0\{\sum_{t=0}^{\infty}\beta^t[(C_t-\mathfrak{H}_t)^{1-\gamma}-1]/(1-\gamma)\}$, where $\mathfrak{H}_t$ is the level of (exogenous) habit and other terms are standard. The *surplus-consumption ratio* is $S_t^c \equiv (C_t-\mathfrak{H}_t)/\mathfrak{H}_t$. Log dynamics are $s_{t+1}^c = (1-\phi)\overline{s}^c + \phi s_t^c + \lambda(s_t^c)\varepsilon_{t+1}$, $c_{t+1} = g + c_t + \varepsilon_{t+1}$, and $d_{t+1} = g + d_t + \eta_{t+1}$, where $\varepsilon_{t+1} \overset{\text{i.i.d.}}{\sim} \mathcal{N}(0,\sigma_\varepsilon^2)$, $\eta_{t+1} \overset{\text{i.i.d.}}{\sim} \mathcal{N}(0,\sigma_\eta^2)$, $\text{Corr}(\varepsilon_{t+1},\eta_{t+1}) = \rho$, and the *sensitivity function* is $\lambda(s_t^c) = \left[\frac{1}{\overline{S}^c}\sqrt{1-2(s_t^c-\overline{s}^c)}-1\right]\mathbb{1}\{s_t^c \leqslant s_{\max}^c\}$, with $\overline{S}^c = e^{\overline{s}^c} = \sigma_\varepsilon\sqrt{\frac{\gamma}{1-\phi}}$ and $s_{\max}^c = \overline{s}^c + (1-\overline{S}^c)^2/2$. The SDF evolves according to $M_{t,t+1} = \beta\left(\frac{C_{t+1}}{C_t}\right)^{-\gamma}\left(\frac{S_{t+1}^c}{S_t^c}\right)^{-\gamma}$, so

$$\frac{\mathbb{E}_t[M_{t,T} \mid R_T^m = \theta_j]}{\mathbb{E}_t[M_{t,T} \mid R_T^m = \theta_{j+1}]} = \frac{\mathbb{E}_t\left[\exp\left(\sum_{\tau=0}^{T-t-1} -\gamma\left(1+\lambda(s_{t+\tau}^c)\right)\varepsilon_{t+\tau+1}\right) \;\middle|\; R_T^m = \theta_j\right]}{\mathbb{E}_t\left[\exp\left(\sum_{\tau=0}^{T-t-1} -\gamma\left(1+\lambda(s_{t+\tau}^c)\right)\varepsilon_{t+\tau+1}\right) \;\middle|\; R_T^m = \theta_{j+1}\right]}.$$

   For a counterexample to constant ϕ_t, set $T=2$ and $\rho=1$ (so $\Delta c_t = \Delta d_t$, as in the simplest case considered by Campbell and Cochrane). A sufficient condition for non-constant ϕ_t is $\text{Cov}_0(\phi_1, \mathbb{E}_1[M_{1,2} \mid R_2^m = \theta_{j+1}]) \neq 0$, as this gives $\mathbb{E}_0[\phi_1] \neq \phi_0$. As of $t=0$, both ε_1 and ε_2 are relevant for R_2^m and $M_{0,2}$: ε_1 determines s_1^c and thus $\lambda(s_1^c)$. As of $t=1$, the only source of uncertainty for both R_2^m and $M_{1,2}$ is ε_2: s_2^c and d_2 determine R_2^m, and conditional on time-1 variables, these depend only on ε_2. Write ε_j^1 for the realization of ε_2 needed to generate $R_2^m = \theta_j$ given ε_1 — i.e., $\varepsilon_j^1 \equiv \{\varepsilon_2 : R_2^m = \theta_j \mid \varepsilon_1\}$ — and similarly write ε_{j+1}^1 for θ_{j+1}. Then we have $\mathbb{E}_1[M_{1,2} \mid R_2^m = \theta_{j'}] = \exp(-\gamma(1+\lambda(s_1^c))\varepsilon_{j'}^1)$ for $j' = j, j+1$, so $\phi_1 = \exp(-\gamma(1+\lambda(s_1^c))(\varepsilon_j^1 - \varepsilon_{j+1}^1))$. Thus $\text{Cov}_0(\phi_1, \mathbb{E}_1[M_{1,2} \mid R_2^m = \theta_{j+1}]) = \text{Cov}_0(\exp(-\gamma(1+\lambda(s_1^c))(\varepsilon_j^1 - \varepsilon_{j+1}^1)), \exp(-\gamma(1+\lambda(s_1^c))\varepsilon_{j+1}^1))$. Given Gaussian ε_1, this value is generically non-zero.

6. Take the two-agent CRRA case considered in Section 5 of Basak (2000), with notation adopted directly. Basak's Proposition 7 shows that when extraneous risk matters, state prices (and thus the SDF) depend on both the stochastic weighting process $\eta(t)$ and the aggregate endowment $\varepsilon(t)$. These two processes are driven respectively by independent shocks, $dW_z(t)$ (extraneous risk) and $dW_\varepsilon(t)$ (fundamental risk). Asset returns thus do not pin down the SDF realization, generating a generically path-dependent SDF and thus time-varying ϕ_t (see also the discussion in Atmaz and Basak, 2018, footnote 17). □

Proof of Proposition 7. Given that ϕ_t can change, we explicitly allow it to depend on the signal history. RN beliefs are thus now denoted by $\pi_t^*(H_t) = \frac{\phi_t(H_t)\pi_t(H_t)}{(\phi_t(H_t)-1)\pi_t(H_t)+1}$, where we use the simpler notation from Section 2 for clarity throughout. Uncertainty about θ is again resolved by period T, and we again consider X^* from 0 to T. Since $\pi_T \in \{0,1\}$ implies $\pi_T^* = \pi_T$, time variation in ϕ_t has no effect on X^* for $t > T-1$.

Toward a contradiction, assume that there exists some DGP(s) in which ϕ_t changes such that $\mathbb{E}_t[\phi_{t+1}] \leqslant \phi_t$ and expected RN movement is higher than the bounds in Proposition 2 for some T. Consider a DGP from this set with the highest expected RN movement. We now consider the last

meaningful movement of ϕ in this DGP. Specifically, given that ϕ_t is assumed to change at some point, but ϕ_t is constant when $t \geqslant T$, there must exist some history H_t in which $\pi_t \in (0,1)$, ϕ_t can change between t and $t+1$ (i.e., there exists a signal s_{t+1} for which $\phi_{t+1}(H_t \cup s_{t+1}) \neq \phi_t(H_t)$, where s_{t+1} includes the signal $s_{\phi_{t+1}}$) but for which ϕ_t is constant after $t+1$. Following any H_t, by assumption, $\phi_{t+1}(H_t \cup s_{t+1})$ can take two values: $\phi^H_{t+1} > \phi_t$ following signal s^H_{t+1} with probability $q^H > 0$, and $\phi^L_{t+1} < \phi_t$ following signal s^L_{t+1} with probability $q^L = 1 - q^H > 0$. We start by assuming that ϕ_t evolves as a martingale:

$$\sum_{i \in \{L,H\}} q^i \cdot \phi^i_{t+1} = \phi_t. \tag{B.1}$$

Given the maintained assumption that π_t does not evolve in the same period as ϕ_t and therefore is constant immediately following history H_t, $\pi^*_t(H_t \cup s_{t+1})$ can take at most two values: $\pi^{*i}_{t+1} = \frac{\phi^i_{t+1} \cdot \pi_t}{(\phi^i_{t+1}-1)\pi_t+1}$ for $i \in \{L,H\}$. Now consider expected RN movement following H_t. From period t to $t+1$, given signal s^i_{t+1}, RN beliefs move from π^*_t to π^{*i}_{t+1}, leading to per-period RN movement

$$\begin{aligned}\mathbb{E}[\mathsf{m}^*_{t,t+1} | H_t \cup s^i_{t+1}] = (\pi^*_t - \pi^{*i}_{t+1})^2 &= \left(\frac{\phi_t \cdot \pi_t}{(\phi_t - 1)\pi_t + 1} - \frac{\phi^i_{t+1} \cdot \pi_{t+1}}{(\phi^i_{t+1} - 1)\pi_{t+1} + 1} \right)^2 \\ &= \left(\frac{\phi_t \cdot \pi_t}{(\phi_t - 1)\pi_t + 1} - \frac{\phi^i_{t+1} \cdot \pi_t}{(\phi^i_{t+1} - 1)\pi_t + 1} \right)^2.\end{aligned}$$

Given that the postulated ϕ_t process is constant after $t+1$, at that point our main bounds hold with π^*_0 replaced with π^{*i}_{t+1} and ϕ replaced with ϕ^i_{t+1}. Thus given signal s^i_{t+1},

$$\begin{aligned}\mathbb{E}[\mathsf{m}^*_{t+1,T} | H_t \cup s^i_{t+1}] &= \mathbb{E}[X^*_{t+1,T} | H_t \cup s^i_{t+1}] + \mathbb{E}[\mathsf{r}^*_{t+1,T} | H_t \cup s^i_{t+1}] \\ &\leqslant (\pi^{i*}_{t+1} - \pi_{t+1}) \cdot \pi^{i*}_{t+1} + (1 - \pi^{i*}_{t+1}) \cdot \pi^{i*}_{t+1} = (1 - \pi_{t+1}) \cdot \pi^{i*}_{t+1} \\ &= (1 - \pi_{t+1}) \cdot \frac{\phi^i_{t+1} \cdot \pi_{t+1}}{(\phi^i_{t+1} - 1)\pi_{t+1} + 1} = (1 - \pi_t) \cdot \frac{\phi^i_{t+1} \cdot \pi_t}{(\phi^i_{t+1} - 1)\pi_t + 1},\end{aligned}$$

where the second line plugs in our bound for excess RN movement and uncertainty reduction given that uncertainty is zero at period T, and the third line states everything in terms of ϕ_t and π_t and uses the assumption that $\pi_t = \pi_{t+1}$. Therefore, expected RN movement from period t onward following history H_t is bounded above by:

$$\begin{aligned}\mathbb{E}[\mathsf{m}^*_{t,T} | H_t] &= \mathbb{E}[\mathsf{m}^*_{t,t+1} | H_t] + \mathbb{E}[\mathsf{m}^*_{t+1,T} | H_t] \\ &\leqslant \sum_{i \in \{L,H\}} q^i \cdot \Big(\big(\frac{\phi_t \cdot \pi_t}{(\phi_t - 1)\pi_t + 1} - \frac{\phi^i_{t+1} \cdot \pi_t}{(\phi^i_{t+1} - 1)\pi_t + 1} \big)^2 + (1 - \pi_t) \cdot \frac{\phi^i_{t+1} \cdot \pi_t}{(\phi^i_{t+1} - 1)\pi_t + 1} \Big).\end{aligned}$$

We now show that this DGP will have higher RN movement if ϕ_t is constant from H_t onward. To see this, consider the "worst-case" DGP in Proposition 4 in which ϕ remains constant at ϕ_t.

In this case, RN movement is (arbitrarily close to) $\mathbb{E}_{maxDGP}[\mathsf{m}^*_{t,T}|H_t] = (1-\pi_t)\cdot\frac{\phi_t\cdot\pi_t}{(\phi_t-1)\pi_t+1}$. We now subtract the expected RN movement given changing ϕ ($\mathbb{E}[\mathsf{m}^*_{t,T}|H_t]$) from the worst-case RN movement ($\mathbb{E}_{maxDGP}[\mathsf{m}^*_{t,T}|H_t]$) and show it is positive given the assumption that ϕ_t evolves as a martingale. The difference is positive if and only if

$$(1-\pi_t)\cdot\frac{\phi_t\cdot\pi_t}{(\phi_t-1)\pi_t+1} - \sum_{i\in\{L,H\}} q^i\cdot\left((\frac{\phi_t\cdot\pi_t}{(\phi_t-1)\pi_t+1} - \frac{\phi^i_{t+1}\cdot\pi_t}{(\phi^i_{t+1}-1)\pi_t+1})^2 + (1-\pi_t)\cdot\frac{\phi^i_{t+1}\cdot\pi_t}{(\phi^i_{t+1}-1)\pi_t+1}\right) > 0.$$

Using (B.1) in this inequality gives that $\mathbb{E}_{maxDGP}[\mathsf{m}^*_{t,T}|H_t] - \mathbb{E}[\mathsf{m}^*_{t,T}|H_t] > 0$ if and only if

$$\frac{\pi_t^3(1-\pi_t)^2(\phi^H_{t+1}-\phi_t)(\phi_t-\phi^L_{t+1})((\phi^H_{t+1}-\phi_t)+(\phi^L_{t+1}-1)+(\pi_t)(2+\pi_t(\phi_t-1))(\phi^H_{t+1}-1)(\phi^L_{t+1}-1))}{(1+\pi_t(\phi_t-1))^2(1+\pi_t(\phi^H_{t+1}-1))^2(1+\pi_t(\phi^L_{t+1}-1))^2} > 0.$$

It is straightforward to see that the expression on the left side of this inequality is positive: every parentheses contains a positive value as $\phi^H_{t+1} > \phi_t > \phi^L_{t+1} \geqslant 1$ and $\pi_t \in (0,1)$. Therefore, we conclude that expected RN movement can be increased if ϕ_t remains constant following H_t rather than changing. But this gives us a contradiction, as it violates the assumption that the DGP with ϕ_t moving following H_t has the highest possible movement. Therefore, we conclude that there does not exist a DGP satisfying in which ϕ evolves as a martingale that produces more expected RN movement than the bound in Proposition 2.

We now extend this observation to DGPs in which movement in ϕ is a supermartingale rather than a martingale. We do so by showing that if there exists a DGP where ϕ evolves as supermartingale and leads to expected movement that is higher than our bound, there there must exist a martingale that leads to higher expected movement. Given the previous martingale result, this is impossible. Formally, assume that there exists a DGP_{super} in which ϕ evolves as a supermartingale such that the expected movement of this DGP is higher than our bound for a given T. Consider the supermartingale DGP with the maximum expected movement, and consider a period t (history H_t) with the last meaningful movement in ϕ in which ϕ is a strict supermartingale. If this period does not exist, the process is a martingale, and the previous results hold. Note that, following this movement, there cannot be further change in ϕ. If there were and ϕ were a martingale, the previous result shows that no change in ϕ would produce more expected movement, contradicting the assumption that this DGP produces the highest expected movement in the class. If instead there was movement and the change in ϕ was a strict supermartingale, it would contradict the assumption that the previous movement was the last meaningful movement of that type.

Now, we show that it is possible to adjust DGP_{super} following history H_t to increase expected movement following H_t by adjusting the change in ϕ from period t to period $t+1$ to be a martingale rather than a supermartingale. To do so, we first show that any upward movement from ϕ_t to $\phi_{t+1} > \phi_t$ always leads to more total movement following H_t than any downward movement from ϕ_t to $\phi_{t+1} < \phi_t$. Consider total expected movement from H_t onward given a change from ϕ_t to ϕ_{t+1}:

$$\mathbb{E}[\mathsf{m}^*_{t,T}|H_t,\phi_t,\phi_{t+1}] = (\frac{\phi_t\cdot\pi_t}{(\phi_t-1)\pi_t+1} - \frac{\phi_{t+1}\cdot\pi_t}{(\phi_{t+1}-1)\pi_t+1})^2 + (1-\pi_t)\cdot\frac{\phi_{t+1}\cdot\pi_t}{(\phi_{t+1}-1)\pi_t+1}.$$

Our claim is that this is higher if $\phi_{t+1} > \phi_t$ than if $\phi_{t+1} < \phi_t$. To see this, compare the above with movement if $\phi_{t+1} = \phi_t$. In this case, $\mathbb{E}[\mathsf{m}^*_{t,T}|H_t, \phi_t = \phi_{t+1}] = (1-\pi_t) \cdot \frac{\phi_t \cdot \pi_t}{(\phi_t - 1)\pi_t + 1}$. Subtracting from above and writing $\pi = \pi_t$ for simplicity yields:

$$\begin{aligned}
&\mathbb{E}[\mathsf{m}^*_{t,T}|H_t, \phi_t, \phi_{t+1}] - \mathbb{E}[\mathsf{m}^*_{t,T}|H_t, \phi_t = \phi_{t+1}] \\
&\quad = \frac{(\pi-1)^2 \cdot \pi \cdot (1 + \pi \cdot (2 + \pi \cdot (\phi_t - 1)) \cdot (\phi_{t+1} - 1)) \cdot (\phi_t - \phi_{t+1})}{(1 + \pi(\phi - 1))^2 \cdot (1 + \pi(\phi_{t+1} - 1))^2}.
\end{aligned}$$

As with the inequality in the martingale case, every component in this expression is weakly positive (as $0 < \pi < 1$ because the ϕ movement is meaningful and $\phi \geqslant 1$), except for $(\phi_t - \phi_{t+1})$. Therefore, this equation is positive if $\phi_{t+1} < \phi_t$ and negative if $\phi_{t+1} > \phi_t$. But then it must be that $\mathbb{E}[\mathsf{m}^*_{t,T}|H_t, \phi_t, \phi_{t+1}]$ is greater if $\phi_{t+1} > \phi_t$ than if $\phi_{t+1} < \phi_t$. In this case, we can adjust the evolution of ϕ following history H_t — which was assumed to be a supermartingale — to be a martingale by taking a probability from downward change in ϕ and shifting it to an upward change in ϕ. Specifically, if ϕ_t is a strict supermartingale at H_t, there must be at least some probability on a realization of $\phi_{t+1} < \phi$. Consider the lowest possible realization of ϕ^L_{t+1} with associated probability q^L. There are two possibilities. First, there is some value $\phi^H_{t+1} > \phi$ such shifting the probability q^L from ϕ^L_{t+1} to ϕ^H_{t+1} makes ϕ a martingale. Second, there is some $q^H < q^L$ such that shifting q^H from ϕ^L_{t+1} to ϕ^H_{t+1} makes ϕ a martingale. In either case, we are shifting probability from $\phi^L_{t+1} < \phi_t$ to $\phi^H_{t+1} > \phi_t$. But, as just proven above, it must be that $\mathbb{E}[\mathsf{m}^*_{t,T}|H_t, \phi_t, \phi_{t+1}]$ is greater if $\phi_{t+1} > \phi_t$ than if $\phi_{t+1} < \phi_t$. But then the total movement of the change from ϕ at H_t must increase. This implies that there exists a martingale process for ϕ at H_t that has higher expected movement than the strict supermartingale process for ϕ at H_t. This contradicts the assumption that the strict supermartingale process has the highest movement in the class of supermartingale processes (which includes martingales), completing the proof. □

Proof of Proposition 8. In what follows, we often use $\mathbb{E}_i[\cdot]$ to make explicit that we are taking expectations over DGPs indexed by i, and we continue to use the notational simplifications used in the statement of the proposition. For (i), fixing $\pi^*_{0,i} = \pi^*_0$ across i and applying Proposition 1,

$$\begin{aligned}
\mathbb{E}_i[\mathbb{E}[X^*_i]] &= \mathbb{E}_i[(\pi^*_0 - \pi_{0,i}) \cdot \triangle_i] = \pi^*_0 \cdot \mathbb{E}_i[\triangle_i] - \mathbb{E}_i[\pi_{0,i}] \cdot \mathbb{E}_i[\triangle_i] \\
&= (\pi^*_0 - \mathbb{E}_i[\pi_{0,i}]) \cdot \mathbb{E}_i[\triangle_i] = \mathbb{E}_i[\pi^*_0 - \pi_{0,i}] \cdot \mathbb{E}_i[\triangle_i] \\
&= \mathbb{E}_i\left[\pi^*_0 - \frac{\pi^*_0}{\phi_i + (1-\phi_i)\pi^*_0}\right] \cdot \mathbb{E}_i[\triangle_i] \qquad \text{(B.2)}
\end{aligned}$$

where the last equality in the first line follows from the assumption that $\mathrm{Cov}(\pi_{0,i}, \triangle_i) = 0$.

Now consider $\zeta_1(\phi_i, \pi^*_0) \equiv \pi^*_0 - \frac{\pi^*_0}{\phi_i + (1-\phi_i)\pi^*_0}$. This function is concave in ϕ_i: $\frac{\partial^2 \zeta_1}{\partial \phi_i^2} = \frac{-2\pi^*_0(1-\pi^*_0)^2}{(\pi^*_0 + \phi(1-\pi^*_0))^3}$, which is weakly negative given $\pi^*_0 \in [0,1]$ and $\phi \geqslant 1$. Thus by Jensen's inequality, the expectation of ζ_1 over ϕ_i is less than ζ_1 evaluated at $\underline{\phi} \equiv \mathbb{E}_i[\phi_i]$, so $\mathbb{E}_i\left[\pi^*_0 - \frac{\pi^*_0}{\phi_i + (1-\phi_i)\pi^*_0}\right] \leqslant \pi^*_0 - \frac{\pi^*_0}{\underline{\phi} + (1-\underline{\phi})\pi^*_0}$.

Returning to (B.2), suppose that $\mathbb{E}_i[\triangle_i] > 0$. In this case,

$$\mathbb{E}_i[\mathbb{E}[X_i^*]] = \mathbb{E}_i[\pi_0^* - \frac{\pi_0^*}{\phi_i + (1-\phi_i)\pi_0^*}] \cdot \mathbb{E}_i[\triangle_i]] \leqslant (\pi_0^* - \frac{\pi_0^*}{\underline{\phi} + (1-\underline{\phi})\pi_0^*}) \cdot \mathbb{E}_i[\triangle_i].$$

Now assume that $\mathbb{E}_i[\triangle_i] \leqslant 0$. Then, as $\pi_0^* - \frac{\pi_0^*}{\phi_i + (1-\phi_i)\pi_0^*} = \pi_0^* - \pi_0 \geqslant 0$ given $\phi_i \geqslant 1$,

$$\mathbb{E}_i[\mathbb{E}[X_i^*]] = \mathbb{E}_i[\pi_0^* - \frac{\pi_0^*}{\phi_i + (1-\phi_i)\pi_0^*}] \cdot \mathbb{E}_i[\triangle_i] \leqslant 0.$$

Taken together, $\mathbb{E}_i[\mathbb{E}[X_i^*]] \leqslant \max\{0, (\pi_0^* - \frac{\pi_0^*}{\underline{\phi} + (1-\underline{\phi})\pi_0^*}) \cdot \mathbb{E}_i[\triangle_i]\}$.

For part (ii), first consider the situation in which $\pi_{0,i}^*$ is constant and equal to π_0^*. As above,

$$\mathbb{E}_i[\mathbb{E}[X_i^*]] \leqslant \mathbb{E}_i[(\pi_0^* - \pi_{0,i}) \cdot \pi_0^*] = \mathbb{E}_i[\pi_0^* - \pi_{0,i}] \cdot \pi_0^* = \mathbb{E}_i\left[\pi_0^* - \frac{\pi_0^*}{\phi_i + (1-\phi_i)\pi_0^*}\right] \cdot \pi_0^*.$$

As above, given the concavity of $\zeta_2 \equiv \pi_0^* - \frac{\pi_0^*}{\phi_i + (1-\phi_i)\pi_0^*}$ with respect to ϕ_i and the fact that $\pi_0^* \geqslant 0$,

$$\mathbb{E}_i[\mathbb{E}[X_i^*]] \leqslant \mathbb{E}_i\left[\pi_0^* - \frac{\pi_0^*}{\phi_i + (1-\phi_i)\pi_0^*}\right] \cdot \pi_0^* \leqslant \left(\pi_0^* - \frac{\pi_0^*}{\underline{\phi} + (1-\underline{\phi})\pi_0^*}\right) \pi_0^*,$$

as stated in the second inequality. Now allowing $\pi_{0,i}^*$ to vary, write the bound for $\mathbb{E}[X^*]$ in Proposition 2 as $\zeta_{2'}(\phi_i, \pi_{0,i}^*) \equiv \left(\pi_0^* - \frac{\pi_0^*}{\phi_i + (1-\phi_i)\pi_0^*}\right) \pi_{0,i}^*$. Again since $\partial^2 \zeta_{2'} / \partial \phi_i^2 \leqslant 0$, for any arbitrary realization of $\pi_{0,i}^* = \varrho$, we have from the application of Jensen's inequality above (now dropping the dependence of $\mathbb{E}$ on i) that $\mathbb{E}[\zeta_{2'}(\phi_i, \pi_{0,i}^*) \mid \pi_{0,i}^*] \leqslant \zeta_{2'}\left(\mathbb{E}[\phi_i \mid \pi_{0,i}^* = \varrho], \varrho\right)$. Using Proposition 2 and applying LIE to this inequality,

$$\mathbb{E}[X_i^*] \leqslant \mathbb{E}[\zeta_{2'}(\phi_i, \pi_{0,i}^*)] \leqslant \mathbb{E}\left[\zeta_{2'}\left(\mathbb{E}[\phi_i \mid \pi_{0,i}^*], \pi_{0,i}^*\right)\right] \leqslant \mathbb{E}\left[\zeta_{2'}(\overline{\phi}, \pi_{0,i}^*)\right], \tag{B.3}$$

where $\overline{\phi}$ is as in the proposition statement and where the last inequality uses $\partial \zeta_{2'} / \partial \phi_i \geqslant 0$. Substituting the definition of $\zeta_{2'}$ into this inequality yields equation (16).

For part (iii), as $(\pi_{0,i}^* - \frac{\pi_{0,i}^*}{\overline{\phi} + (1-\overline{\phi})\pi_{0,i}^*}) \leqslant \pi_{0,i}^*$ for any $\overline{\phi} \geqslant 1$, $\mathbb{E}[X_i^*] \leqslant \mathbb{E}[(\pi_{0,i}^* - 0)\pi_{0,i}^*] = \mathbb{E}[(\pi_{0,i}^*)^2]$, as stated. (Equivalently, one can use (B.3) and note again that $\partial \zeta_{2'} / \partial \overline{\phi} \geqslant 0$, so that the bound is most slack as $\overline{\phi} \to \infty$, giving the same bound.)

For part (iv), Corollary 2 gives that if $\mathbb{E}[X^* | \theta = 0] \leqslant \mathbb{E}[X^* | \theta = 1]$, then $\mathbb{E}[X^*] \leqslant 0$. Therefore, if $\mathbb{E}[X_i^* | \theta = 0] \leqslant \mathbb{E}[X_i^* | \theta = 1]$ for all i, then $\mathbb{E}[X_i^*] \leqslant 0$ over all streams, completing the proof. □

B.3 Proofs for Section 5

Proof of Proposition 9. For part (i), first define the likelihood of a prior π_0 as

$$\mathcal{L}(\pi_0) \equiv \frac{\pi_0}{1 - \pi_0}, \tag{B.4}$$

and the likelihood of a signal s_t as

$$\mathcal{L}(s_t) \equiv \frac{DGP(s_t|\theta=1)}{DGP(s_t|\theta=0)},$$

where the dependence of the latter on H_{t-1} is left implicit for simplicity. The likelihood for any belief π_t is defined as well following (B.4). The above likelihoods are well-defined for interior priors (as we assume given finite L in the proposition) and for $DGP(s_t|\theta=0, H_{t-1}) > 0$ (we return to the situation in which $DGP(s_t|\theta=0, H_{t-1}) = 0$ shortly). From Bayes' rule, beliefs satisfy $\mathcal{L}(\pi_t) = \mathcal{L}(\pi_0) \cdot \mathcal{L}(s_1) \cdot \mathcal{L}(s_2) \cdots \mathcal{L}(s_t)$. Now note from (5) that $\mathcal{L}(\pi_0^*) \equiv \frac{\pi_0^*}{1-\pi_0^*} = \phi \frac{\pi_0}{1-\pi_0}$, from which it follows that under Bayesian updating,

$$\mathcal{L}(\pi_t^*) = \mathcal{L}(\pi_0^*) \cdot \mathcal{L}(s_1) \cdot \mathcal{L}(s_2) \cdots \mathcal{L}(s_t) = \phi \mathcal{L}(\pi_0) \cdot \mathcal{L}(s_1) \cdot \mathcal{L}(s_2) \cdots \mathcal{L}(s_t).$$

For a fictitious agent with a rational prior, one could replace $\mathcal{L}(\pi_0)$ with $\mathcal{L}(\mathbb{P}_0(\theta=1))$. In our case, given the incorrect prior (but correct Bayesian updating), we have $\frac{\pi_t^*}{1-\pi_t^*} = \check{\phi} \frac{\mathbb{P}_0(\theta=1)}{1-\mathbb{P}_0(\theta=1)}$, where $\check{\phi} \equiv \phi L$, with L defined as in the proposition. We can therefore write

$$\mathcal{L}(\pi_t^*) = \check{\phi} \mathcal{L}(\mathbb{P}_0(\theta=1)) \cdot \mathcal{L}(s_1) \cdot \mathcal{L}(s_2) \cdots \mathcal{L}(s_t).$$

As the likelihood ratios for the RN beliefs in this case are equal to those of a fictitious agent with a correct prior $\check{\pi}_0 = \mathbb{P}_0(\theta=1)$ and $\check{\phi}$ in place of ϕ, we conclude that the RN beliefs are as well. Finally, for the case in which $DGP(s_t|\theta=0, H_{t-1}) = 0$ and this signal s_t is observed, the person will update to $\pi_t = 1$, matching the belief of a rational agent again. We have thus shown part (i).

We can thus treat the agent with the incorrect prior as if she were rational (satisfying Assumption 2) but with $\check{\phi}$ in place of ϕ. Further, $\check{\phi}$ satisfies Assumption 4, since L is constant and ϕ is constant by that assumption as well. For part (ii) of the proposition, if $\check{\phi} \geqslant 1$, then Assumption 3 holds as well, so all three assumptions are satisfied, and the stated results carry through.

For part (iii), assuming $0 < \check{\phi} < 1$ (so Assumption 3 no longer holds for the fictitious rational agent), note first that the proof of Proposition 1 never employs Assumption 3 and therefore still holds straightforwardly, as we can write $\mathbb{E}[X^*] = (\pi_0^* - \check{\pi}_0)\triangle$ without use of this assumption. For Proposition 2, the result as stated for a rational agent requires that $\pi_0^* > \check{\pi}_0$, which is not true for $\check{\phi} < 1$. But an alternative bound can be shown for this case, by obtaining a lower bound for $\triangle$ similar to the upper bound in Lemma A.2. Starting from (A.7) but solving now for $\mathbb{E}[\mathsf{m}^*|\theta=1]$, $\mathbb{E}[\mathsf{m}^*|\theta=1] = (1-\pi_0^*) - \frac{1-\pi_0^*}{\pi_0^*} \cdot \mathbb{E}[\mathsf{m}^*|\theta=0]$. Using this in (A.6),

$$\triangle = \mathbb{E}[\mathsf{m}^*|\theta=0] - \left((1-\pi_0^*) - \frac{1-\pi_0^*}{\pi_0^*} \cdot \mathbb{E}[\mathsf{m}^*|\theta=0] \right) = \frac{1}{\pi_0^*} \cdot \mathbb{E}[\mathsf{m}^*|\theta=0] - (1-\pi_0^*).$$

Then, given that $\frac{1}{\pi_0^*} \geqslant 0$ and $\mathbb{E}[\mathsf{m}^*|\theta=0] \geqslant 0$, $\triangle$ must be bounded below by $-(1-\pi_0^*)$. Returning

to the formula from Proposition 2, if $\check{\phi} < 1$, then $\pi_0^* - \check{\pi}_0 \leqslant 0$, which gives

$$\mathbb{E}[X^*] = (\pi_0^* - \check{\pi}_0)(\triangle) \leqslant (\check{\pi}_0 - \pi_0^*)(1 - \pi_0^*). \tag{B.5}$$

Further, as $\check{\pi}_0 \leqslant 1$, $\mathbb{E}[X^*] \leqslant (\check{\pi}_0 - \pi_0^*)(1 - \pi_0^*) \leqslant (1 - \pi_0^*)(1 - \pi_0^*) = (1 - \pi_0^*)^2$, as stated. And taking (ii) and (iii) together, we have that $\mathbb{E}[X^*] \leqslant \max(\pi_0^{*2}, (1 - \pi_0^*)^2)$. □

Proof of Corollary 3. Case (iii) from the previous proof applies, with ϕ in place of $\check{\phi}$ and π_0 in place of $\check{\pi}_0$ (since the agent now has RE but $\phi < 1$). Thus (B.5) applies with these substitutions. The second expression for the bound given in the corollary then substitutes for π_0 (using (8)) and simplifies. Equivalently, by swapping the labels of states 0 and 1, the swapped RN beliefs become $1 - \pi_t^*$ in place of π_t^* and the swapped SDF ratio becomes $\frac{1}{\phi}$ in place of ϕ. As $\phi < 1$, $\frac{1}{\phi} > 1$. Therefore, all of our results hold, with π_t^* replaced by $1 - \pi_t^*$ and ϕ replaced by $\phi^{-1} > 1$. □

Proof of Proposition 10. Under the stated assumptions for ϵ_t, observed RN movement satisfies

$$\begin{aligned}
\mathbb{E}[\widehat{\mathsf{m}}_{t,t+1}^*] &= \mathbb{E}[(\widehat{\pi}_{t+1}^* - \widehat{\pi}_t^*)^2] = \mathbb{E}\Big[\big((\pi_{t+1}^* - \pi_t^*)^2 + (\epsilon_{t+1} - \epsilon_t)\big)^2\Big] \\
&= \mathbb{E}[\mathsf{m}_{t,t+1}^*] + 2\mathbb{E}[\pi_{t+1}^*\epsilon_{t+1} - \pi_t^*\epsilon_{t+1} - \pi_{t+1}^*\epsilon_t + \pi_t^*\epsilon_t] + \mathbb{E}[(\epsilon_{t+1} - \epsilon_t)^2] \\
&= \mathbb{E}[\mathsf{m}_{t,t+1}^*] + \mathbb{E}[\epsilon_t^2 + \epsilon_{t+1}^2].
\end{aligned}$$

For the observed counterpart of uncertainty resolution $\mathsf{r}_{t,t+1}^* \equiv (\mathsf{u}_t^* - \mathsf{u}_{t+1}^*)$,

$$\mathbb{E}[\widehat{\mathsf{r}}_{t,t+1}^*] = \mathbb{E}[(\pi_t^* + \epsilon_t)(1 - \pi_t^* - \epsilon_t) - (\pi_{t+1}^* + \epsilon_{t+1})(1 - \pi_{t+1}^* - \epsilon_{t+1})] = \mathbb{E}[\mathsf{r}_{t,t+1}^*] + \mathbb{E}[\epsilon_{t+1}^2 - \epsilon_t^2].$$

Combining these two, with $\mathrm{Var}(\epsilon_t) \equiv \mathbb{E}[(\epsilon_t - \mathbb{E}[\epsilon_t])^2] = \mathbb{E}[\epsilon_t^2]$ and $X_{t,t+1}^* \equiv \mathsf{m}_{t,t+1}^* - \mathsf{r}_{t,t+1}^*$,

$$\mathbb{E}[\widehat{X}_{t,t+1}^*] = \mathbb{E}[X_{t,t+1}^*] + 2\mathrm{Var}(\epsilon_t). \qquad \square$$

Appendix C. Additional Technical Material

C.1 Simulations for the Relationship of RN Prior and DGP with $\triangle$

As noted in Section 2.3, we run numerical simulations of a large number of DGPs and priors in order to understand the precise impact of the RN prior and DGP on $\triangle$ (and therefore $\mathbb{E}[X^*]$). We consider the universe of history-independent binary-signal DGPs with a prior π_0^* where $s_t \in \{l, h\}$ and $\mathbb{P}[s_t = h|\theta = 1]$ and (assumed lower) $\mathbb{P}[s_t = h|\theta = 0]$ are constant over t. These signal distributions imply likelihood ratios for the signals of $L_h \equiv \frac{\mathbb{P}[s_t=h|\theta=1]}{\mathbb{P}[s_t=h|\theta=0]} > 1$ and $L_l \equiv \frac{\mathbb{P}[s_t=l|\theta=0]}{\mathbb{P}[s_t=l|\theta=1]} > 1$. We use a fine grid to discretize π_0^*, L_h, and L_l, then conduct 1000 simulations with $T = 100$ and calculate $\triangle$ in all cases. We find:

1. When π_0^* is low, $\triangle > 0$ is very unlikely: the percentage of DGPs with positive $\triangle$ given a $\pi_0^* < .25$ is 2%. For $\pi_0^* < .5$, it is 11%.

Figure C.1: Contour Plot: Simulations for $\triangle$ by DGP and π_0^*

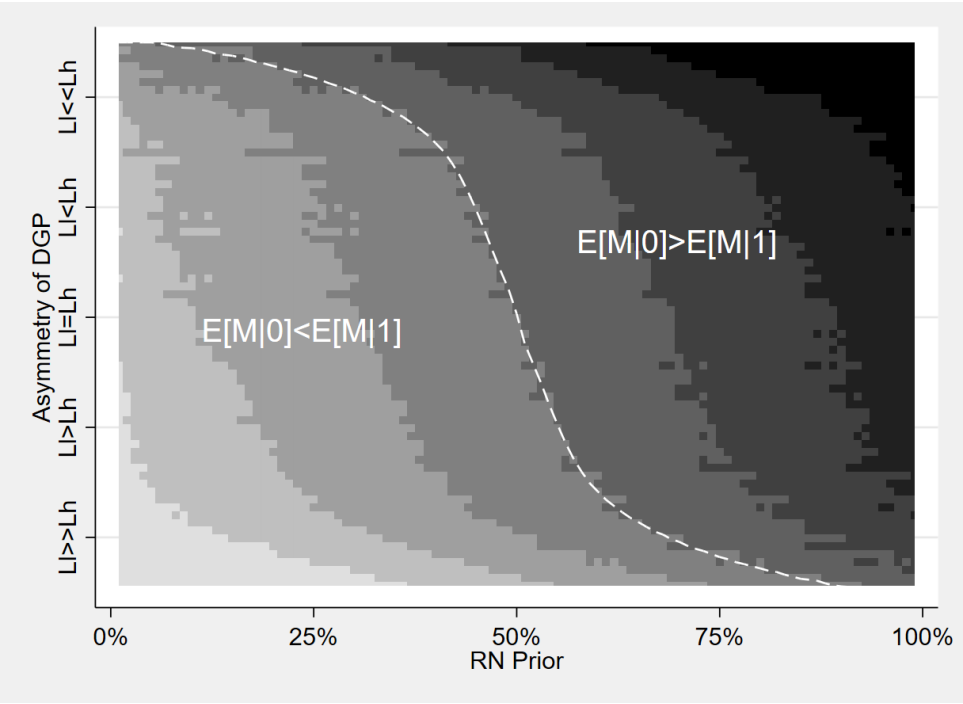

Note: See text in Appendix C.1 for description of simulations and discussion of results.

2. When π_0^* is low, the only DGPs in which $\triangle > 0$ are very asymmetric and extreme. For example, when $\pi_0^* = .25$, $\triangle > 0$ only occurs if $\mathbb{P}[s_t = h|\theta = 1] > .95$ and $L_l > 2 \cdot L_h$.
3. The converse is true when π_0^* is high: $\triangle < 0$ is rare and only occurs given a very asymmetric and extreme DGP.
4. For symmetric DGPs ($L_h = L_l$), $\triangle \gtreqless 0$ when $\pi_0^* \gtreqless .5$.
5. Holding the DGP constant, $\triangle$ rises with π_0^*.
6. Holding all else constant, as L_h rises and the size of upward updates rises, $\triangle$ falls. As L_l rises and the size of upward-updates rises, $\triangle$ rises.

We present these results visually in Figure C.1. We reduce the dimensionality of the setting by focusing on the *likelihood ratio* $\frac{L_h}{L_l}$ rather than L_h and L_l individually. (While the impact of both L_h and L_l on $\triangle$ appears monotonic, the impact of $\frac{L_h}{L_l}$ is only monotonic on average, leading to a slightly messier graph.) The figure shows a contour plot with the RN prior on the x-axis, with the y-axis stacking all of the DGP combinations in order of the likelihood ratio, and the contour colors showing the approximate value of $\triangle$ (darker colors corresponding to higher values) for each prior and DGP (with the dotted line highlighting the points at which $\triangle = 0$). For example, drawing a vertical line at a prior of $\pi_0^* = 0.25$ suggests that a large portion of DGPs produce a $\triangle < 0$, and the only DGPs that produce $\triangle > 0$ have extreme likelihood ratios.

C.2 Risk-Neutral Beliefs and Time-Varying Discount Rates

This section provides further context on the relationship between RN beliefs and discount rates, as discussed in Section 4.1 in the main paper. We again work in the setting in Section 2 here for simplicity of exposition. The price of the terminal consumption claim is given in equilibrium in by $P_t(C_T) = \mathbb{E}_t\left[\beta_t^{T-t}\frac{U'(C_T)}{U'(C_t)}C_T\right]$, where β_t is now the agent's (possibly time-varying) time discount factor. Defining the gross return $R^C_{t,T} \equiv \frac{C_T}{P_t(C_T)}$, rearranging this equation for $P_t(C_T)$ yields

$$\mathbb{E}_t[R^C_{t,T}] = \frac{1 - \text{Cov}_t\left(\beta_t^{T-t}\frac{U'(C_T)}{U'(C_T)}, C_T\right)}{\mathbb{E}_t\left[\beta_t^{T-t}\frac{U'(C_T)}{U'(C_t)}\right]} = \frac{\frac{U'(C_t)}{\beta_t^{T-t}} - \text{Cov}_t(U'(C_T), C_T)}{\mathbb{E}_t[U'(C_T)]},$$

as usual. We can write $\mathbb{E}_t[U'(C_T)] = \pi_t U'(C_{\text{low}}) + (1-\pi_t)U'(C_{\text{high}})$ in our two-state setting, and $\text{Cov}_t(U'(C_T), C_T)$ can be similarly rewritten as a function of π_t, C_T, and $U'(C_T)$. In this setting, discount-rate variation can arise from four sources:

1. Changes in the time discount factor β_t.
2. Changes in contemporaneous marginal utility $U'(C_t)$.
3. Changes in the relative probability π_t.
4. Changes in state-contingent terminal consumption C_i or marginal utility $U'(C_i)$.

Our framework allows for *any* discount-rate variation arising from the first three sources, but restricts the last one: under CTI, it must be the case that any changes to (expected) $U'(C_i)$ are proportional across states. (More generally, as in Section 4.1, permanent changes to the SDF are admissible, which by itself greatly generalizes this setting relative to one with constant discount rates.) With constant discount rates, meanwhile, none of the four changes are admissible, or any such changes must offset perfectly.

C.3 Simulations with Time-Varying ϕ_t

This section provides further detail for the simulations discussed in Section 4.3 and shown in Figure 4. First consider the baseline situation in which $\pi_0^* = 0.5$ and $\phi_t = 3$ for all t. There is thus only uncertainty about θ, and $\mathbb{E}[\mathsf{m}^*]$ varies depending on the signal DGP. To trace the distribution of $\mathbb{E}[\mathsf{m}^*]$ across DGPs, we attempt to cover the space of binary DGPs in which the signal strengths are constant over time. We start by looping over $\mathbb{P}[s_t = h|\theta = 1]$ from {1,.99,.98,...,.01}. Then we loop over $\mathbb{P}[s_t = l|\theta = 0]$ from {.01,.02,.03,....99} while constraining $\mathbb{P}[s_t = h|\theta = 1] > \mathbb{P}[s_t = l|\theta = 0]$ such that the h signal leads to an upward movement. This process leads to 5052 DGPs. For each of these DGPs, we simulate 100 random streams of $T = 200$ periods, after which the state is perfectly observed. This number of periods allows beliefs to get very close to certainty prior to the resolving signal. We calculate m^* for each stream, from which we calculate the average m^* statistic as an estimate of $\mathbb{E}[\mathsf{m}^*]$ for each DGP. The distribution of $\mathbb{E}[\mathsf{m}^*]$ values across all such simulated DGPs is shown in the dark line in Figure 4.

Next, we allow additional uncertainty about the conditional realizations of the SDF M_T, so that ϕ_t also evolves over time. For each state (j and $j+1$), we allow M_T to take two possible values with equal probability, where we choose the values such that $\phi_0 = 3$. Here, we start to run into calculation timing constraints such that we limit the possible signal strengths. In particular, we allow signal strengths for the high signal of .55,.75,.95 and for the low signal of .05,.25,.45 for both states. Therefore we simulate nine DGPs for learning about M_T in state j and nine DGPs for learning about $j+1$, leading to 81 combined DGPs to learn about M_T. We combine each such DGP with each of the DGPs for θ discussed above, and we again simulate 100 random draws of movement of 200 periods. Each line in Figure 4 represents a different $\mathbb{E}[\mathsf{m}^*]$ distribution given variation in the signal strengths for θ, with the different lines showing different signal strengths for learning about the conditional values of M_T (and thus ϕ). In the "Low ϕ Uncertainty" case, M_T in state j can take the values 2.5 or 3.5 with equal probability and in state $j+1$ can take the values 0.833 or 1.167 with equal probability. Consequently, $\phi_0 = 3$, and ϕ_T can vary from 2.14 to 4.2 (with a coefficient of variation of 12%). In the "Medium ϕ Uncertainty" case, M_T in state j can be 2 or 4 and in state $j+1$ can be 0.667 or 1.333, so that ϕ_T can vary from 1.5 to 6 (with a coefficient of variation of 54%). Finally, in the "High ϕ Uncertainty" case, M_T in state j can be 1.5 or 4.5 and in state $j+1$ can be 0.5 or 1.5, so that ϕ_T can vary from 1 to 9 (with a coefficient of variation of 100%).

C.4 Solution Method and Simulations for Habit Formation Model

See the proof of statement 5 in Appendix B.2 for a description of the model, and the calibrated parameters are identical to those used by Campbell and Cochrane (1999, Table 1), converted to daily values, for the version of their model with imperfectly correlated consumption and dividends. We consider 90-day option-expiration horizons (i.e., $T_i - 0_i = 90$), and after solving the model for the price-dividend ratio, we then solve for the joint distribution for returns (from t to T_i) and the SDF at every point in a gridded state space as of $t = T_i - 1$, then $t = T_i - 2$, and so on, as below.

The initial market index value is normalized to $V^m_{0_i} = 1$, and the joint CDF for the SDF realization and the return as a function of the current surplus-consumption state is then solved by iterating backwards from T_i: after solving the model for the price-dividend ratio as a function of the surplus-consumption value, we then calculate the $T_i - 1$ CDF for any possible surplus-consumption value by integrating over the distributions of shocks to consumption (and thus surplus consumption) and dividends at T_i; we then project this CDF onto an interpolating cubic spline over the three dimensions $(S^c_{T_i-1}, M_{T_i}, \log(R^{m,e}_{T_i}))$; we then calculate the $T_i - 2$ CDF by integrating over the distribution of shocks at $T_i - 1$ *and* the projection solutions for the conditional distribution functions for $(T_i - 1) \rightarrow T_i$ obtained in the previous step; and so on. These CDFs are then used for the model simulations.

We conduct 25,000 simulations, where each simulation runs from 0_i to T_i, and for which the initial surplus-consumption state is drawn from its unconditional distribution. For each period in each simulation, we evaluate risk-neutral beliefs over return states at every point in the space Θ and use these to calculate the set of conditional risk-neutral beliefs $\{\widetilde{\pi}^*_{t,i,j}\}_j$. Further, we store

Figure C.2: Estimates of SDF Slope in Habit Formation Model Simulations

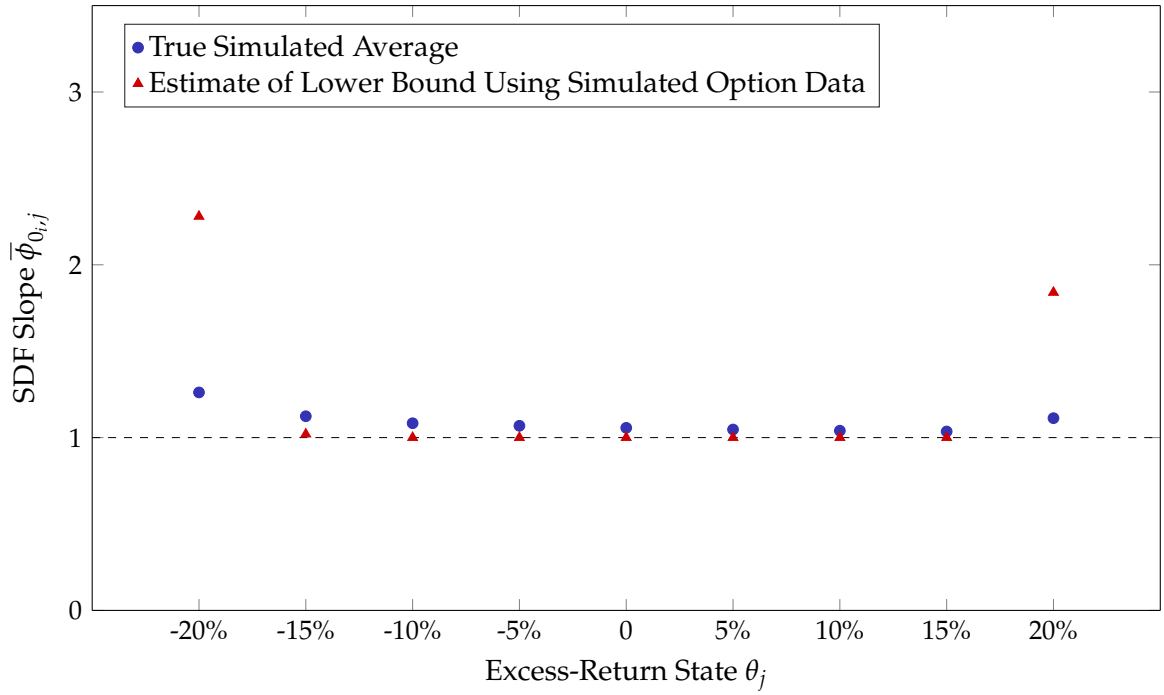

Note: See text in Appendix C.4 for description of simulations.

the associated set of expected SDF slopes $\{\phi_{t,i,j}\}_j$. We can thus calculate the true average values of these objects of interest, $\overline{\phi}_{0_i,j} \equiv \widehat{\mathbb{E}}[\phi_{0_i,i,j}]$, where $\widehat{\mathbb{E}}[\cdot]$ denotes the expectation over all simulations i and we have fixed the state pair j. And using the risk-neutral beliefs series, we can naively apply our conservative bound in Proposition 8 to obtain lower-bound estimates for those SDF slopes and compare those estimates to the true simulated values. Relative risk aversion for this model's representative agent does not match the definition used in Proposition 6, as this agent's utility does not depend only on terminal wealth (see Campbell and Cochrane, 1999, Section IV.B), so we accordingly present estimates for the SDF slope rather than for relative risk aversion.

Figure C.2 presents these simulation results. The blue circles show the true simulated average values of the SDF slopes $\overline{\phi}_{0_i,j}$, while the red triangles show the naive lower-bound estimates of these values using our theoretical bound on the simulated RN beliefs data. It is clear in both cases that these SDF-slope values are far below those obtained from our empirical estimates, so the model does not replicate the observed variation in RN beliefs even with the violation of CTI. We can understand the validity of the theoretical bound for the interior states by way of Proposition 7, which shows that the bounds hold approximately for violations of CTI for which the $\phi_{t,i,j}$ process is close to a martingale. In our simulations, the values $|\widehat{\mathbb{E}}[\phi_{t+1,i,j} - \phi_{t,i,j}]|$ for different state pairs j range from 0.00002 to at most 0.00011, which is not large enough to invalidate the bounds.

C.5 Data Cleaning and Measurement of Risk-Neutral Distribution

Before detailing measurement of the risk-neutral distribution, we note that we must collect additional data in order to follow the procedure below. In particular, in order to obtain the ex post return state for each option expiration date T_i (and thereby assign probability 1 to that state on date T_i, so that our streams are resolving), we need S&P 500 index prices used as option settlement values. Our first step in this exercise is therefore to obtain end-of-day index prices (which we take as well from OptionMetrics). But the settlement value for many S&P 500 options in fact reflects the opening (rather than closing) price on the expiration date; for example, the payoff for the traditional monthly S&P 500 option contract expiring on the third Friday of each month depends on the opening S&P index value on that third Friday morning, while the payoff for the more recently introduced end-of-month option contract depends on the closing S&P index value on the last business day of the month.[2] To obtain the ex-post return state for A.M.-settled options, we hand-collect the option settlement values for these expiration dates from the Chicago Board Options Exchange (CBOE) website, which posts these values.

In addition, in order to measure the risk-neutral distribution *and* to measure realized excess index returns, we need risk-free zero-coupon yields R^f_{t,T_i} for $t = 0_i, \ldots, T_i - 1$. To obtain these, we follow van Binsbergen, Diamond, and Grotteria (2022) and obtain the relevant yield directly from the cross-section of option prices by applying the put-call parity relationship. We apply their "Estimator 2," which obtains $R^f_{t,T_i} = \beta^{-1/T}$ from Theil–Sen (robust median) estimation of $q^{m,\text{put}}_{t,i,K} - q^{m,\text{call}}_{t,i,K} = \alpha + \beta K + \varepsilon_{t,i,K}$. This provides a very close fit to the option cross-sections (see van Binsbergen, Diamond, and Grotteria, 2022, for details) and thus produces a risk-free rate consistent with observed option prices, as is necessary to correctly back out the risk-neutral distribution.

Finally, for both the OptionMetrics end-of-day and CBOE intraday data, we apply standard filters (e.g., Christoffersen, Heston, and Jacobs, 2013; Constantinides, Jackwerth, and Savov, 2013; Martin, 2017) to the raw option-price data before estimating risk-neutral distributions. We drop any options with bid or ask price of zero (or less than zero), with uncomputable Black–Scholes implied volatility or with implied volatility of greater than 100 percent, with more than one year to maturity, or (for call options) with mid prices greater than the price of the underlying; we drop any option cross-section (i.e., the full set of prices for the pair (t, T_i)) with no trading volume on date t, with fewer than three listed prices across different strikes, or for which there are fewer than three strikes for which both call and put prices are available (as is necessary to calculate the forward price and risk-free rate); and after transforming the data to a risk-neutral distribution as below, we keep only conditional RN belief observations $\widetilde{\pi}^*_{t,i,j}$ for which the non-conditional beliefs satisfy $\pi^*_t(R^m_{T_i} = \theta_j) + \pi^*_t(R^m_{T_i} = \theta_{j+1}) \geqslant 5\%$. Our bounds can be calculated using data of arbitrary frequency, so we calculate $X^*_{i,j}$ using changes in RN beliefs over whatever set of trading days are left in the sample after this filtering procedure.

As introduced in Section 6.1, we measure the risk-neutral return distribution by applying the

[2] See http://www.cboe.com/SPX for further detail. For our dataset, the majority (roughly 2/3) of option expiration dates correspond to A.M.-settled options.

following steps to the remaining option prices (for which we use mid prices), following Malz (2014):

1. Transform the collections of call- and put-price cross-sections (for example, for call options on date t for expiration date T_i, this set is $\{q^m_{t,i,K}\}_{K\in\mathcal{K}}$) into Black–Scholes implied volatilities.
2. Discard the implied volatility values for in-the-money calls and puts, so that the remaining steps use data from only out-of-the-money put and call prices (as, e.g., in Martin, 2017). Moneyness is measured relative to the at-the-money-forward price, measured (again following Martin, 2017) as the strike K at which $q^{m,\text{put}}_{t,i,K} = q^{m,\text{call}}_{t,i,K}$.
3. Fit a cubic spline to interpolate a smooth function between the points in the resulting implied-volatility schedule for each trading date–expiration date pair. The spline is *clamped*: its boundary conditions are that the slope of the spline at the minimum and maximum values of the knot points $\mathcal{K}$ is equal to 0; further, to extrapolate outside of the range of observed knot points, set the implied volatilities for unobserved strikes equal to the implied volatility for the closest observed strike (i.e., maintain a slope of 0 for the implied-volatility schedule outside the observed range).
4. Evaluate this spline at 1,901 strike prices, for S&P index values ranging from 200 to 4,000 (so that the evaluation strike prices are $K = 200, 202, \ldots, 4000$), to obtain a set of implied-volatility values across this fine grid of possible strike prices for each (t, T_i) pair.[3]
5. Invert the resulting smoothed 1,901-point implied-volatility schedule for each (t, T_i) pair to transform these values back into call prices, and denote this fitted call-price schedule as $\{\hat{q}^m_{t,i,K}\}_{K\in\{200,202,\ldots,4000\}}$.
6. Calculate the risk-neutral CDF for the date-T_i index value at strike price K using $\mathbb{P}^*_t(V^m_{T_i} < K) = 1 + R^f_{t,T_i}(\hat{q}^m_{t,i,K} - \hat{q}^m_{t,i,K-2})/2$. (See the proof of equation (13) in Appendix B.1 for a derivation of this result; the index-value distance between the two adjacent strikes is equal to 2 given that we evaluate the spline at intervals of two index points.)
7. Defining $V^m_{i,j,\max}$ and $V^m_{i,j,\min}$ to be the date-T_i index values corresponding to the upper and lower bounds, respectively, of the bin defining return state θ_j,[4] we then calculate the risk-neutral probability for state θ_j will be realized at date T_i, referred to with slight notational abuse as $\mathbb{P}^*_t(\theta_j)$, as

$$\mathbb{P}^*_t(\theta_j) = \mathbb{P}^*_t(V^m_{T_i} < V^m_{i,j,\max}) - \mathbb{P}^*_t(V^m_{T_i} < V^m_{i,j,\min}),$$

   where the CDF values are taken from step 6 using linear interpolation between whichever two strike values $K \in \{200, 202, \ldots, 4000\}$ are nearest to $V^m_{i,j,\max}$ and $V^m_{i,j,\min}$, respectively.

Steps 1 and 2 represent the only point of distinction between our procedure and that of Malz, who assumes access to a single implied-volatility schedule without considering put or call prices directly; our procedure is accordingly essentially identical to his. Note that we transform the option

[3] This set of ∼1,900 strike prices is on average about 20 times larger than the set of strikes for which there are prices in the data, as there is a mean of roughly 90 observed values in a typical set $\{q^m_{t,i,K}\}_{K\in\mathcal{K}}$.

[4] That is, formally, $V^m_{i,j,\min} = R^f_{0_i,T_i} V^m_{T_0} \exp(\theta_j - 0.05)$ and $V^m_{i,j,\max} = R^f_{0_i,T_i} V^m_{0_i} \exp(\theta_j)$. For example, for excess return state θ_2, we have $V^m_{i,j,\min} = R^f_{0_i,T_i} V^m_{0_i} \exp(-0.2)$ and $V^m_{i,j,\max} = R^f_{0_i,T_i} V^m_{T_0} \exp(-0.15)$.

prices into Black–Scholes implied volatilities simply for purposes of fitting the cubic spline and then transform these implied volatilities back into call prices before calculating risk-neutral beliefs, so this procedure does *not* require the Black–Scholes model to be correct.[5] The clamped cubic spline proposed by Malz (2014), and used in step 3 above, is chosen to ensure that the call-price schedule obtained in step 5 is decreasing and convex with respect to the strike price outside the range of observable strike prices, as required under the restriction of no arbitrage. Violations of these restrictions *inside* the range of observable strikes, as observed infrequently in the data, generate negative implied risk-neutral probabilities; in any case that this occurs, we set the associated risk-neutral probability to 0.

As noted in step 3, the clamped spline is an *interpolating* spline, as it is restricted to pass through all the observed data points so that the fitted-value set $\{\hat{q}^m_{t,i,K}\}$ contains the original values $\{q^m_{t,i,K}\}$. Some alternative methods for measuring risk-neutral beliefs use smoothing splines that are not constrained to exhibit such interpolating behavior. To check the robustness of our results to the choice of measurement technique, we have accordingly used one such alternative method proposed by Bliss and Panigirtzoglou (2004). Empirical results obtained using risk-neutral beliefs calculated in this alternative manner are unchanged as compared to the benchmark results in Section 6.4.

We have also conducted robustness tests with respect to the fineness of the grid on which we evaluate the spline in step 4 and calculate the risk-neutral CDF in step 6, with results from these exercises also indistinguishable from the benchmark results.

C.6 Noise Estimation and Matching to X^* Observations

As introduced in Section 6.2, we first estimate $\text{Var}(\epsilon_t) = \text{Var}(\epsilon_{t,i,j})$ separately for each combination of trading day t, expiration date T_i, and return state pair j in our intraday sample.[6] Our ReMeDI estimator for this noise variance follows the replication code provided by Li and Linton (2022): $\widehat{\text{Var}}(\epsilon_t) = \frac{1}{N_{\epsilon,n}} \sum_{i=2k_n}^{N_{\epsilon,n}-k_n} (\widehat{\pi}^*_{t_i} - \widehat{\pi}^*_{t_i-2k_n})(\widehat{\pi}^*_{t_i} - \widehat{\pi}^*_{t_i+k_n})$. We select k_n for each return state using the algorithm in Section F.1 of the Online Appendix of Li and Linton (2022).

We must then match the noise estimates (which are obtained only for a subsample of days) to the observed excess movement observations in our original daily data. To do so, we take advantage of the fact that the best predictors of $\widehat{\text{Var}}(\epsilon_{t,i,j})$ are (i) state pair j (we see more noise for tail states) and (ii) the observed RN belief of either θ_j or θ_{j+1} being realized, $\Sigma^*_{t,i,j} \equiv \pi^*_t(R^m_{T_i} = \theta_j) + \pi^*_t(R^m_{T_i} = \theta_{j+1})$ (conditional beliefs are noisier when the underlying sum $\Sigma^*_{t,i,j}$ is lower, as $\Sigma^*_{t,i,j}$ enters into the denominator of $\widetilde{\pi}^*_{t,i,j}$). We thus partition $\Sigma^*_{t,i,j}$ into 5-percentage-point bins ($[0, 0.05), [0.05, 0.1], \ldots$), and then calculate the average noise $\widehat{\sigma}_{\epsilon,j,\Sigma} \equiv \overline{\widehat{\text{Var}}(\epsilon_{t,i,j})}$ for each combination of state pair j and bin for $\Sigma^*_{t,i,j}$. We then match $\widehat{\sigma}_{\epsilon,j,\Sigma}$ to each observed one-day excess movement observation $\widehat{X}^*_{t,t+1,i,j}$ in our original end-of-day data, based on that observation's state j and total probability $\Sigma^*_{t,i,j}$.

[5] We conduct this transformation following Malz (2014), as well as much of the related literature, which argues that these smoothing procedures tend to perform slightly better in implied-volatility space than in the option-price space given the convexity of option-price schedules; see Malz (1997) for a discussion.

[6] For this exercise, to increase our available observations, we do not condition on the ex post state being θ_j or θ_{j+1}.

C.7 Details of Bootstrap Confidence Intervals

Our block-bootstrap resampling procedure is described in Section 6.4, and we provide further details on how we construct one-sided confidence intervals for Table 3 here. Fixing a given $\overline{\phi}$, denote the point estimate for $\overline{e_i^{\text{main}}(\phi)}$ by $\widehat{e}(\overline{\phi})$. The null that $\overline{e_i^{\text{main}}(\phi)} = 0$ is rejected at the 5% level if $2\widehat{e}(\overline{\phi}) - e^*_{(0.95)}(\overline{\phi}) > 0$, where $e^*_{(0.95)}(\overline{\phi})$ is the 95$^{\text{th}}$ percentile of the bootstrap distribution of $\overline{e_i^{\text{main}}(\phi)}$ statistics (i.e., it is rejected if it is outside of the one-sided 95% basic bootstrap CI for $\overline{e_i^{\text{main}}(\phi)}$). We conduct this procedure for all possible $\overline{\phi}$ values, and we obtain $\widehat{\phi}_{LB} = \min_{\overline{\phi}}$ s.t. $2\widehat{e}(\overline{\phi}) - e^*_{(0.95)}(\overline{\phi}) \leqslant 0$.

A more straightforward procedure for conducting inference on $\overline{\phi}$ would be to construct the basic bootstrap CI directly for $\overline{\phi}$ (i.e., $\widehat{\phi}_{LB} = 2\widehat{\phi} - \phi^*_{(0.95)}$). The challenge preventing us from doing so is that in nearly all cases, the 95$^{\text{th}}$ percentile of the bootstrap distribution for $\widehat{\phi}$ is ∞, given how large our point estimates are (and how much excess movement we observe in our data). This motivates our use of a test-inversion confidence interval using the residuals for different possible values of $\overline{\phi}$, which solves this problem. These CIs achieve asymptotic coverage of at least the nominal level under weak conditions (discussed further below), given the duality between testing and CI construction; see, e.g., Carpenter (1999). We find that our procedure performs quite well, with unbiased and symmetric bootstrap distributions around the full-sample point estimate.

We note that our bootstrap procedure fully preserves the groupings of return-state pairs (indexed by $j = 1, \ldots, J-1$) for each set of observations indexed by i (corresponding to the option expiration date) within each block, as we split the observations into blocks only by time and not by return states. We do so in order to obtain valid inference for the aggregate value $\overline{\boldsymbol{\phi}}$, which uses observations for state pairs $(\theta_2, \theta_3), \ldots, (\theta_{J-2}, \theta_{J-1})$, in the face of arbitrary dependence for the observations across those state pairs and a fixed number of return states J (whereas we assume $N \to \infty$, and further the number of blocks $B \to \infty$ according to a sequence such that $(T_N + 1)/B \to \infty$). In this way our procedure is in fact a *panel* (or *cluster*) *block bootstrap*; see, for example, Palm, Smeekes, and Urbain (2011). Lahiri (2003, Theorem 3.2) provides a weak condition on the strong mixing coefficient of the relevant stochastic process — in our case, $\{(X^*_{i,j}, \widetilde{\pi}^*_{0,i,j}, \{\widehat{\text{Var}}(\epsilon_{t,i,j})\})_{t,j}\}_i$ — under which the blocks are asymptotically independent and the bootstrap distribution estimator is consistent for the true distribution under the asymptotics above, so that our test-inversion confidence intervals have asymptotic coverage probability of at least 95% for the population parameters of interest in the presence of nearly arbitrary (stationary) autocorrelation and heteroskedasticity.[7] This coverage rate may in fact be greater than 95% given that we are estimating lower bounds for the parameters of interest rather than the parameters themselves, and this motivates our use of one-sided rather than two-sided confidence intervals, as in Section 6.4.

[7] There are additional conditions required for the result of Lahiri (2003, Theorem 3.2) to hold, but they will hold trivially in our context under the RE null given the boundedness of the relevant belief statistics. Our block bootstrap is a non-overlapping block bootstrap (NBB); others (e.g., Künsch, 1989) have proposed a *moving* block bootstrap (MBB) using overlapping blocks, among other alternatives. While the MBB has efficiency gains relative to the NBB, these are "likely to be very small in applications" (Horowitz, 2001, p. 3190), so we use the NBB for computational convenience.

C.8 Variable Construction for RN Excess Movement Regressions

As discussed in Section 6.5, we consider reduced-form evidence on the macroeconomic and financial correlates of RN excess movement, with results presented in Table 4. The dependent variable in all cases is the monthly average of noise-adjusted RN excess movement $X^*_{t,t+1,i,j}$, with the average calculated across all available expiration dates and interior state pairs for all trading days t in a month. For the dependent variables, from top to bottom in the table, option bid-ask spread is the volume-weighted average bid-ask spread for all S&P 500 options with less than a year to maturity and positive bid prices in the given month. Option volume is total monthly dollar trading volume in that same sample, detrended using an estimated exponential trend given the steady growth in option volume over the sample. RN belief stream length is the average full-stream length $\overline{T_i}$ over all contracts i active in that month. VIX^2 is calculated using the average VIX in the given month. The variance risk premium is VIX^2 minus realized variance, and we use the data provided by Lochstoer and Muir (2022) for this VRP. (We thank these and subsequent authors for making the relevant data available.) The risk-aversion proxy ra_t^{BEX}, as discussed in footnote 37 in the text, is obtained from Nancy Xu's website (https://www.nancyxu.net/risk-aversion-index), and we take the sum of squared daily changes in ra_t^{BEX} in a given month (winsorized at the 5$^{\text{th}}$ and 95$^{\text{th}}$ percentiles) to measure the volatility of this risk-aversion proxy. We obtain the monthly repurchase-adjusted log price-dividend ratio pd_t from Nagel and Xu (2022), and we calculate the absolute value of its deviation from its sample mean $\overline{pd}$. The 12-month S&P 500 change is calculated as the log change in the S&P price from month $t-12$ to t, using data from Robert Shiller's website (http://www.econ.yale.edu/~shiller/data.htm). All variables (both dependent and dependent) are normalized to have zero mean and standard deviation of 1, and all regressions include a constant.

Appendix References

ATMAZ, A. AND S. BASAK (2018): "Belief Dispersion in the Stock Market," *Journal of Finance*, 73, 1225–1279.

AUGENBLICK, N. AND M. RABIN (2021): "Belief Movement, Uncertainty Reduction, and Rational Updating," *Quarterly Journal of Economics*, 136, 933–985.

BASAK, S. (2000): "A Model of Dynamic Equilibrium Asset Pricing With Heterogeneous Beliefs and Extraneous Risk," *Journal of Economic Dynamics & Control*, 24, 63–95.

VAN BINSBERGEN, J. H., W. F. DIAMOND, AND M. GROTTERIA (2022): "Risk-Free Interest Rates," *Journal of Financial Economics*, 143, 1–29.

BLACK, F. AND M. SCHOLES (1973): "The Pricing of Options and Corporate Liabilities," *Journal of Political Economy*, 81, 637.

BLISS, R. R. AND N. PANIGIRTZOGLOU (2004): "Option-Implied Risk Aversion Estimates," *Journal of Finance*, 59, 407–446.

BREEDEN, D. T. AND R. H. LITZENBERGER (1978): "Prices of State-Contingent Claims Implicit in Option Prices," *Journal of Business*, 51, 621–651.

BROWN, D. J. AND S. A. ROSS (1991): "Spanning, Valuation and Options," *Economic Theory*, 1, 3–12.

CAMPBELL, J. Y. (2018): *Financial Decisions and Markets: A Course in Asset Pricing*, Princeton: Princeton University Press.

CAMPBELL, J. Y. AND J. H. COCHRANE (1999): "By Force of Habit: A Consumption-Based Explanation of Aggregate Stock Market Behavior," *Journal of Political Economy*, 107, 205–251.

CARPENTER, J. (1999): "Test Inversion Bootstrap Confidence Intervals," *Journal of the Royal Statistical Society, Series B*, 61, 159–172.

CHRISTOFFERSEN, P., S. HESTON, AND K. JACOBS (2013): "Capturing Option Anomalies with a Variance-Dependent Pricing Kernel," *Review of Financial Studies*, 26, 1962–2006.

CONSTANTINIDES, G. M., J. C. JACKWERTH, AND A. SAVOV (2013): "The Puzzle of Index Option Returns," *Review of Asset Pricing Studies*, 3, 229–257.

EPSTEIN, L. G. AND S. E. ZIN (1989): "Substitution, Risk Aversion, and the Temporal Behavior of Consumption and Asset Returns: A Theoretical Framework," *Econometrica*, 57, 937–969.

GABAIX, X. (2012): "Variable Rare Disasters: An Exactly Solved Framework for Ten Puzzles in Macro-Finance," *Quarterly Journal of Economics*, 127, 645–700.

HANSEN, L. P., J. C. HEATON, AND N. LI (2008): "Consumption Strikes Back? Measuring Long-Run Risk," *Journal of Political Economy*, 116, 260–302.

HOROWITZ, J. L. (2001): "The Bootstrap," in *Handbook of Econometrics*, ed. by J. J. Heckman and E. Leamer, Amsterdam: Elsevier, vol. 5, chap. 52, 3159–3228.

KOCHERLAKOTA, N. R. (1990): "Disentangling the Coefficient of Relative Risk Aversion from the Elasticity of Intertemporal Substitution: An Irrelevance Result," *Journal of Finance*, 45, 175–190.

KÜNSCH, H. R. (1989): "The Jackknife and the Bootstrap for General Stationary Observations," *Annals of Statistics*, 17, 1217–1241.

LAHIRI, S. N. (2003): *Resampling Methods for Dependent Data*, New York: Springer.

LI, Z. M. AND O. B. LINTON (2022): "A ReMeDI for Microstructure Noise," *Econometrica*, 90, 367–389.

LOCHSTOER, L. A. AND T. MUIR (2022): "Volatility Expectations and Returns," *Journal of Finance*, 77, 1055–1096.

MALZ, A. M. (1997): "Option-Implied Probability Distributions and Currency Excess Returns," *Federal Reserve Bank of New York Staff Report No. 32*.

——— (2014): "A Simple and Reliable Way to Compute Option-Based Risk-Neutral Distributions," *Federal Reserve Bank of New York Staff Report No. 677*.

MARTIN, I. (2017): "What Is the Expected Return on the Market?" *Quarterly Journal of Economics*, 132, 367–433.

NAGEL, S. AND Z. XU (2022): "Asset Pricing with Fading Memory," *Review of Financial Studies*, 35, 2190–2245.

PALM, F. C., S. SMEEKES, AND J.-P. URBAIN (2011): "Cross-Sectional Dependence Robust Block Bootstrap Panel Unit Root Tests," *Journal of Econometrics*, 163, 85–104.

VRINS, F. (2018): "Sampling the Multivariate Standard Normal Distribution Under a Weighted Sum Constraint," *Risks*, 6, 1–13.